BUILDING INTERVAL VELOCITY MODELS FOR DEPTH CONVERSION

WITHIN THE TWENEBOA-ENYERA-NTOMME (TEN) OIL DISCOVERY AREA

By

Bannor Antwi-Boasiako Kakra

(BSc Physics)

A Thesis submitted to the Department of Physics, Kwame Nkrumah University of Science and Technology in partial fulfilment of the requirements for the degree

MASTER OF SCIENCE

(Geophysics)

College of Science

June 2013

Supervisors:

Prof. S. K. Danuor (Head of Department, Physics Dept, KNUST)

Mr. Gabriel Osatey (Chief Geophysicist, Ghana National Petroleum Corporation, GN'PC)

DECLARATION

I hereby declare that this submission is my own work towards the MSc and that, to the best of my knowledge, it contains no material previously published by another person nor material which has been accepted for the award of any other degree of the University, except where due acknowledgement has been made in text.

BANNOR
ANTWI-
KAKRA Consta

.?.G.Q.s.1ß..u..... NOVEMBER 4, 2013.

Student Name & ID Signature Date

Certified by:

Prof. S.K. Danuor

o

((—11— 13

Supervisor's Name Signature Date

Certified By:

Prof. S.K. Danuor 04-11-13

Head of Dept. Name Signature Date

ABSTRACT

Seismic velocity relates seismic data, acquired in the time domain, to prospect evaluation, reservoir modelling and well engineering which are all undertaken in the

depth domain. Areal interval macrovelocity models were built for an area within the Deepwater Tano of the Western Basin, offshore Ghana. They were built from both well (checkshot) data and seismic data using regression geostatistical technique. The research was aimed at understanding the interval velocity variations within the subsurface, depth converting seismic time data and studying the possible effects of fan systems on depth conversions. Two main interval velocity models were built: Constant Interval Velocity (CIV) and Mapped Interval Velocity (MIV) models. CIV models were essentially step plots built using Grapher 8 software. They represented 1Dimensional interval velocity models for each of the wells. They revealed the vertical variation of interval velocities at well positions. Seismic-Micro Technology (SMT) software, Kingdom Suite, was used to build MIV models from interval velocity regression functions and seismic time data. These mapped models were generated for three grouped lithostratigraphic layers and were used for the depth conversions. The built interval velocity models proved reliable for the time-depth conversion because the maÑmum percentage deviation computed between the observed field data and the

converted depths at well positions, was less than 3 0/0. An average percentage deviation of 0.97 % and average depth difference of 26 m were the average error margins for the built interval velocity models. The interval velocity models gave an understanding how the interval velocity vary laterally and vertically at the area. The MIV models and their converted depths honoured lithological trends and geologic features within the subsurface. The research was also able to prove that the presence of fans within the subsurface with different lithological infill could adversely affect interval velocity models and consequently depth conversions. Depth converted

seabed and subsurface horizons, generally, sloped southwards in the Deepwater Tano area.

Table of Contents

LIST OF FIGURES

LIST OF TABLES

ACKNOWLEDGEMENTS

Firstly, thanks go to the Almighty God who has kept me through the period of the project. Secondly, my supervisors Professor S. K. Danuor and Mr Gabriel Osatey who have been excellent at guiding me to this point of my studies and I greatly appreciate their support. I thank the Geophysics Manager, Mr Theophilus Ahwireng and the entire staff of Geophysics Department, Ghana National Petroleum

Corporation (GNPC) for their unflinching support. Finally, I am immensely grateful to my family.

DEDICATION

This work is dedicated to God who has shared His glory with me and my family who have been my support in many ways.

CHAPTER 1:

1.1 INTRODUCTION

The transformation of recorded seismic reflection data into structural images of the subsurface requires the use of seismic velocity models. Since traveltime is converted into distance by using velocity, it is apparent that knowledge of seismic velocities is essential to seismic imaging and 'depthing', prospect evaluation, reservoir modelling and well engineering. Seismic velocity is generally defined as the distance travelled by seismic energy per unit time in a given direction through the Earth. Seismic velocities are of great importance in exploration. They are widely used in the conversion of time to depth and vice versa. Velocities are used in well logging to compute porosities and then seismic stratigraphers use seismic velocities to assist in mapping lithofacies.

Seismic velocities actually depend on the ratio of elastic modulus to density, the modulus and density effects "fight" each other, hence, velocities may not always follow any particular trend (Mavko, 1990). Since rocks are of various compositions, textures porosities and pore fluids, they differ in elastic moduli and densities and consequently in eir seismic velocities. For a range of sedimentary rocks, the _____ compressional wave velocity is related to density, and well established velocity— density curves have been published. Hence, the densities of inaccessible subsurface formations may be estimated if their velocities are known from seismic surveys (Kearey et al, 2002).

Velocities, generally, increase with effective pressure due to greater degrees of compaction caused by thickening overburden. To a first order, only the difference between confining pressure and pore pressure are known to matter, not the absolute levels of each — "effective pressure laW'. The pressure dependence results from the closing of cracks, flaws, and grain boundaries, which elastically stiffens the rock mineral frame.

Velocities are known to be sensitive to the fluid content of pores. The compressional wave (P-wave) velocity is usually more sensitive than the shear wave (S-wave) velocity. In sandstone and shales, together with overburden pressure, velocities show systematic increase with age due to the combined effect of compression and cementation (Kearey et al, 2002).

Seismic velocities may be attained from sonic logs, Vertical Seismic Profiles (VSps)/ Checkshots, seismic sections or in the laboratory using suitably prepared rock samples (Keary et al, 2002). The sonic log approximates a log of instantaneous velocity in the direction of the borehole. It practically measures the average velocity of a headwave over a short interval. The Borehole Compensated (BHC) sonic and the Long Spaced Sonic (LSS) logs use the principle of differencial measurements which are averaged in order to provide compensation for borehole rugosity (Marsden, 1998).

Vertical seismic profiling (VSP) is a seismic method where seismic signals generated at the surface of the Earth are recorded by the geophones placed at various depths in a well. If the source is located close to the well, a zero-offset VSP is obtained, and if the source is at some distance from the well, an offset VSP is obtained. A full seismic trace is recorded in order to enable correlation between borehole depths and seismic events. First break on each of the traces gives the time-depth records which correspond to the checkshot records. Generally, well data are accurate, often vertical, finely sampled in depth and afford good volume models, analytic functions and deterministic depth conversions (Marsden, 1998).

Velocities from seismic sections are known as 'provelocities' (Etris et al, 2001) because these velocity estimations derived from processing of seismic data. These velocities help in improving the seismic data and provide better imaging. Seismic

data, in terms of accuracy and resolution, depend on spread length, stacking fold, Signal-toNoise ratio, muting, time gate length, velocity sampling, choice ofcoherency measure, true departures from hyperbolic moveout and bandwidth of data. These velocities are regarded as 'soft' and are coarsely sampled in depth but finely sampled horizontally. They provide good horizontal models, deterministic and stochastic depth conversions (Marsden, 1998). Seismic processing velocities present the control needed to extrapolate the velocity field away from the wells (Dheasúna et al, 2012).

Sonic logs and VSPs provide direct measurements of the velocity with which seismic waves travel through the Earth as a function of depth whereas seismic data provide indirect estimate of the velocity. The resolution of the VSP data is higher than the one characteristic ofthe traditional seismic but then lower than the sonic logs. VSPs enable the distinction of subtle features that cannot be defined by surface seismic and better

correlation ofthe well and traditional seismic data. Joint use ofthe various data enables them to overcome the limitations of each of the individual datasets and construct a more reliable model, providing the valuable information about the structure and stratigraphy of the reservoir (Kissinger, n.d). In the absence of borehole velocity surveys, pseudo velocities become quite handy. They are estimates of average velocities calculated from seismic reflection times and measured well depths (Marsden, 1998).

Finally, velocities are determined in the laboratories by measuring the traveltimes of high-frequency (about 1 MHz) acoustic pulses travelling through cylindrical rock specimens. With this mode of velocity determination, the effects of temperature,

confining pressure, pore fluid pressure or composition on velocity may be quantitatively assessed (Keary et al, 2002).

The velocity that can reliably be derived from seismic data is the velocity that gives the best Common Mid-Point (CMP) stack. Assuming a layered media, stacking velocity (the velocity that stacks the CMP gathers) is related to normal moveout (NMO) velocity, VNMO, (the velocity required to best NMO correct the data using the hyperbolic NMO assumption). This, in turn, is related to the root mean square velocity, Vrms, from which the average and interval velocities, Vint, are derived. Vint is a velocity measurement made over the interval between two different depths, times, horizons or reflections. The values ofVrms down to different reflectors are used to compute interval velocities, Vint, via the Dix formula (Dix, 1955). C Hewitt Dix showed that given 'n' horizontal beds, travel times can be related to actual paths taken, using the Vrms.

Generally, where there are n horizontal beds and At is the one-way time through the bed, then:

$$V_{rms}^2 = \frac{\sum_{i=1}^{n} V_i^2 \Delta t_i}{\sum_{i=1}^{n} \Delta t_i} \quad \text{.....1.1}$$

From this equation, Vintis calculated from the Vnns using the Dix equation:

$$V_{\text{int}} = \left[\frac{V_{rms,n}^2 \tau_n - V_{rms,n-1}^2 \tau_{n-1}}{\tau_n - \tau_{n-1}} \right]^{1/2} \quad \text{.....1.2}$$

Where is the one-way travel time.

In the simplest scenario ofhorizontal reflectors in a medium with only vertical velocity inhomogeneity (ID case), the stacking velocity values obtained from

stacking velocity analysis in a CMP gather are sufficient to construct a ID interval velocity model by applying Dix inversion. In laterally inhomogeneous media, the Dix inversion is in such cases, usually, used to obtain a simple initial model which is then updated. Consequently, virtually all velocity model estimation techniques proceed iteratively, either by updating an initial model locally or globally, or by performing layer-stripping (Etris et al, 2001).

The instantaneous velocity, Vinst, is most truly representative of the layered sediments and is what is measured by a sonic log. The interval velocities that are measured over large layer thicknesses are actually averaged instantaneous velocities. Check shot surveys and VSPs furnish us with such averaged interval velocities. The average velocity, Vavg, is the depth divided by the two way time to any interface and is often used_for depth con2gsionAonetheless, it is only valid where the velocity varies only vertically (Marsden, 1998). Instantaneous Velocity, Vinst, is the average velocity at a certain point within a layer or a geological formation. These velocities with which seismic waves travel through the Earth, as a function of depth, can also be obtained from sonic logs and Vertical Seismic Profiling (VSPs) or checkshots.

Generally, names of velocities are derived from how they are measured and will generally not agree with one another due to inherent consistent errors. Integrating all available velocity information into a velocity model increases the accuracy of the model by offsetting the weakness of one data type with the strengths of another. Integrated model building is outstanding due to its ability to integrate all available data into one velocity model. Integration is essential for generating subsurface images that accurately position reflections both horizontally and vertically. (Lorie et al, 2005).

First use of a velocity model has been time-depth conversion of seismic horizons interpreted in regional mapping projects (Dalfen, 2006). Depth conversion methods can be grouped into two major categories: direct time-depth conversion and velocity

modelling for depth conversion. The reliability of either method for depth conversion is in its accuracy at tying existing wells and predicting depths at new well locations.

Depth conversion is a way to reduce structural ambiguity inherent in time and verify structures. Explorationists have to structures to ascertain the presence of a structural trap when planning an exploration well, or to determine the spill point and gross thickness of a prospect to establish volumetrics for economic calculations, or to define unswept structural highs to drill with infill wells to tap attic oil (Etris et al, 2001). Rojano et al (2005) mentioned in their research that the ability to integrate seismic-and well data allows for the creation of high-confidence static and dynamic reservoir models.

Velocity models can be used indirectly through their influence on reflection coefficients and amplitudes for purposes such as the detection of Direct Hydrocarbon Indicators (DHI) (Yilmaz, 1987). An important use in geophysical interpretation is in differentiating between overlapping primary returns from deeper layers and multiple reflections from shallow reflectors on continuous profiling records. The usually higher velocities of deeper strata make it possible to distinguish the two types of returns (Leverette, 1977).

They provide an indication of the lithology of a rock or, in some cases, the nature of the pore fluids contained within it. This is because S-waves will not travel through pore spaces and thus depends only on the matrix grain properties and their texture whereas the P-wave velocity is also influenced by the pore fluids. Hence, if both the P-wave and S-wave velocities of a formation are known, detecting variations in pore fluid becomes possible. This methodology is used to detect gas-filled pore spaces in underground hydrocarbon reservoirs (Kearey et al, 2002).

According to Stanford University (n.d), the relationship between the derived or measured velocities or reflectivities and intrinsic rock properties is needed before seismic survey results can be interpreted quantitatively in terms of lithology. Velocity models for various formations afford an understanding of the variation of velocity in a reservoir, a field or an area. It also provides a medium for converting time structure maps to depth structure maps.

Huge sums of money are invested in drilling wells for appraising, developing and production of reservoirs. Correct depths of formations are of utmost importance for well designing and subsequently the acquisition of appropriate materials such as casing and suitable drilling mud. Thus, resources are maximized and proper and appropriate well-casing programs and cementing practices are ensured.

The need for accurate depths of target formations and over-pressured zones cannot be overemphasized in any petroleum-well drilling operation. These are crucial in any drilling work because appropriate permits and requisite agreements must be sought and signed, with regards to depths oftarget zones and total depths, before actual work can begin. Besides, some companies drill dry holes, desert the area they drilled, only for other companies to drill deeper and encounter hydrocarbons due to better depth conversions. Guilbot et al (2002) points out that reservoir engineers use the results of 4-1) constrained depth conversion to update key parameters of their geomechanical and porosity-log decompaction models. Besides, precise depth conversion is a critical step for creating static and dynamic reservoir models that incorporate seismic attributes and also mandatory for accurate planning of horizontal wells (Rojano et al, 2005).

Blowouts are dangerous and expensive accidents in drilling operations. It is defined as the loss of control over formation pressure which causes an unrestrained flow of

mud, oil, gas, or water at the surface, often accompanied by injury to personnel, loss of hole or equipment, or other appreciable damage. Among other causes, blowouts can easily result when wells encounter over-pressured formations at shallower depths than anticipated from inaccurate depth conversions. Such unfortunate incidents have daunting and calamitous effects on health, safety and environment. Hence, generating representative and reliable velocity models are of immense value in the petroleum industry.

Velocity models can be evaluated numerically, visually, intuitively for reasonableness and also usually employs the use of velocity information from both seismic and wells if available. Thus, it presents a wider scope for critical review and quality control (Etris et al, 2001).

1.2 AREA GEOLOGY

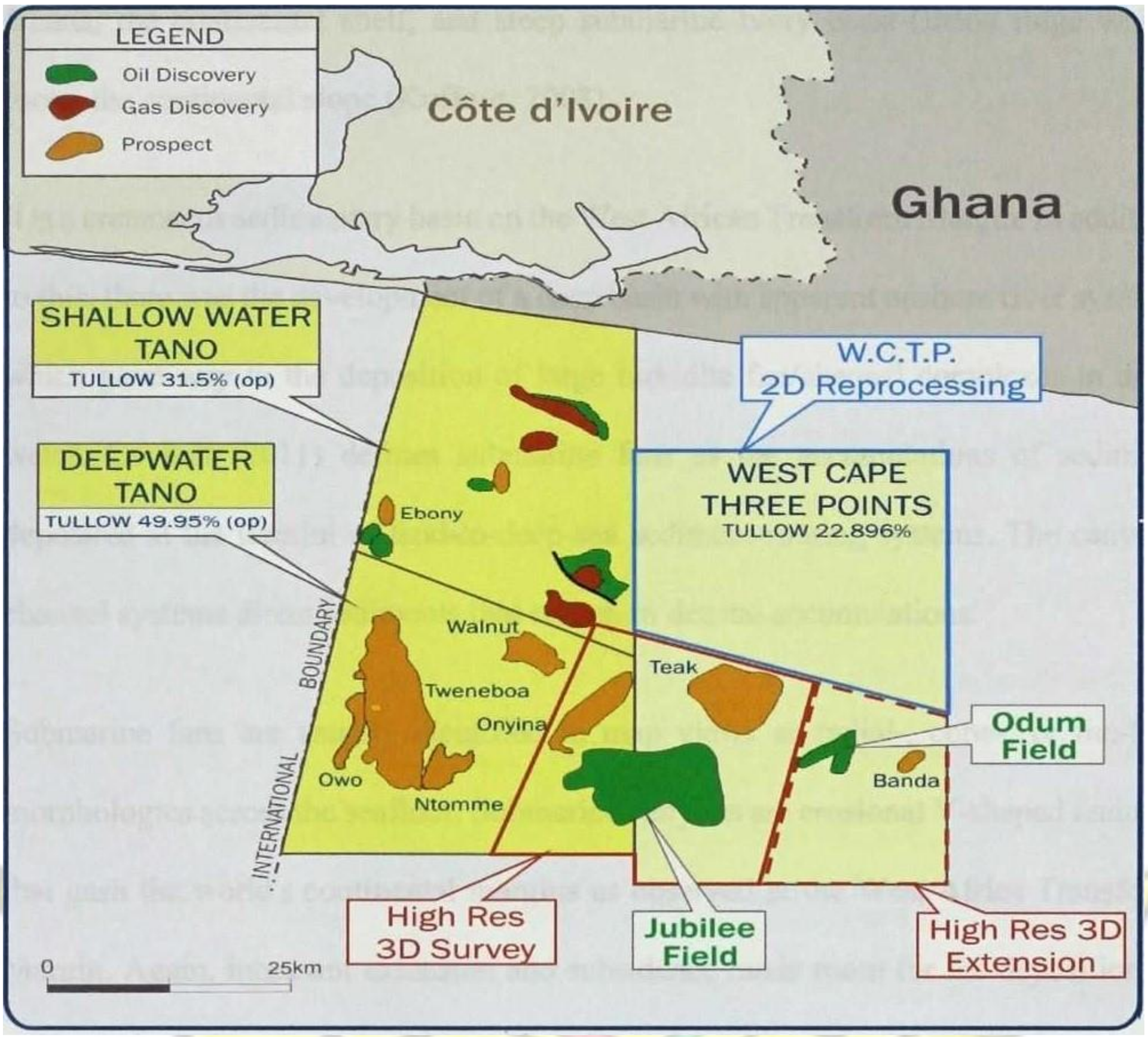

Figure 1.1 : Tano Basin (Kuffuor, 2008)

The Tano Basin (Western Basin, as defined by GNPC), Figure 1 : 1, is within the larger Ghana-Ivory Coast intra-cratonic Basin found in the Gulf of Guinea, West Africa. The location is about 40 46' North latitude and about 30 West longitude. It is an East-West onshore-offshore structural basin. The basin covers an area of 1,165 km2 between the mouths of the Ankobra River to the east, and the Tano River to the west (Atta-Peters et al, 2004) and bounded to the south by the Romanche Fracture Zone and to the north by the St. Paul Fracture Zone. It stretches over an area of at least 3000 square kilometers in offshore and narrow onshore segment of the south-western corner of the Republic of Ghana. It includes the narrow Mesozoic coastal strip of south-

western Ghana, the continental shelf, and steep submarine Ivory coast-Ghana ridge which forms the continental slope (Kuffour, 2008).

It is a cretaceous sedimentary basin on the West African Transform Margin. In addition to this, there was the development of a deep basin with apparent onshore river systems which gave way to the deposition of large turbidite fan/channel complexes in deep water. Covault (2011) defines submarine fans as the accumulations of sediment deposited at the termini of land-to-deep-sea sediment-routing systems. The canyonchannel systems direct sediments that end up in detrital accumulations.

Submarine fans are usually identified in map views as radial-, cone-, or fan-like morphologies across the seafloor. Submarine canyons are erosional V-shaped features that gash the world's continental margins as observed at the West Africa Transform Margin. Again, incessant extension and subsidence made room for the deposition of thick shale and sandstones which formed stratigraphic traps for oil in the margin (Sutherland, 2008).

The overall deepening of the basin after Cenomanian age led to the depositions of many cayon sands —_ng-uHge from Turonian to possibly Lower Palaeocene. Tano Basin, as part of an extensional Rift Basin system, received substantial clastic sediment input from the African continent. These sands are primary slope turbidites, funnelled offshore from the shelf following major erosional events that formed the submarine cayons (Fuller et al, 2009). It has over 4000 m of lower cretaceous shale and sandstone, where thick sandstone formation makes up the hydrocarbon reservoir for three wells, northern part of the Western basin (Kuffour, 2008).

Middle and Upper Albian sedimentation in the Western Basin (Tano) is characterized by shallow marine shelf to shore face sandstones and shales in several depositional units, including newly-named Bonyere, Voltano, and Domini and Tano formations (Kuffour, 2008)

The Deepwater Tano area ofthe Tano basin, Figure 1.2, is the first deepwater field to be developed in offshore Ghana. There are three oil and gas fields which are part of the Deepwater Tano license: Tweneboa, Enyenra (formerly, Owo) and Ntomme. Tweneboa, Enyenra and Ntomme, collectively known as TEN. The TEN Cluster Development consists of three discoveries in the Deepwater Tano Block, Tweneboa, Enyenra, and Ntomme, offshore Ghana in water depths ranging from 1,000 to 2,000 meters. Partners in the block include Tullow Oil plc (49.95 percent working interest and operator), Kosmos Energy (18 percent working interest), Anadarko (18 percent) Sabre Oil & Gas Holdings Ltd (4.05 percent working interest) and the Ghana National Petroleum Corporation (10 percent carried interest) (http://www.subseaiq.com/datanroject.aspx?project id=1038&AspxAutoDetectCookieSupport=1, May 10, 2013).

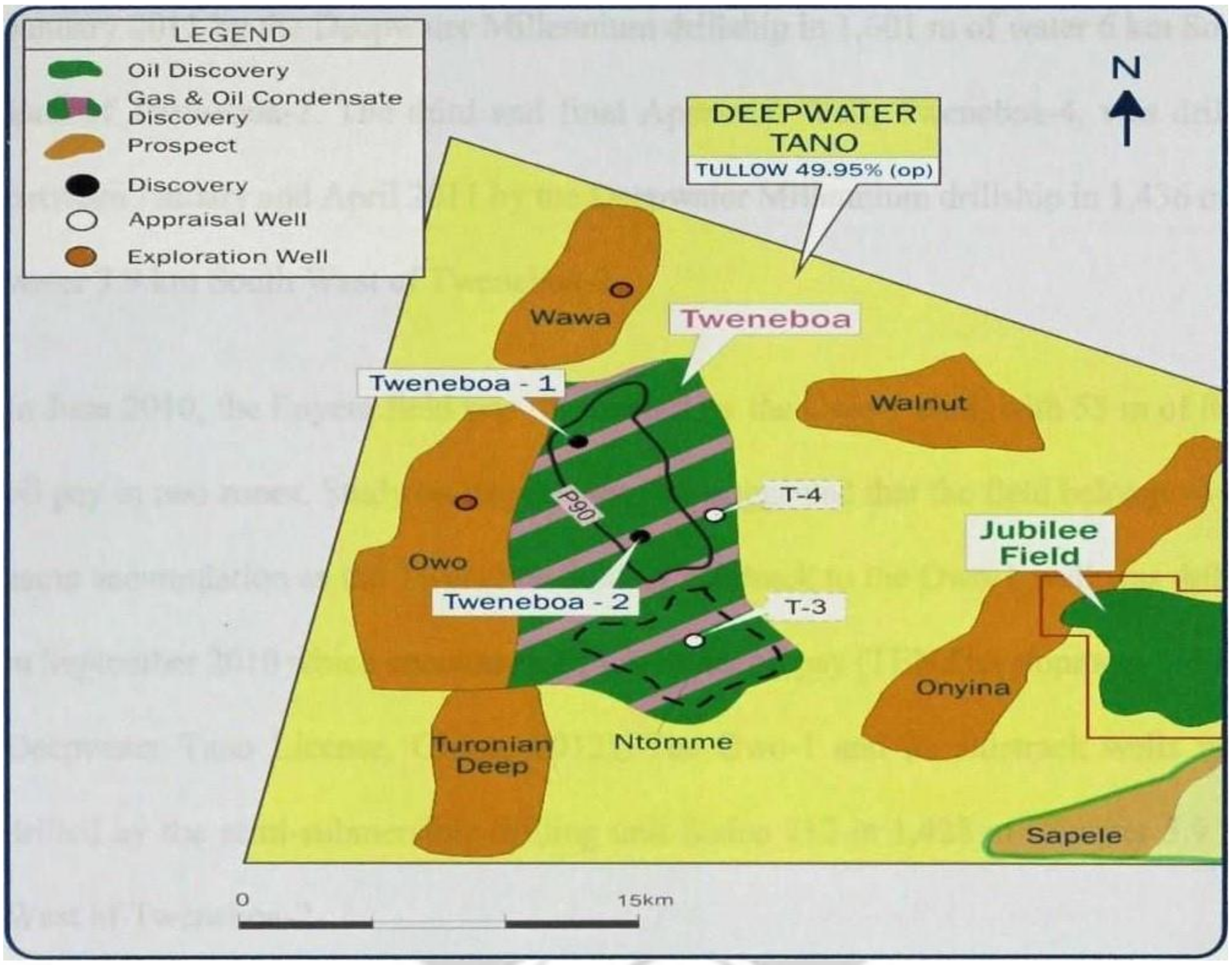

Figure 1.2: Tano basin showing the Deepwater Tano area (2010 Capital Markets Event -Ghana, Tullow)

Discovery of the Tweneboa field was made by Tweneboa-l well in March, 2009 with 21 m of net pay and 4 m of oil-bearing sand on the edge of a giant 200 sq km fan system related to the Jubilee play. In addition, it encounted a 4 m over-pressured oilbearing sand and an over-pressured zone at total depth (Tullow Oil Ghana, 2012). Tweneboa-l well was drilled by the semi-submersible drilling unit Erik Raude in 1, 149

m of water some 25 km North West of Hyedua-l in the Jubilee Field. The Appraisal Programme required the drilling of three Appraisal Wells: Tweneboa-2, Tweneboa-3 (3ST) and Tweneboa-4.

Tweneboa-2, was drilled 6 km South East of Tweneboa-l between December 2009 and February 2010 by the semi-submersible Atwood Hunter in 1,321 m of water. Appraisal Wells Tweneboa-3 and 3ST were drilled between November 2010 and January 2011 by the Deepwater Millennium drillship in 1,601 m of water 6 km South East of

Tweneboa-2. The third and final Appraisal Well, Tweneboa-4, was drilled between January and April 2011 by the Deepwater Millennium drillship in 1,436 m of water 3.9 km South West of Tweneboa-2.

In June 2010, the Enyera field was discovered by the Owo-l well, with 53 m of light oil pay in two zones. Study on its pressure data suggested that the field belongs to the same accumulation as the Tweneboa field. A sidetrack to the Owo-l well was drilled in September 2010 which encountered 16 m ofnet oil pay (TEN Development Project, Deepwater Tano License, Ghana, 2012). The Owo-l and its sidetrack wells were drilled by the semi-submersible drilling unit Sedco 712 in 1,428 m of water 5.9 km West of Tweneboa-2.

Appraisal Well Enyenra-2A was drilled between January and March 2011 by the Deepwater Millennium drillship in 1,673 m ofwater 7 km South South-East of Owo1 & Owo-l ST. The well was designed to test the South-Central part of the Enyenra channel system. Appraisal Well Enyenra-3A was drilled between April and September 2011 by the Deepwater Millennium drillship in 1,103 m of water 6.5 km north of Owo1 & Owy-1ST. The well was designed to test the Northern extent of the Enyenra

Discovery. Appraisal Well Enyenra-4A was drilled between January and March 2012 by the Olympia drillship in 1,877 m of water 7 km South West of Enyenra-2A. The well was designed to test the downdip southerly extent of the Enyenra oil Discovery.

The Ntomme Discovery was made by Tweneboa Discovery Appraisal Well Tweneboa-3 and its geological sidetrack Tweneboa-3ST 650 m to the West. Appraisal Well Ntomme-2A was drilled 4.3 km South of Tweneboa-3ST between November

2011 and March 2012 by the Olympia drillship in 1,730 m of water.

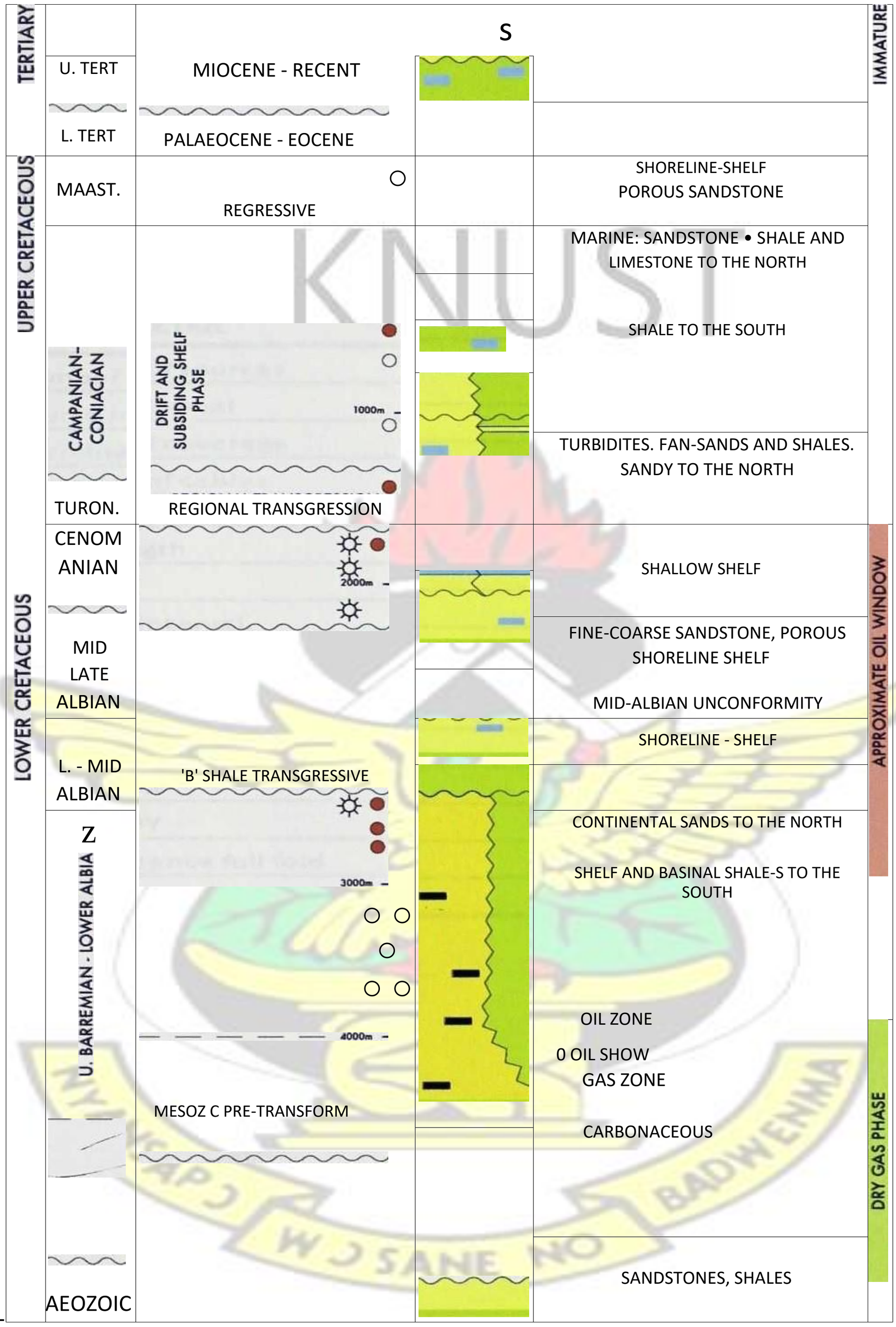

Figure 1.3: Generalized Stratigraphy of the South Tano (Ghana-Tano-BasinPresentationAGM)

A Deepwater Tano 3D seismic survey, acquired by Dana Petroleum in 1995 and reprocessed (pre-stack migration in

2007) was used in this study. The acquisition was done by CGGVeritas in 2000. The acquisition parameters are given in table 1.4.

Table 2.1 Acquisition Parameters

PARAMETER	FIGURE
Num ber Of s our-ces	2
Source interval	50.00 m
Nor-mina l coverage	51 m
Number Of ca bles	6
Cable interval	100
Cable length	5100
Trace length	12.50 m
CDP line	6.25 m
CDP line interval	1007
Distance between sail lines	300 m
Bin size DX	6.25 m
Bin size DY	25 m
Total Distance full fold	4551.4 km
Number of sail lines	109

1.3 PROBLEM STATEMENT

The present development targets in the petroleum industry in Ghana require detailed information about the subsurface. With the large amount of seismic and log data that has been acquired in the Tano basin, an aerial velocity model for the Deepwater Tano of that part ofthe basin is key to understanding the vertical and horizontal variation of velocities of the reservoirs and their depths of occurrences.

The Deepwater Tano has its seabed characterized by canyons and it is also known to have fans, including the campanian fans, within the subsurface. These phenomena have significant effects on the velocity and subsequent depths estimates.

1.4 OBJECTIVES OF RESEARCH

The area under investigation has both 3D data and well logs. The major objectives of the study are:

a) To image the subsurface of Deepwater Tano area by building an interval macrovelocity model that would appropriately convert seismic time data to depths.

b) To investigate the effects the campanian fans on these velocity models.

1.5 JUSTIFICATION OF THE OBJECTIVES

When dealing with complex geology, the conventional seismic imaging approaches may fail and result in non-negligible errors in the interpretation and construction ofthe geological models. Wrong estimation of depths is one ofthe common reasons for the failure of explorative wells incurring avoidable costs and jeopardizing Health, Safety and Environment (HS&E). This works seeks to build an interval macrovelocity model that most appropriately converts seismic time data sets to seismic depth data sets in the Deepwater Tano area.

CHAPTER 2: LITERATURE REVIEW

The variation of seismic velocity with depth is a fundamental aspect of seismic work (Al-Chalabi, 1997) and various kinds of velocity models are desired for different purposes such as stacking, migration and depth conversion. When velocity modelling is done as channel for time-depth conversion, the aim is to construct a representative model that accurately predicts true vertical velocity at and between wells and beyond (Etris et al, 2001).

Given the number of velocities that can be used in the development of models for the conversion of time data to depths, the choice of velocity and procedure used for the modelling is largely determined by available data, lithology of the area of study and parameters employed in the geophysical acquisition and processing. Whether using direct mapping from time to depth or migrating original data with a prestack depth migration algorithm to mitigate structural errors, it is required to convert time migration velocity to a velocity model in depth (Cameron et al, 2006). Although the principal objective in determining velocities is to allow an accurate structural

interpretation to be made from seismic reflection data, an important secondary objective is to get so—ithelogical information (Dix, 1955).

Since 1930 several analytic expressions had been developed to describe the variation of seismic velocity with depth (Al-Chalabi, 1997). After analysing data from some 500 seismic well surveys in the United States and Canada, Larry Faust plotted velocities of sand and shale series of different stratigraphic ages against depth on log/log axes for various stratigraphic units. He then concluded that a relationship exists of the form:

$$V_{\text{int}} = \alpha(ZT)^{1/6} \quad \text{.....2.1,}$$

Where Vint is the interval velocity connected with mean velocity by Vint = 6/5 (Vmean), a is a constant (125.3 for velocity in feet/s and Z in feet; 46 for velocity in m/s and Z in m), Z is the depth and T is the geologic age of the stratum at depth Z (Süss et al, 2003). These relations describe the primary influence of depth on seismic velocity but has the limitations of being generally ineffective for layers near the surface (<1000 m) where compaction gradients are high. Also, it is unable to describe lateral velocity variations that may result from sedimentary facies changes or other processes and empirical relations derived in one basin may not be applicable to other basins with different compositions or geologic histories (Cordier, 1985). Some of the challenges are sorted by adapting Faust's exponent, 1/6, in the formula, and/or adjusting a. The exponent was assumed to reflect the compaction-related behaviour of the rock and a was understood to relate to the sand/shale ratio (Süss et al, 2003).

Hudson's study (as cited by Uduanochie, 2011) indicates that the physical properties of the rocks in the earth are effectively and accurately estimated using the PP-wave seismic reflection technique. Also the extent of mineral and natural reservoirs in the earth and the geological structures that contain them can now be predicted, inferred and their position estimated-with some accuracy. Velocity analysis combines the

mathematical laws that describe seismic wave propagation and the sensitivity of imaging to velocity (Andreoletti, 2012). Three techniques of velocity analysis are widely used: velocity semblance analysis, prestack depth migration, and seismic tomography.

Velocity semblance analysis is based on flattening of events in common midpoint gathers and it is used to determine stacking velocities to enable velocity estimations for areas where the structure is simple (Yilmaz, 1987). Prestack depth migration is an effective method for determining velocities because of the sensitivity of the migrated image to the velocity model (Kissinger, n.d). Both the semblance and the migration velocity analyses are "local" methods of velocity determination. Seismic tomography provides a sliced picture of the velocity distribution in the Earth and combines geologic property estimation and imaging into one concept. While other approaches separate velocity model building from imaging, traveltime tomography determines both interval velocities and reflection interfaces (Kissinger, n.d).

Andreoletti et al (2012) built a velocity model by Migration Velocity Analysis (MVA) using hard data from wells and structural information from images as constraints. The methodology is so called because of the continuous interplay between migration and velocity analysis, where one depends on the other. Simulated reflection traveltimes in a model via ray tracing were matched with observed traveltimes then the velocity model was derived by solving a non-linear optimization problem that updated velocity according to traveltime misfit until the misfit itselfwas minimized. The match between the estimated velocity and sonic log, jointly with traveltime match, imaging quality and fault focusing, generated a three-layer anisotropic model which honoured all the information coming from the well (sonic log and markers) and also produced the best

imaging.

Marsden (1989) used and analyzed the use of layer cake velocity model for depth conversion. The simplest method of this technique is to attend to separate lithologic units and define each by different mathematical function. He indicated that this method of depth conversion breaks down in areas of complex structure, tectonic inversion or lateral lithology change where insufficient well control exists to adequately define the velocity variations in the different lithologic units by mathematical functions. The simplest functions of all assume that each lithologic unit has a constant but different interval velocity.

He derived functions for the layers by plotting two-way traveltime (obtainable from the integrated sonic log, check shot, or VSP) against the isopach, depth thickness, for a number of wells in the mapping area and then fitted a regression line to the data points. Masden indicated that these empirical functions often work well within a restricted area yet have proved not to be theoretically exact. The scatter of data points about the regression lines, caused by geologic factors such as varying lithology, pressure regimes, and tectonic history, leads to errors in the depth conversion.

Dalfsen et al (2006) also generated a velocity model based on lithostratigraphic layers in Netherlands. The model was based on the Vint-Zmid method applied to the layers. At borehole locations, Vo was calibrated such that traveltime through the layer according to the linear velocity model equalled the traveltime according to the borehole data. A kriging procedure was applied to the calibrated vo(x, y)-values resulting in an estimated Vo-value at any other location. The model Vo-values were determined on an areal grid with cells of 1 km x 1 km.

In Canyon-ãõóVGulf of Mexico, velocity models were built for deepwater area by Uduanochie (2011) using 4C-3D ocean-bottom seismic data from that region. He employed ray-tracing and anisotropic velocity model-building techniques. The research estimated shallow Vp and Vs in the range of 1560 ms-I and 147 ms-I,

respectively with Vp/Vs values of 10 in the shallow areas and VpNs values of 4 above the salt body and for anisotropy equations. The estimated velocities, he asserted, focused the data better after being compared with mudline and estimated velocities from surrounding wells in the region.

Regional velocity models can also be used in the area of earthquake hazard assessment including the processing of seismic reflection profiles, precise earthquake relocations and forward modelling of wave propagation for strong ground motion predictions as was undertaken by Süss et al (2003). By constructing triangulated surfaces consisting of topography, bathymetry and the top of basement, a three-dimensional (3-1)) volumetric description of the basin sediments was generated. Within these enveloping surfaces, three topologic regular grids, representing the models of different resolution, were used to interpolate the velocity structure.

When an optimum velocity model for depth conversions in regional studies is being derived from stacking and imaging velocities, careful integration of the depth information provided by wells, and in particular, check shot data is needed (Dheasúna et al, 2012). In the report of Dheasúna et al (2012), Aker Geo and Searcher Seismic collaborated to generate a regionally consistent velocity model (hiQbeTM) for depth conversion in the Carnarvon, offshore Canning, and Browse basins of the Northwest Shelf.

Due to-ševere disto •on of wavefronts or scattering of energies by complexly shaped ____salt bodies, seismic imaging of hydrocarbon accumulations below salt has proven to be a challenge. Wang et al (2008) highlighted some advances in building a velocity model for subsalt imaging. Their study enumerated three main stages in velocity model building: suprasalt velocity determination, salt-model definition and subsalt velocity update. Incorporating volumetric high-resolution tomography and high-

velocity contrast boundaries a good sediment velocity model was built before building the salt model for the Gulfof Mexico.

Higginbotham et al (2010) presented a wave equation velocity update scheme making use of the time-shift imaging condition. The approach was robust under salt and in a land fault shadow example with limited acquisition effort. Nonetheless, wave equation migration is criticized for its difficulty in efficiently obtaining 3D angle gathers (incidence, azimuth, and dip angle).

Rojano et al (2005) introduced an iterative approach to building their velocity-model which accommodated the problematic nature of integrating seismic and well data in mature fields. Using the Poza Rica Field, a giant oil and gas field in Veracruz, México, as the research area, they propose an initial creation of velocity model by combining seismic velocities and checkshots, followed by calibration interpreted seismic horizons with the equivalent well tops and then the smoothening of the model over twice the nominal well spacing, introducing geologic consistency to the model. Recalibration is done on the smoothed model with the well tops and depth errors between the two are used to flag problematic wells or seismic data. They asserted that these iterations, which involves the confirmation of well positions and seismic interpretations reevaluation, are ntended to reduce the sources oferrors associated with mature fields

such as incorrect well postings or inconsistencies in the interpreted tops.

In areas characterized by dramatic changes of velocity resulting from thick carbonate or evaporate units alternating with thick elastic units, complex structures, tectonic inversions or lateral lithology change, Alaminiokuma et al (2010) suggests that the layer cake model which deals each lithologic init separately and defines unit by a different mathematical function may be appropriate for depth conversion. Their study

essentially derived top interface velocity, Vo, compaction factor, k and a velocity function useful for predicting lateral and vertical velocity structure of the deep subsurface and converting time-to-depth section in the Niger Delta.

Olabode et al (2008) analysed seismic time-depth conversion using geostatisticallyderived average Velocities over "Labod" Field, Niger Delta, Nigeria. Geostatistics, they referenced as the application of statistical estimation techniques to spatially correlate random variables for geological and geophysical applications. The research justified this methodology saying that since a unique velocity solution is presumed inadequate, a probabilistic model ofthe velocity stood to be realistic. The geostatistical techniques employed were variogram analysis, Regression and Kriging. These were used to generate average velocity maps that were used for time-depth conversion.

After conversion of data in the time domain to depth via a velocity model, it is quite tempting to use the same model to convert it back to the time domain in the situation where additional processing and interpretation needs to be done. The lack of smoothness which is inherent in time migrated velocity field but not in depth migrated data thepþecomes a challenge. Jones (2009) brings to bear the inappropriateness of

using tune-to-depth velocity model for depth-to-time conversions and showed in his _——tutorial the subtle difference between the two methodologies.

This research seeks to build an interval macrovelocity model that integrates velocities from checkshot data and the geology of the Deepwater Tano area to convert seismic time data to depths.

CHAPTER 3: METHODOLOGY

Time to depth conversion is about building a model of the seismic velocities that incorporates velocity information (e.g. from existing wells) and makes predictions about the rock velocities away from well control. A representative interval velocity model should tie well control and honour structural trends of the seismic data. For depth conversions from checkshots, depths need to be expressed as a function of reflection time, z=f(t) (Marsden, 1998).

Eight wells were used as constraints for the study from the Deepwater Tano area. Checkshot data and formation tops of the following wells were provided:

- Enyera 2A
- Enyera 4A
- Ntomme 2A
- Ntomme
- Tweneboa 1
- Tweneboa 2
- Tweneboa 3ST1
- Tweneboa 4A

The intervalVelocity-mOðêTÇóbuilt from checkshots and seismic sections for the identified lithostratigraphic layers between the Tertiary and just above the Cenomanian within the late Cretaceous. The checkshots and formation tops were loaded in Seismic Micro Technology (SMT) and using their time-depth graphs, T-D charts, the two-way traveltimes were estimated for the depths of formation tops.

Using Microsoft Excel, the interval velocities of the formations were calculated with equation 3.1 and assigned to calculated middle depths of the layers, equation 3.2:

$$V_{int} = \frac{(Z_b - z_t)}{A_t} \quad \text{.. ....(3.1)}$$

$$- \frac{(Z_t + Z_b)}{2} \quad \text{.....} \quad (3.2)$$

where At is the one-way isochron, Zt and Zb are, respectively, the depths of the top and bottom of the formation from checkshot data.

Crossplots of Vint against Zmid were plotted to get the parameters, Vo , a constant and K, indicating the rate of change of velocity with respect to depth, Figures 4.2, 4.4 and 4.7. Any scatter in the crossplot indicates variations in the key factors which control seismic velocity in rocks-lithology, pressure, fluid content and depth of burial (Masden, 1992). These functions are fit separately for each layer to ensure geological consistency and usually employ the simplest model that fits the data well (Etris et al, 2001).

The lithostratigraphic layers were put into four main groups for the depth conversion:

- Layer 1: Seabed - Miocene Unconformity, Seabed Group (SB).
- Layer 2: Miocene Unconformity — Upper Campanian, Miocene Unconformity Group (MU).
- Layer 3: Upper Campanian — Turonian, Campanian Group (CAM).
- Layer 4: Turonian — Total Depth of well, Turonian Group (TUR).

With the exception of Tweneboa 1 , all the wells had information ofthe grouped layers. The Miocene Unconformity was not present (identified) at Tweneboa 1 well location.

Table 3.1 : Showing the lithology of the grouped formations at the various wells

FORMATION TOPS	ENYERA 2A	ENYERA 4A	NTOMME (TWENEBOA 3)	NTOMME 2A	TWENEBOA 2A	TWENEBOA-3ST1	TWENEBOA 4A
MU	Claystone with minor sands	Claystones with occational sandstone beds	Claystone with occasional sandstone interbeds	Claystone with occasional sandstone beds	Claystone with minor sands	Claystone with occasional sandstone interbeds	Claystone with occasional sandstone interbeds
CAMI	Clay/ silts/ sand	Claystones with ,Minor thin sanstones, (sandstones, some massive, sand/shale interbeds)	Sandstone massive of interbedded with claystone	Sandstone, some massive, sand/shale interbeds	Claystone/sandstone/minor	Sandstone massive of interbedded with claystone	Sandstone massive of interbedded with claystone
TUR	Sands/ shales	Sandstones, some massive, sand/shale interbeds (thin sand shale interbeds)	Thick sandstone/occassional claystone interbeds	Sandstone, some massive, sand/shale interbeds	Thick sandstone/ claystone interbeds	Thick sandstone occassional claystone interbeds	Thick sandstone occassional claystone interbeds

The Campanian group has fans: Upper and Lower Campanian fans. The upper Campanian fan is encountered as the top of the Campanian group at the Enyera wells and Ntomme 2A well. The top of the Turonian fan was generally picked for the Turonian Group.

3.1 STEP VELOCITY MODEL

Constant interval velocity (CIV) is the simplest multilayer velocity model. Each layer of the model is represented by one velocity:

$V_{i,m} = V_{0,m}$ ....(3.3)

The velocity model used is of the layer cake type: seismic velocity is modelled according to lithostratigraphic layer and hence the horizons are useful to represent subsurface structure. Each horizon marks, in the time domain, a surface at which the acoustic impedance of the rock (solids and fluids) above is assumed to contrast that of the rock below (TNO, 2007).

Step plots were dravm for the grouped formation tops to give impressions of how the velocities varied vertically down the stratigraphy at the well locations. Using equation 3.2, interval velocities of the grouped formation tops were calculated in Microsoft Excel and assigned to the depth ofthe tops for each of the given wells.

The data was then loaded in Grapher 8 software and step plots of depths of formation tops against interval velocities were plotted. This was done for each well and then wells from the same discoveries. Finally all the wells were placed on one plot for comparison, Tables 4.3-4.6. These represented vertical I-Dimensional interval velocity models through the subsurface for each of the wells. Each of these plots represents a constant interval velocity (CIV) model. This type of modelling has the advantage ofaccounting for rapidly changing bed thicknesses ofcontrasting velocities.

When all the I-Dimensional modelled well interval velocities are put on the same graph, they present a spatially variable average velocity model for the formations (Grouped layers). Nonetheless, it falls short in not being able to account for velocity variations within a layer or bed (Marsden, 1998).

3.2 MAPPED INTERVAL VELOCITY

Seismic interpretation was carried out on the seismic sections to generate seismic time maps. These were achieved using formation tops from wells as markers to pick the Seabed, Miocene Unconformity, Top Upper Campanian (Fan) and the Top Turonian (Fan) on seismic time data. These were gridded and contoured to produce two-waytime maps, Figure 4.10. Geostatistical technique, regression, was used to produce interval velocity maps which were used for the time-depth conversion.

A 664.611 square kilometer area within the Tano Shallow and Deep Water 3D merged, Tullow reprocessed 16FSIA107TTPWCGG survey was considered for the research.

The area of interest has the coordinates, in meters, A (477929.9, 522469.7), B (504309.2, 517865.0), C

(499789.1, 493384.8) and D (473500.8, 498171.5). one hundred and two (102) seismic reflection lines (53 inlines and 49 crosslines) within the area were used for the study.

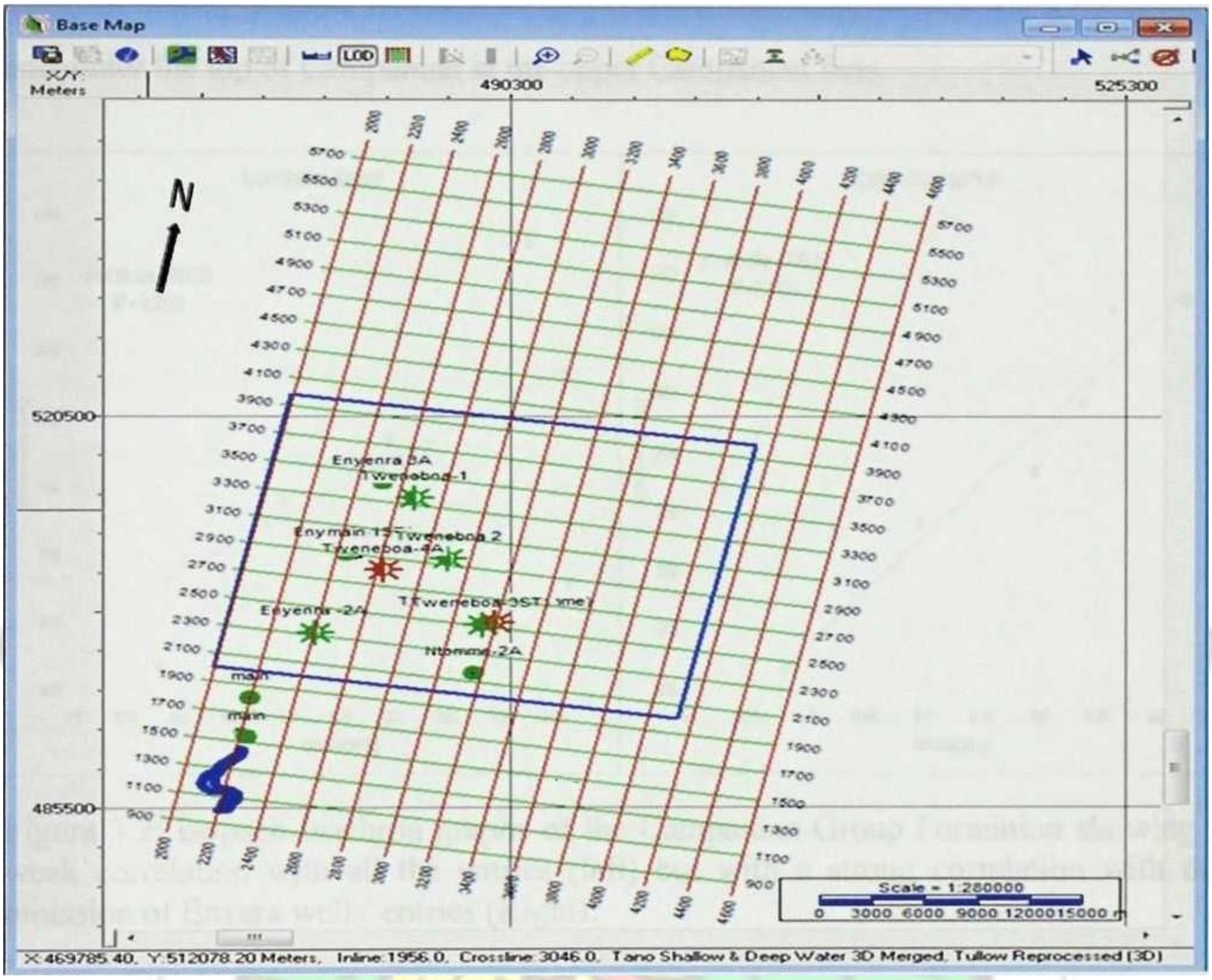

Figure 3.1: Showing survey area and study area (in deep blue outline). Displaying every huríúedth Line (red) and ssline (green)

——-Trom the well data, depth thicknesses (Isopachs) and time thicknesses (isochrons), for the grouped layers were computed, Table 4.1. The Isopach-lsochron pairs for each were grouped according to-layers and then each layer had the Isopachs plotted against the Isochrons, Table 4.2. The slopes of the graphs indicated by the linear least

squares trendline fit to the pairs gave the average interval velocity of the layer:

$$\frac{Z_2 - Z_1}{t_2 - t_1} = V_{int} \quad (3.4)$$

All but the Campanian group gave a strong correlation of above 0.9, Figure 4.7. Isopach-lsochron entries for the Enyera 2A and Enyera 4A had to be omitted to attain a strong correlation of 0.9523 as against 0.2152. This is because the Enyera wells encounter the top of Campanian at the upper Campanian fans.

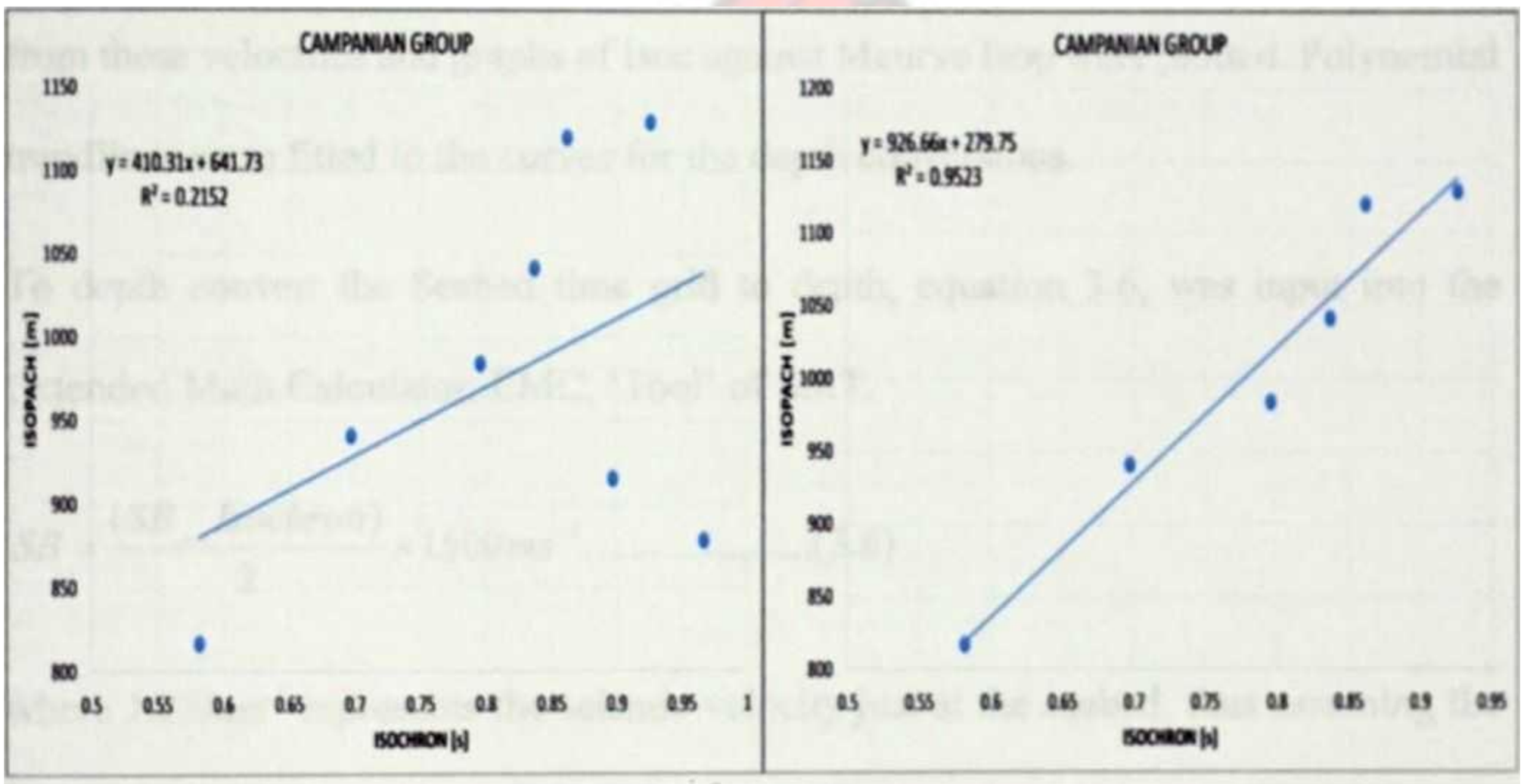

Figure 3.2: Isopach-lsochron graphs of the Campanian Group Formation showing a weak correlation with all the entries (left) but with a strong correlation with the omission of Enyera wells' entries (Right).

From equation (3.4), for very thin layers, giving very short traveltimes, the velocities become infinitely large and must be corrected so that when the traveltime goes to zero, -——The interval velocity would also go to zero. To do this, isochron (iscx) values were generated for the layers starting from zero seconds. Then, using each layer's linear least square trendline fit equation from Figure 4.7 graphs; corresponding were calculated from the isochrons. The Apparent interval velocities, Appar St., of these generated isopach-isochron were then using equation 3.5.

d isopach

.....(3.5) t

isochron

Consequently, this forced the velocity to be zero at zero isochron values, Table 4.3. In spite ofthis, a few Appar Vint were more than 6000ms-l, the maximum seismic velocity for sedimentary rocks (Keary and brooks, 2002). Thus Appar Vint was kept below 6000ms-l , Table 4.3. From this stage, isopach values, Mcurve Isop, were calculated from these velocities and graphs of Isoc against Mcurve Isop were plotted. Polynomial trendlines were fitted to the curves for the depth conversions.

To depth convert the Seabed time grid to depth, equation 3.6, was input into the Extended Math Calculator, EMC, 'Tool' of SMT.

(SB Isochron)

x 1500ms-..... .(3.6)

2

where 1500ms-l represents the seismic velocity just at the seabed, thus assuming the seismic velocity in water. The Depth-converted Seabed grid was contoured, Figure 4.9.

The EMC was used to calculate Isochron grids between Seabed and Miocene Unconformity, Miocene Unconformity and Top Upper Campanian and then finally the Top Upper Campanian and the Turonian groups. Corresponding Isopach grids were generated using the polynomial trendlines equations from the Isoc-Mcurve Isop graphs by inputting them into EMC. Again, using the EMC, the Isopach grids were divided by their Isochron grids to obtain interval velocity models for the intervals between the grouped formation tops, Figures 4.1 la, 4.12a and 4.13a.

Lastly, equation (3.7) was used to convert the time grids ofthe MU, CAMP and TUR to depths by inputting into EMC, Figure 3.3.

$$Di = Di\_l + x\ Isochron \quad \ldots\ldots\ldots\ldots\ldots\ldots\ldots (3.7)$$

This generated depth grids that were contoured, Figures 4.11b, 4.12b and 4.13b.

N.B: the Isochron is not divided by 2 because in equation 3.5, Vint, the isochron is in TWT, thus, these appropriately cancels out to get the right depths. The output of the models were compared with the given well formation tops, Table 4.4.

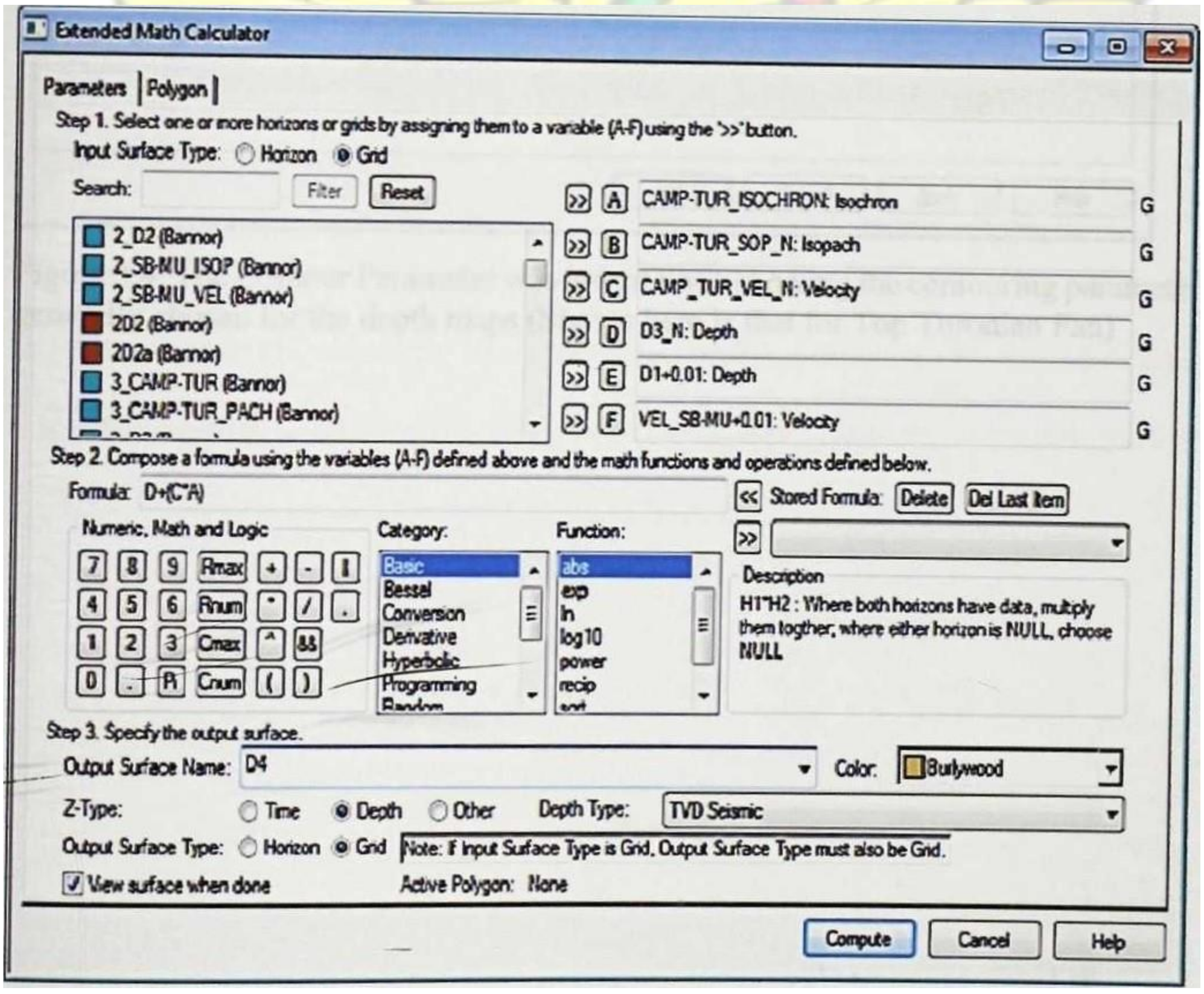

Figure 3.3: External Math Calculator window showing the calculation of D4, Top Turonian (Fan):

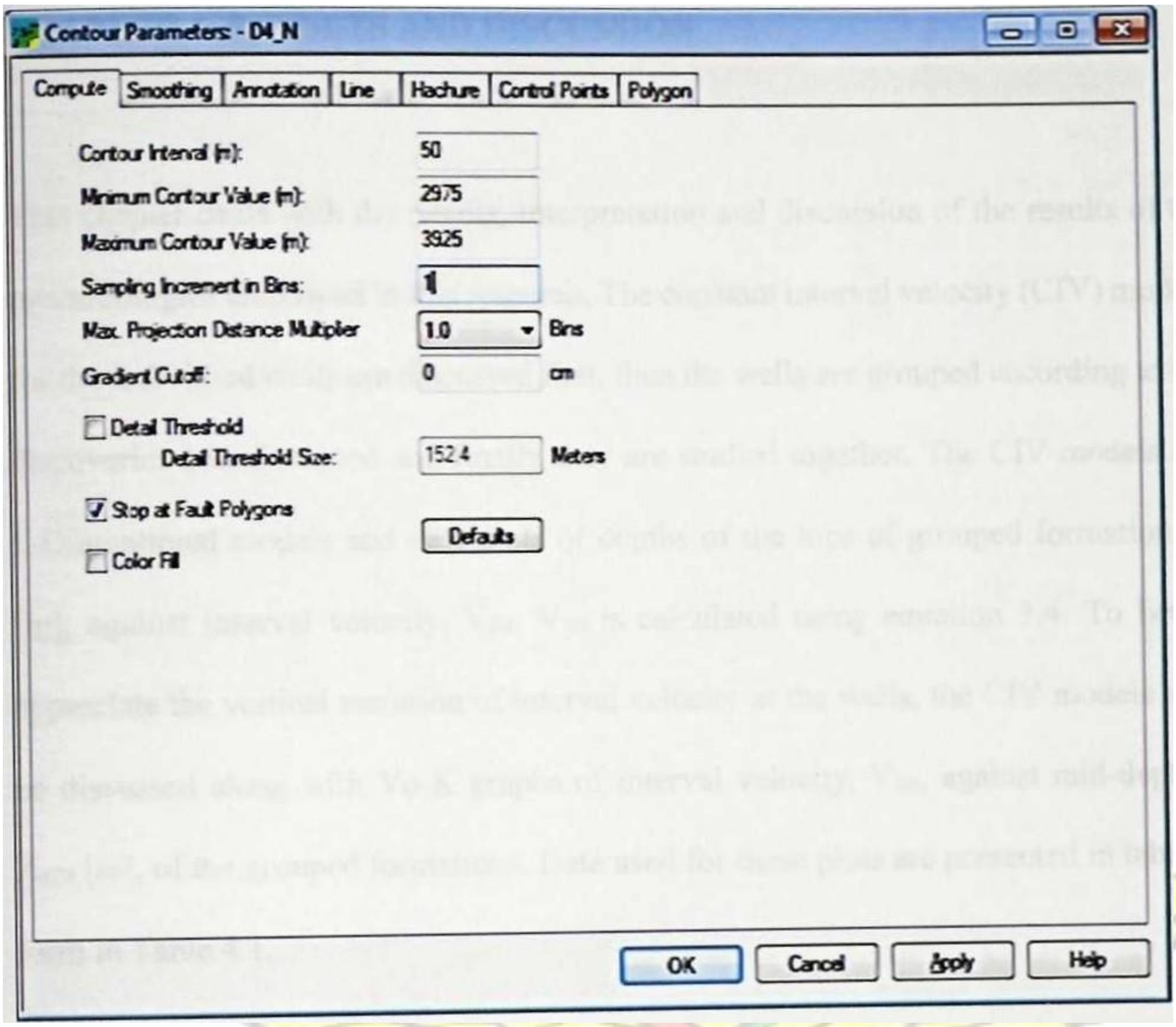

Figure 3.4: The Contour Parameter window ofSMT showing the contouring parameter generally chosen for the depth maps (Shown here is that for Top Turonian Fan)

CHAPTER 4: RESULTS AND DISCUSSION

This chapter deals with the results, interpretation and discussion of the results of the methodologies employed in this research. The constant interval velocity (CIV) models for the individual wells are discussed first, then the wells are grouped according to the discoveries and discussed and finally they are studied together. The

CIV models are I-Dimentional models and step plots of depths of the tops of grouped formation, Z [m], against Interval velocity, Vint. Vint is calculated using equation 3.4. To better appreciate the vertical variation of interval velocity at the wells, the CIV models will be discussed along with Vo-K graphs of interval velocity, Vim, against mid-depths, Zmid [m], ofthe grouped formations. Data used for these plots are presented in tabular form in Table 4.1.

Results for Mapped Interval Velocity (MIV) models used for depth conversions are then presented and discussed. Depth-converted surfaces are also presented and their viabilities are discussed compared to well formation tops. Thus, the appropriateness of the built interval velocities for the study area is ascertained.

Table 4.1 : Showing depths of formation tops, one-way-time and calculated interval velocities at various wells for the grouped formations.

			NTOMME (TWENEBOA 3ST1)	
	Z [m] Zmid [m] INTERVAL VELOCITY [m/s	Z [m] Zmid [m] INTERVAL VELOCITY [m/s	Z [m] Zmid [m] INTERVAL VELOCITY [m/s	Z [m] Zmid [m] INTERVAL VELOCITY [m/s
	lam 171B	215750		
	BR.m	2413.1	n.97	22m
CAM	18110			

		TWREBU2		
	11m] Zridlml lNTEWAIVROOTYlm1sl	Z[ml Zmid [m] INTERVAL VELOCITY [m/s	Z [m] Zmid [m] INTERVAL VELOCITY [m/s	Z [m] Zmid [m] INTERVAL VELOCITY [m/s
	1)7.75			
		3135	028	

4.1 CONSTANT INTERVAL VELOCITY MODELS

4.1.1 Enyera Wells

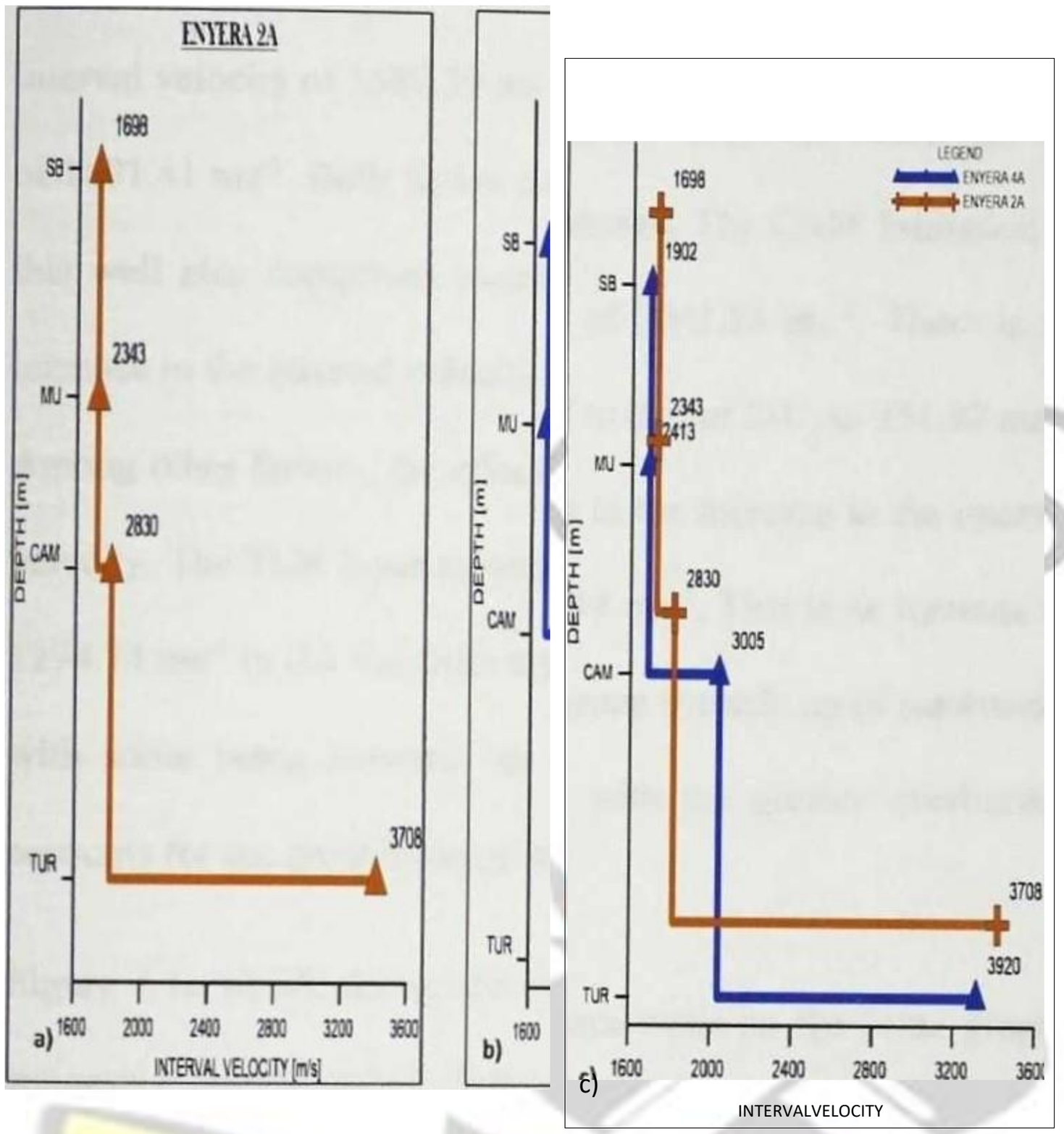

Figure 4.1 : 1 -Dimensional Interval Velocity models For Wells in the Enyera Discovery within Deepwater Tano Area

The CIV model of Enyera 2A, Figure 4.1 a, shows that the well encounters about 1698 m ofwaterup to the seabed. The interval velocity does not vary much between the SB

and MU groups. SB group has a slightly greater Vint value of 1728.53 ms-I relative to ——that of MU which is 1728.48 ms-I Both layers are predominantly made ofclaystones. The CAM group which is made up of sands/shale/silts indicates an increament in the Vint of 1816.60 ms-I. The TUR group shows an increase in Vint of 1690.45 ms-I from that ofthe CAM group. The TUR group ofthe well comprises mainly sands and shales.

The Enyera-4A well is located approximately 7 kilometers south of the Enyenra-2A well. The CIV model of Enyera 4A, located further south of Enyera 2A, encounters the seabed at a depth of 1902 m. Its MU group lies at a depth of 2120 m with a lower interval velocity of 1689.39 ms-I relative to the overburden, SB group, which has Vint of 1691.41 ms-I . Both layers are mainly made of claystones. The CAM formation at this well also comprises mainly claystones with Vint of 2041.26 ms-I. There is an increase in the interval velocity of the CAM, compared to that of MU, to 351.87 ms-I . Among other factors, the effect of overburden features in the increase in the interval velocity. The TUR layer records a higher Vint of 3316.14 ms-I. That is an increase of 1274.74 ms-I in the Vint from that of CAM. The TUR group is made up of sandstones with some being massive. Its composition, together with the greater overburden accounts for the great increase in interval velocity.

Figure 4. lc which shows the CIV models of the Enyera wells on the same graphs suggests a sloping seabed along the Enyera discovery. For both wells, interval velocity for MU is greater than that of SB signifying some consistency between them. Comparatively, for both the SB and MU formations, Enyera 2A records higher Vint even though they lie at shallower depths to those of the Enyera 4A. This is not so for CAM where there is a wide differe e in the interval velocity ofabout 200 ms-I, Figure 4.1c, with Enyera 2A having a lower Vint of 1816.60 ms-I relative to that of Enyera 4A, 2041.26 ms-I. This lateral difference is due to greater overburden at Enyera 4A since it lies deeper than it is in Enyera 2A. Increased overburden results in greater compaction and hence higher interval velocity.

The difference may, as well, be attributed to the lithological composition of the Campanian group at the separate well locations. Enyera 4A's CAMP comprises more of sandstones and claystones as compared to that of2A which is mainly sands/clay/silt, Table 3.1.

The Vint at TUR at Enyera 2A, even though lying shallower than that of Enyera 4A, is higher. This cannot be attributed to greater overburden since Enyera 4A has a higher overburden of about 8 m. There is a difference of about 102.79 ms-I in Vint between them. The lithological difference between the two formations accounts for the variation in the Vim. In general, interval velocity did not vary much within the Grouped formations between the Enyera wells.

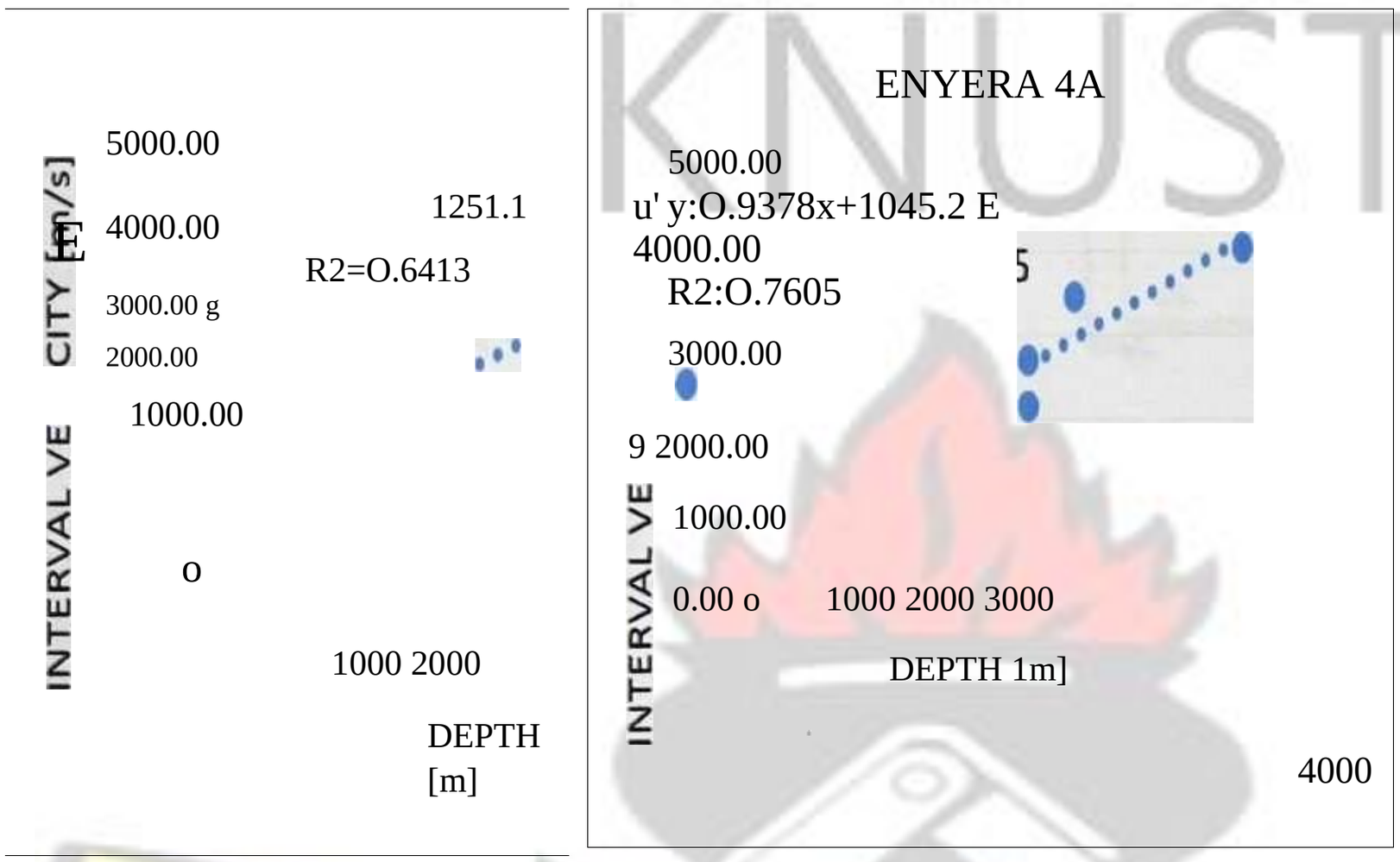

Figure 4.2: Graphs of interval velocity against mid-depths of grouped formations for Enyera 2A and Enyera 4A

Figure 4.2 of graphs of against Zmid shows that K is higher in Enyera 4A, 0.9378 s-l, compared to Enyera 2A, 0.7757 s-l . Thus, it is expected that there will be greater vertical variation in the interval velocities at the Enyera 4A compared to Enyera 2A.

4.1.2 Ntomme Wells

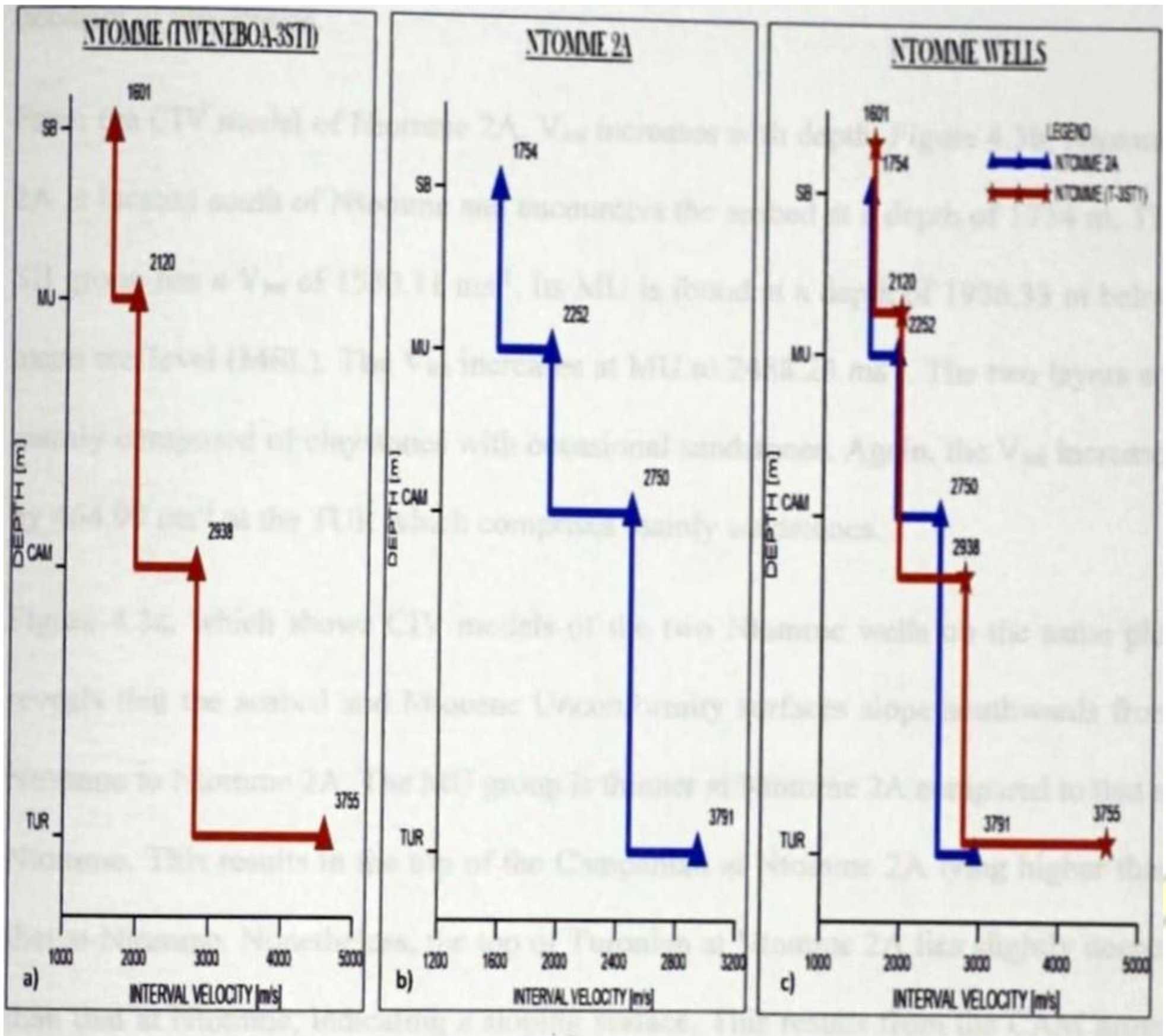

Figure 4.3: I-Dimensional Interval Velocity models For Wells in the Ntomme Discovery within Deepwater Tano Area.

The Tweneboa-3 well was sidetracked about 550 m west, targeting the Ntomme anomaly, amarea of strong seismic response. The CIV model of Tweneboa 3STI

(Ntomme) well is shown in Figure 43a. Generally, Virg, at the well, increases with Increasing depth. The seabed lies at a depth of 1626 m with a of 1630.87 ms-I. The overburden of the SB group, among other factors, increases the Vag of the MU group to 1922.97 ms-I. It lies at a depth of 2120 m and, together with the SB group, is composed of claystones with occasional sandstone interbeds. The CAM layer at the well is made of sandstones and has a higher Vag of 2699.30 ms-I. The top oftE CAM is at a depth

of2800 m. A very high Veg of 4522.60 ms-I is attained for tfrE TUR group which lies at a depth of 3741 m. The layer is made up of thick sanstones with occasional claystones.

From the CIV model of Ntomme 2A, Vint increases with depth, Figure 4.3b. Ntomme 2A is located south ofNtomme and encounters the seabed at a depth of 1754 m. The SB group has a Vint of 1580.11 ms-I. Its MU is found at a depth of 1936.33 m below mean sea level (MSL). The Vint increases at MU to 2488.23 ms-I. The two layers are mainly composed of claystones with occasional sandstones. Again, the Vint increases by 464.99 ms-I at the TUR which comprises mainly sandstones.

Figure 4.3c, which shows CIV models of the two Ntomme wells on the same plot reveals that the seabed and Miocene Unconformity surfaces slope southwards from Ntomme to Ntomme 2A. The MU group is thinner at Ntomme 2A compared to that at Ntomme. This results in the top of the Campanian at Ntomme 2A lying higher than that at Ntomme. Nonetheless, the top of Turonian at Ntomme 2A lies slightly deeper than that at Ntomme, indicating a sloping surface. This results from the CAM group of Ntomme 2A being thicker than that at Ntomme. Vint of SB and MU grouped formations for the Ntomme wells are very close indicating slight Vint variation within the discovery.

The SB fóhmation of Ntomme has ahigher Vint but a lower Vint for MU formation _compared to Ntomme 2A. Since SB formation for Ntomme is slightly thicker than that of Ntomme 2A, greater overburden may account for the higher Vint at Ntomme. The thinner MU formation ofNtomme 2A affords that ofNtomme 2A a higher Vint. There is a wide difference between the Vint of TUR ofNtomme and Ntomme 2A of about 1569 ms-I. The difference in the interval velocity for the Turonian Group may be arising from the fact that the formation at Ntomme includes the Tweneboa fans but that of Ntomme 2A does not. Considering the lithology, Table 3.1, it comes as no surprise that Ntomme has higher Vint since it comprises thicker sandstones.

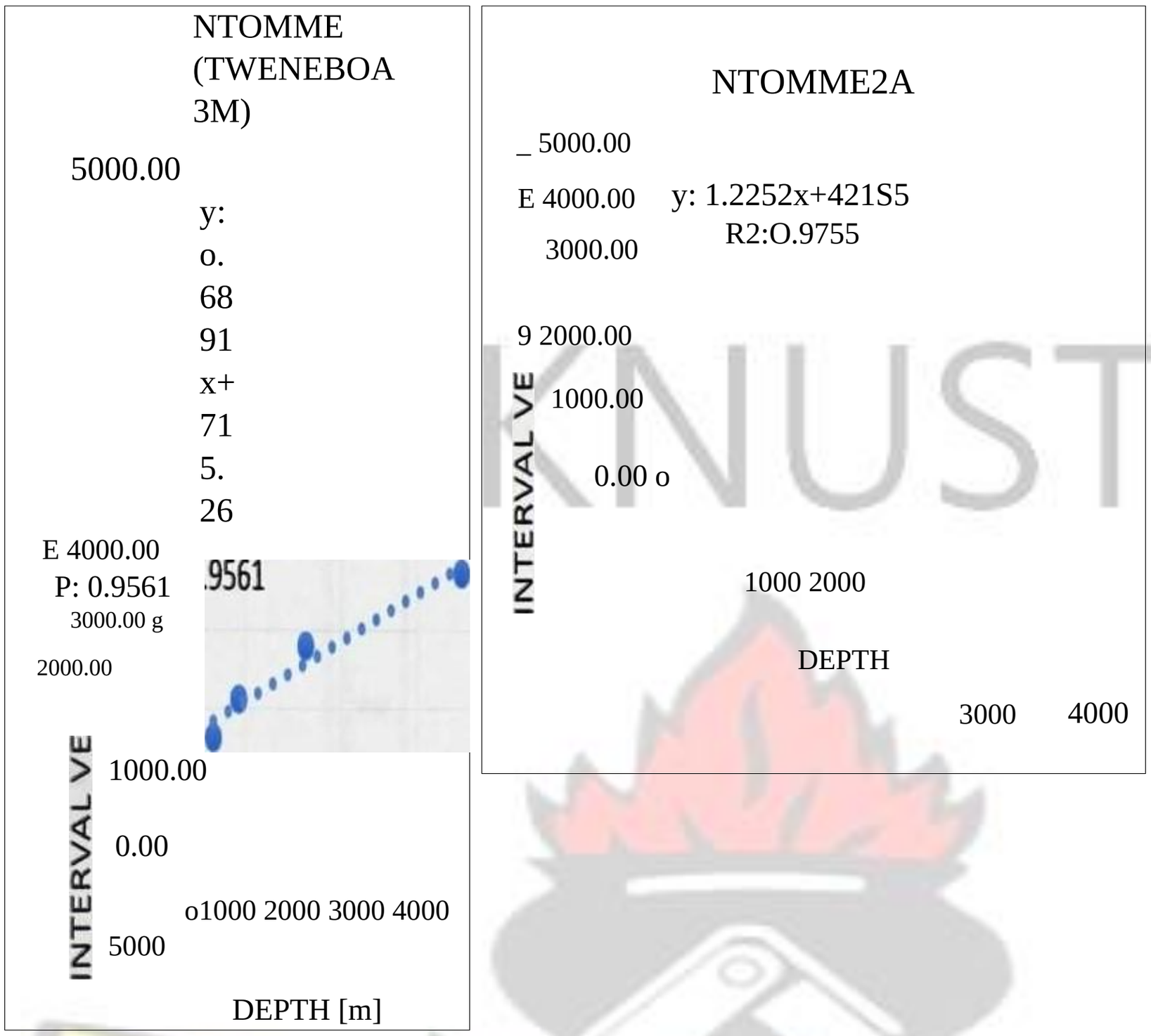

Figure 4.3: Graphs of interval velocity against mid-depths of grouped formations for Ntomme and Ntomme 2A

From Figure 4.4, Ntomme 2A has a higher K of 1.2252 s-l compared to Ntomme, 0.6891 s-l. The higher vertical variation in interval velocity at Ntomme 2A is due to the thinner Miocene Unconformity Group. Hence, this presents greater lithological variation, depth-wise at Ntomme 2A.

4.1.3 Tweneboa wells

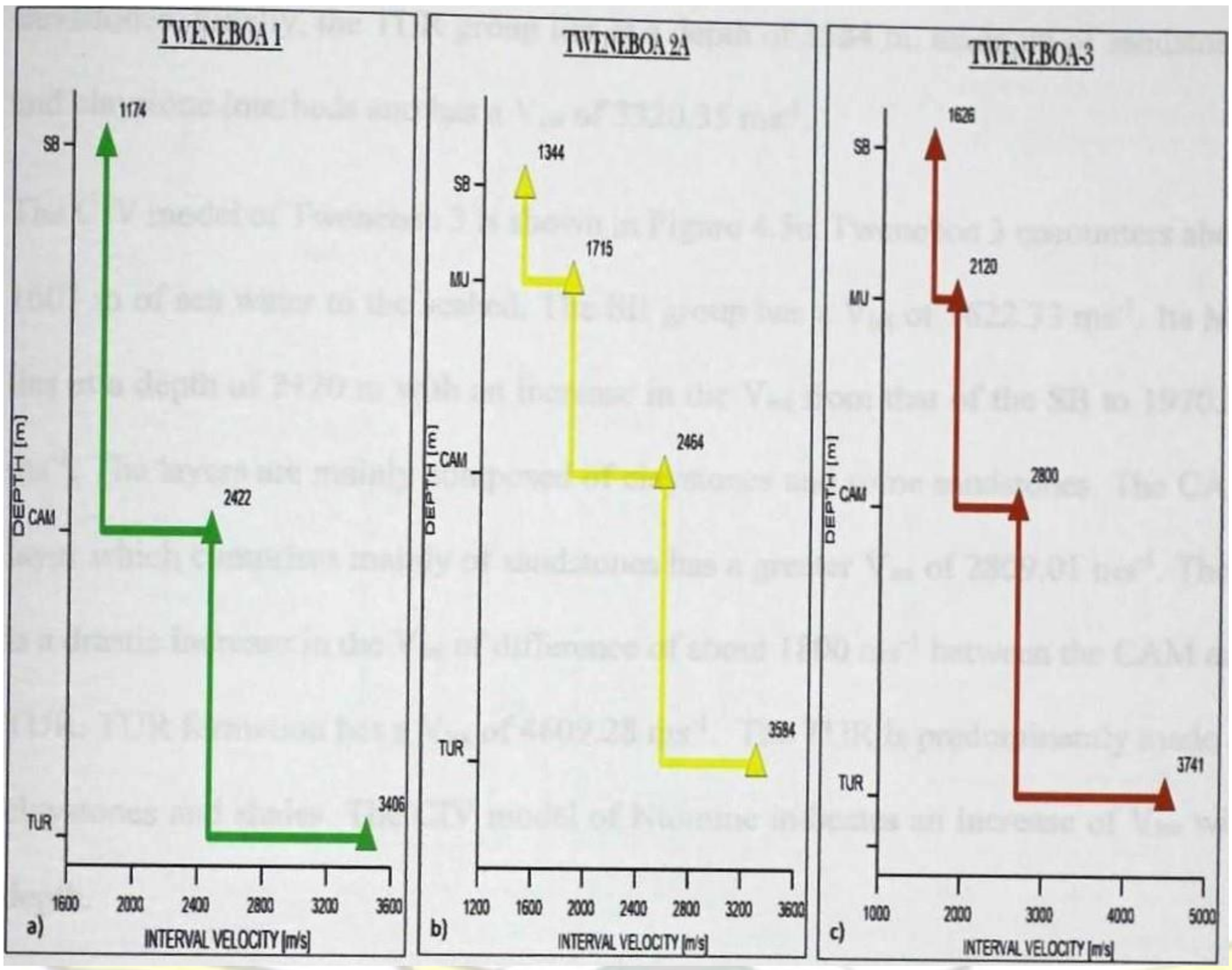

Figure 4.4: I-Dimensional Interval Velocity models for wells in the Tweneboa Discovery within Deepwater Tano Area.

At a depth of 1174 m, Tweneboa 1 well encounters the seabed as shown in Figure 4.5a. The Miocene unconformity top was not picked at this well because it was not identified. The Vint of the seabed to top of Campanian is 1804.01 ms-I. This high Vint value is he results of conšiaæihe depth interval from the seabed to the top of the __Campanian. The CAM group lies at a depth of 2422 m with a Vint of 2474 ms-I. Vint at TUR, picked at a depth of 3406.00 m, is 3454.09 ms 1.

Tweneboa 2 encounters the seabed at a depth of 1344 m., Figure 4.5b. The SB formation has a Vint of 1513.02 ms-I which is close to that of seismic velocity in water. The Vint increases to 1889.56 ms-I at MU group and is encountered at depth 1715.00 m. The two layers are made up of mainly claystones. Top of CAM formation

is encountered at depth of 2463.50 m with Vint of 2599.80 ms-I. The CAM is generally sandstones. Finally, the TUR group lies at a depth of 3584 m, made up of sandstones and claystone interbeds and has a Vint of 3320.35 ms-I.

The CIV model of Tweneboa 3 is shown in Figure 4.5c. Tweneboa 3 encounters about 1601 m of sea water to the seabed. The SB group has a Vint of 1622.33 ms-I. Its MU lies at a depth of 2120 m with an increase in the Vint from that of the SB to 1970.32 ms-I. The layers are mainly composed of claystones and some sandstones. The CAM layer which comprises mainly of sandstones has a greater Vint of 2809.01 ms-I . There is a drastic increase in the Vint of difference of about 1800 ms-I between the CAM and TUR. TUR formation has a Vint of 4609.28 ms-I. The TUR is predominantly made of claystones and shales. The CIV model ofNtomme indicates an increase of Vint with depth.

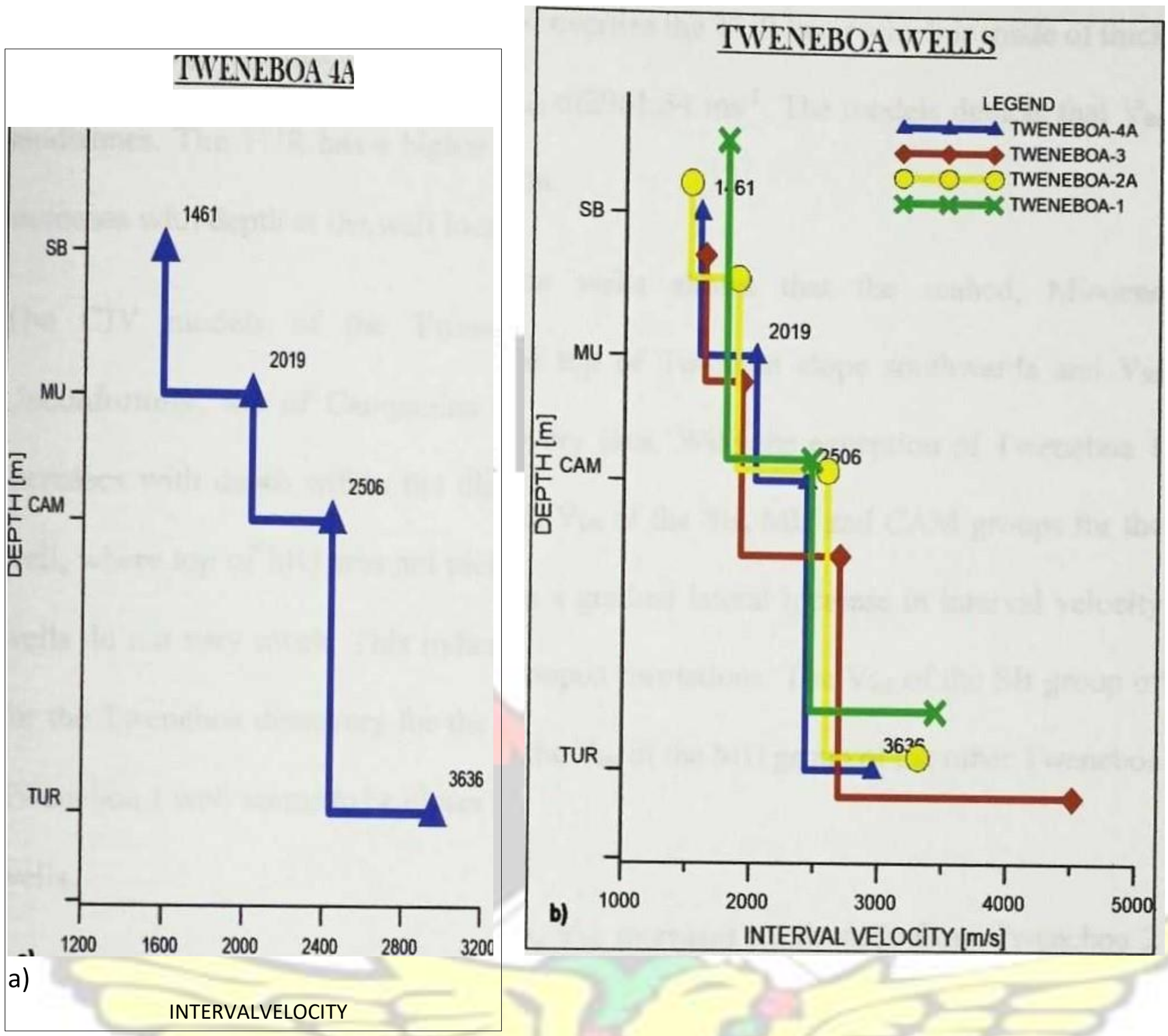

Figure 4.5: CIV models for Tweneboa 4 (left) and for wells in the Tweneboa discovery (Right)

The Tweneboa-4A well, located 3.9 kilometres southwest ofthe Tweneboa-2 appraisal well and was drilled in the western flank of the accumulation to complete the appraisal ofthe Tweneboa gas-condensate discover (bttp://ghanaoilwatch.org/index.php/ghanaoil-and- as-news/1335-tullow-oil.com lete-successful-tweneboa-4-a raisal-welloffshore-ghana, 13 April 2011). CIV model for Tweneboa-4 well in Figure 4.6 shows that the well encounters the seabed at a depth of 1461 m. The SB group has a Vint of 1592.01 ms-I with a thickness of about 558 m. The MU is picked at a measured depth of2019.00 m with a higher Vint of 2035.61 ms-I . The two layers are made up ofmainly claystones with sandstone-

interbeds. The well picks a very thick CAM layer of thickness of about 1129.5 m. This has an interval velocity of 2439.21 ms-I. The layer

is composed of massive sandstones and overlies the TUR layer which is made of thick sandstones. The TUR has a higher Vint of2961.54 ms-I. The models depicts that Vint increases with depth at the well location.

The CIV models of the Tweneboa wells shows that the seabed, Miocene Unconformity, top of Campanian and top of Turonian slope southwards and Vint increases with depth within the discovery area. With the exception of Tweneboa 1 well, where top of MU was not picked, Vint of the SB, MU and CAM groups for the wells do not vary much. This indicates a gradual lateral increase in interval velocity for the Tweneboa discovery for the grouped formations. The Vint of the SB group of Tweneboa 1 well seems to be closer to the Vint ofthe MU group ofthe other Tweneboa wells.

Considering the SB grouped formation, Vint increases southwards from Tweneboa 2 location, through Tweneboa 4 and towards location of Tweneboa 3. For the MU and CAM grouped layers, interval velocity increases laterally in the southeast direction from location Tweneboa 1, Tweneboa 2 to Tweneboa 3 wells. Tweneboa 4A has the highest Vint MU formation but the lowest for the CAM and TUR formations. When TUR group for Tweneboa 3 is not considered, it appears that Vint decreases southwards from Tweneboa 1, Tweneboæ2-to-Tweneboa 4.

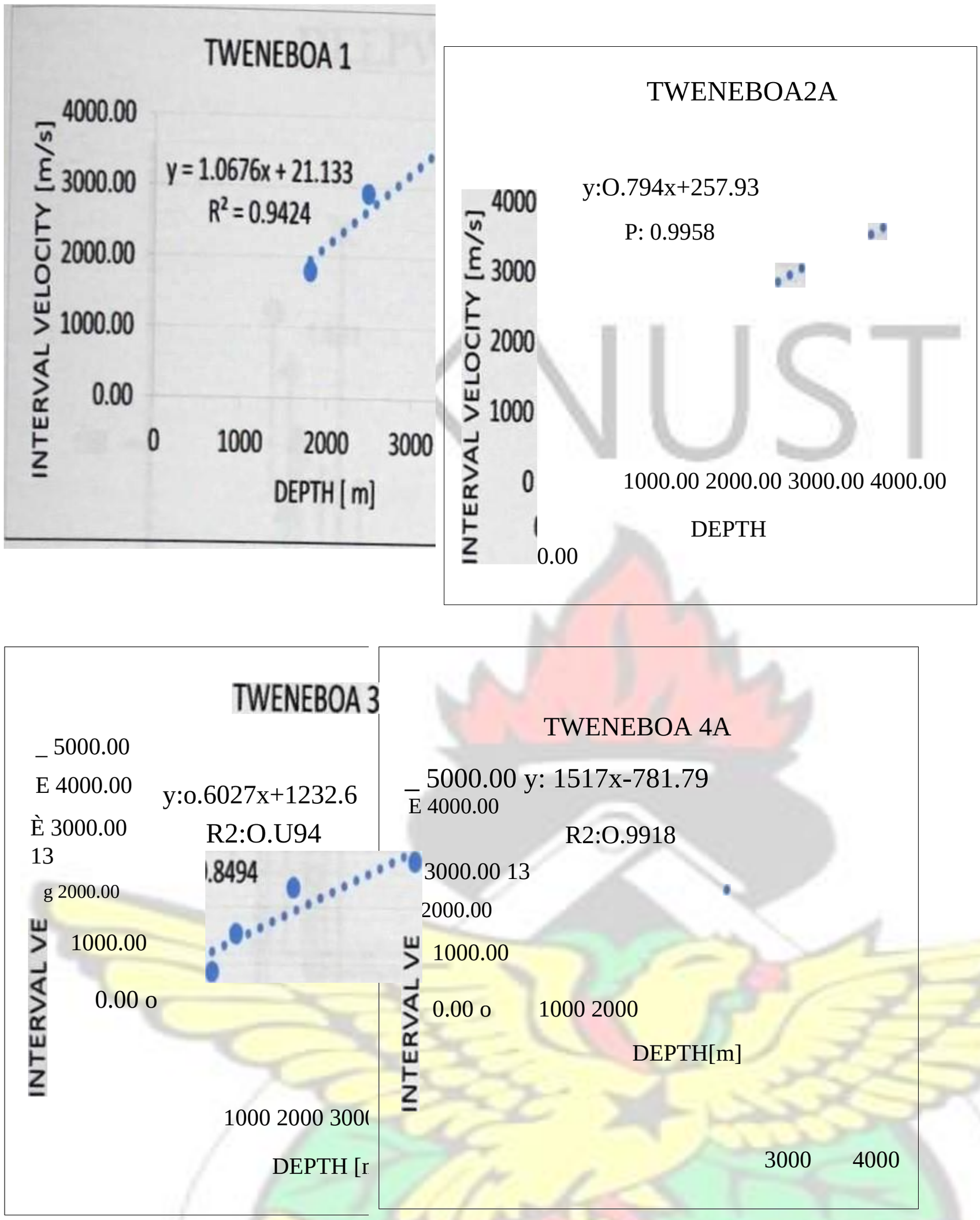

Figure 4.6: Graphs ofinterval velocity against mid-depths ofgrouped formationsfor the Tweneboa wells

The Vo-K graphs for the Tweneboa wells, Figure 4.7, show that Tweneboa 3ST1 has the lowestKValue of0.692TS+WhCreas Tweneboa 4A has the highest, 1.5517 s-l even though from Table 3.1 they appear to have similar lithology. Tweneboa 4A has the thinnest MU layer and could be the reason behind the well having the highest K value, representing the greatest variation of Vint with depth and lithology.

DEEPWATER TANO WELLS

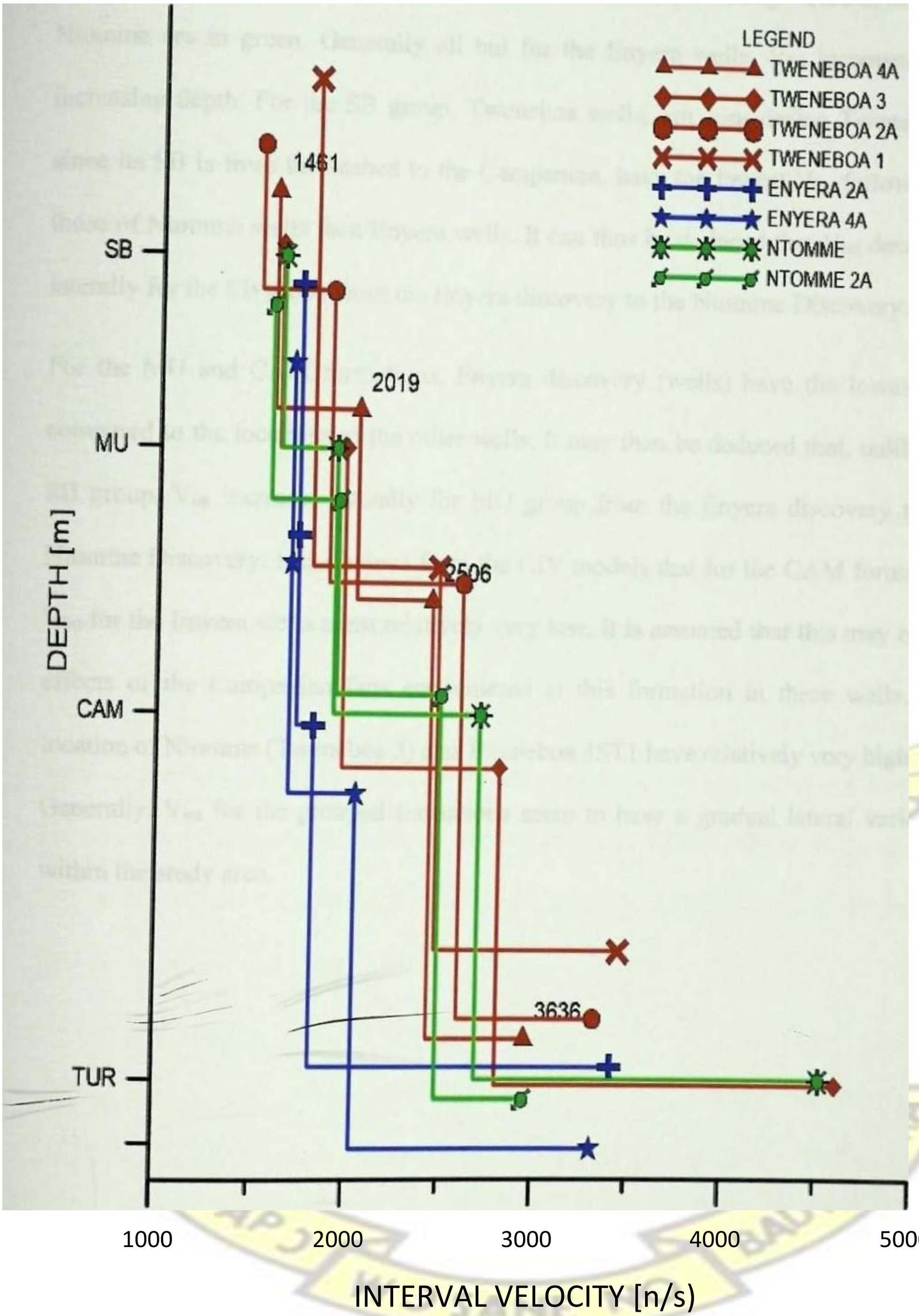

Figure 4.7: Constant Interval Velocity models of Deepwater Tano wells

Figure 4.8 shows the CIV models ofall the available wells ofthe Deepwater Tano area used for the research. The Tweneboa wells are in red step plots, Enyera are in blue and Ntomme are in green. Generally all but for the Enyera wells, Vint increases

with increasing depth. For the SB group, Tweneboa wells, not considering Tweneboa 1 since its SB is from the seabed to the Campanian, have the lowest Vint followed by those of Ntomme wells then Enyera wells. It can thus be deduced that Vint decreases laterally for the SB group from the Enyera discovery to the Ntomme Discovery.

For the MU and CAM formations, Enyera discovery (wells) have the lowest Vint compared to the locations of the other wells. It may then be deduced that, unlike the SB group, Vint increases laterally for MU group from the Enyera discovery to the Ntomme Discovery. It is obvious from the CIV models that for the CAM formation, Vint for the Enyera wells seem relatively very low. It is assumed that this may be the effects of the Campanian fans encountered at this formation in these wells. The location ofNtomme (Tweneboa 3) and Tweneboa 3ST1 have relatively very high Vint. Generally, Vint for the grouped formations seem to have a gradual lateral variation within the study area.

4.2 MAPPED INTERVAL VELOCITY (MN) MODELS

Mapped interval velocity models were built from checkshots and seismic data. Linear regression models from isopach-isochron graphs were derived from checkshots and then essentially used to convert picked horizons on seismic time sections. The horizon picked are the seabed, Miocene unconformity, Top Campanian (fan) and the Top Turonian fan. Three mapped interval velocity models were built and were used for the depth conversions of the Miocene Unconformity, Campanian (fan) and the Turonian fan.

The first MIV model for the SB group was used to depth-convert the Miocene Unconformity, the second for the MU group was used to depth-convert the Campanian time horizon and finally the MIV model for the CAM group was used

for the conversion of the Turonian fan time horizon. A constant velocity of 1500 ms-I was used to depth convert the time-map of the seabed.

After the seabed was picked on the seismic section, it was gridded and contoured, Figure 4.9a. Afterwards, in EMC, the seabed time grid was divided by two since the data is in TWT, and multiplied by 1500 ms-I , equation 3.6. This generated a seabed grid in depth shown in Figure 4.9b.

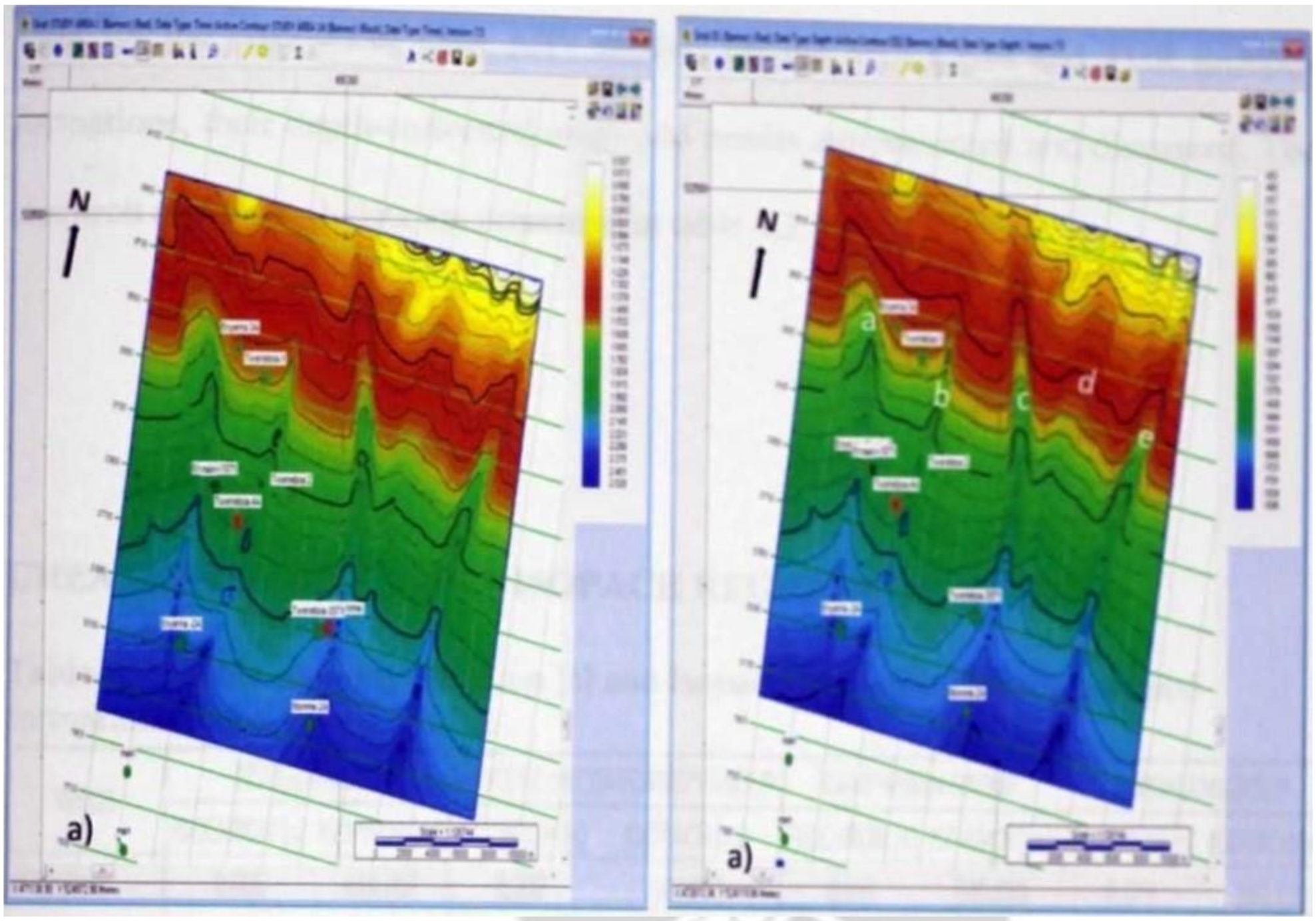

Figure 4.8: Two-Way-Time (TWT) Map of Seabed (a) and Depth Converted Seabed Map (b), showing canyons a, b, c, d and e.

The depth of seabed below mean sea level (MSL) ranges from 403 m to 1896 m. On the colour bar, the white to yellow ranged from 403 m to 805 m. This is followed by red to depths of about 1092 m, then green follows to 1379 m and finally, blue to 1896 m. The seabed slopes southwards and is characterised by canyons a, b, c, d and e. These canyons are visible both on the TWT time map and the depth map ofthe seabed. The canyons a, b and c f0i$KG§s that trend from northwest to southwest. Canyons —a and b seem to merge southwards. Canyons d and e arcs towards the northeast of the area. Canyon d is not prominent and levels up southwards towards deeper depths. Towards the north, all the canyons seem to level up to the general seabed level and become less distinct.

Data for the creation of these MIV models for the MU, CAM and TUR grouped formations, their depth-converted maps and results are presented and discussed. The isochron and isopach data are presented in table 4.2.

CREATION OF ISOCHRON-ISOPACH REGRESSION MODELS

Table 4.2: Table showing Isochron [s] and Isopach [m] values for the grouped formations at the various wells.

WELLS	SEABEDGROUP		MIOCENE NFORMITYGROUP		CAMPANIANGROUP		TURONIANGROUP	
	ISOCHRONIsl	ISOPACHlml	ISOCHRON[sl	ISOPACHlml	ISOCHRON[sl	ISOPACH[ml	ISOCHRON	ISOPACH[m]
NTOMME		494.0	0707		0697	940.880	0.073	165120
NTOMME2A	0630	497.0	0514	497.500	0.837	1041.n	0.137	202000
TWENEBOA4A	0701	558.0	0.478	487.0	0926	1129.500	0.234	346500
MENEBOA3	0640	519.000	0830	8180	0582	817.0	O.ff	151.n
MENEBOA2A	0491	371.500	0.792	748500	0862	1120500	0.259	430400
MENEBOAI	1.384	1248.500			1795	984.000	0.226	401.0
ENYERA4A		511.0	0.700	591.70		915.300	0.153	254.0
ENYEA2A	0.746	645.0	0564	487.000	0.967	878.000	0.202	327.190

These Isopach values, depth thicknesses, from the wells are plotted against their corresponding-isochron values, time thicknesses, for the four grouped layers even

though only the first three were used for the conversion.

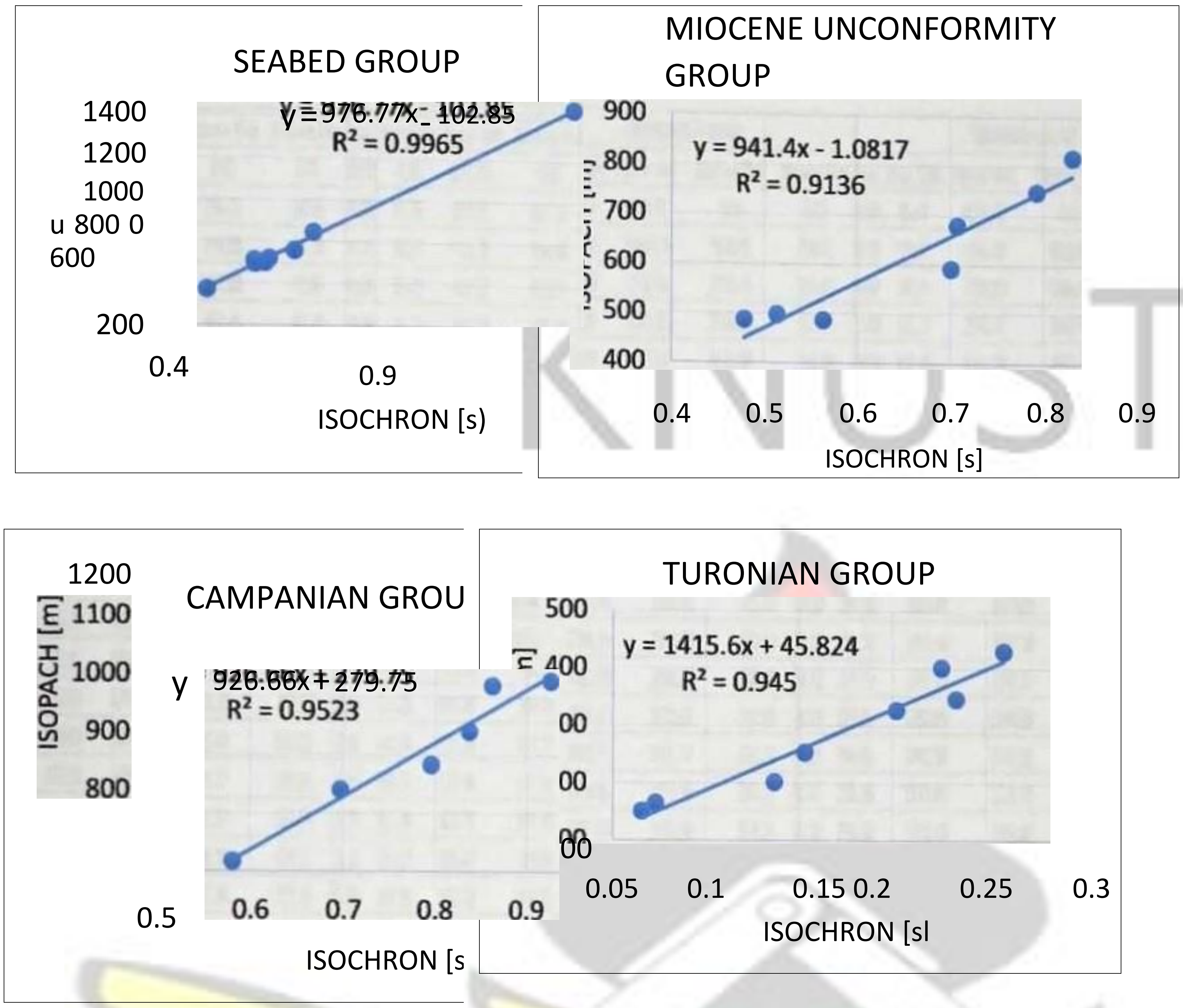

Figure 4.9: Graphs showing Isopach against Isochron for the tops of each of the grouped formation across the wells.

The line of best-fit of the graphs in Figure 4.9 needs to pass through the origin so that the isochron is zero when the isopach is zero. Thus, the modification to ensure this is shown in Table 4.3.

	MOCĐw0NFORMIY6ROUP		TinNlAN601P
Ise Calc vint I,tnelso	nc isop Calc ar int Mcurve Vint Mcurve Isop	Apparint I,brvelsq	lzisop at tint kurefrt
-1025 nvn 10	-10	279.75 01/0! 10 10	0
8103	17.75 07.32 175	101416 7m41 15841	3717
2910 110	04 36.57 914.36 914.36	72141	
8103 291B 015	92137 550	B535 5£16 33535	

920	10 7413 927.8	3510 0.08 353.88 4423.54	1045 2511 811 10245
141B 025 1413	110	010 37142 372116 37242	
	112 1110 1110	112 325791	217133
	114 mn	114 0.48 22487	107
7119 2878	116 93464	016 267510 267510 42802	Isa
3167 045 74814	118 107	118 2408 4465	17123
7711	01 187.1 935B 18720	232541 0.20 465.08 2325.41	110 187.1 1873
0434 70.70	122 548	219825 0.22 483.62 2198.25	111 18218 183218 20154
017	0.24 224.85 936.89 245	124 5215 E29 1828	112 2151 1797.47 215)
16 81847 81847	126 2418 93714 93714	5208 0.26 520.68 2002.62	113 17aŒ
OTI	0.28 8251 9373 8251	192577 53921 128 539.21 1925.77	114 2401 17Q91 17291 2401
057	937.ð 937.79	£7.75 1016	115 816 816
67851	132 mp mil	132 57828 IDS 57628	116 27132 17020 27232
7275	034 311B	1M 9481 17045 17045	18515 18515
77818 S2Q 77618	0.36 337.82 938.40 33782	6135 11874 61335	118 na 167018 157018
15 844	0.38 356.65 938.55	16284 6310 0.38 631.88 1662.84	119
10 8735 8715 8718	0.40 375.48 938.70 37548	10 650.41 1626.04	120
87875	142	IQ 1ĐŽn 85	01
	0.44 413.13 938.94 938.94 41113	15246 87.0 (144 687.48 1562.46	
ILS Iou	146 431.96 939.05 939.05	146 153481 153481	37141 1614B 37141
100.19 11	148	7245 72455	124 3851 3857
125	19 062	15) 14816	125 3Bn
0758	152 B32	152 1161 76161	126 1915 1916 411B
121570	9717 939.40 939.40	7015 14472 144472	
la IHS 1853	15 B.47	ma 142621	128 44219 1579b
	0.58 544.93 939.54 939.54 544B	8171 817.21	029 15n61
	0.60 562.76 939.60 939.60	83575	
	0.62 582.59 939.66	062 5428 137787 137787 828	
	0.64 601.41 939.71 0141	Inn 87181	
	0.66 620.24 939.76 B.76	0135 13952 015	
	0.68 639.07 939.81	13M	

Table 4.3: Showing the optimization using generated isochron values for the grouped formations

0.70 61.99 939.85			2841		92841
171 676.73 939.90		67673	172 946.95 1315.20	131520	9465
0.74 695.55 939.94		055	174 965.48 1304.70	Imo	9650
176 714.38 939.98	nu	71438	0.76 984.01 1294.75		
0.78 733.21 940.01			0.78 1002.54 1285.31	1831	IQ54
	90Œ		0.80 1021.08 1276.35	127835	
			182 10Ð61	1267.82	119.61
			0.84 1058.14 1259.70		
			125195	17515	
			0.88 1095.21 1244.56		
			111374 1237.0	1237.49	
			on 113228		
			0.94 1150.81 1224.27		
			0.96 1169.34 1218.07		1B34
			121112		11871
			1m 11641		

Mcurve Isop values for the various group formations is plotted against the generated Isochron values. Regression equations are derived from the graphs and are shown in Figure 4.11.

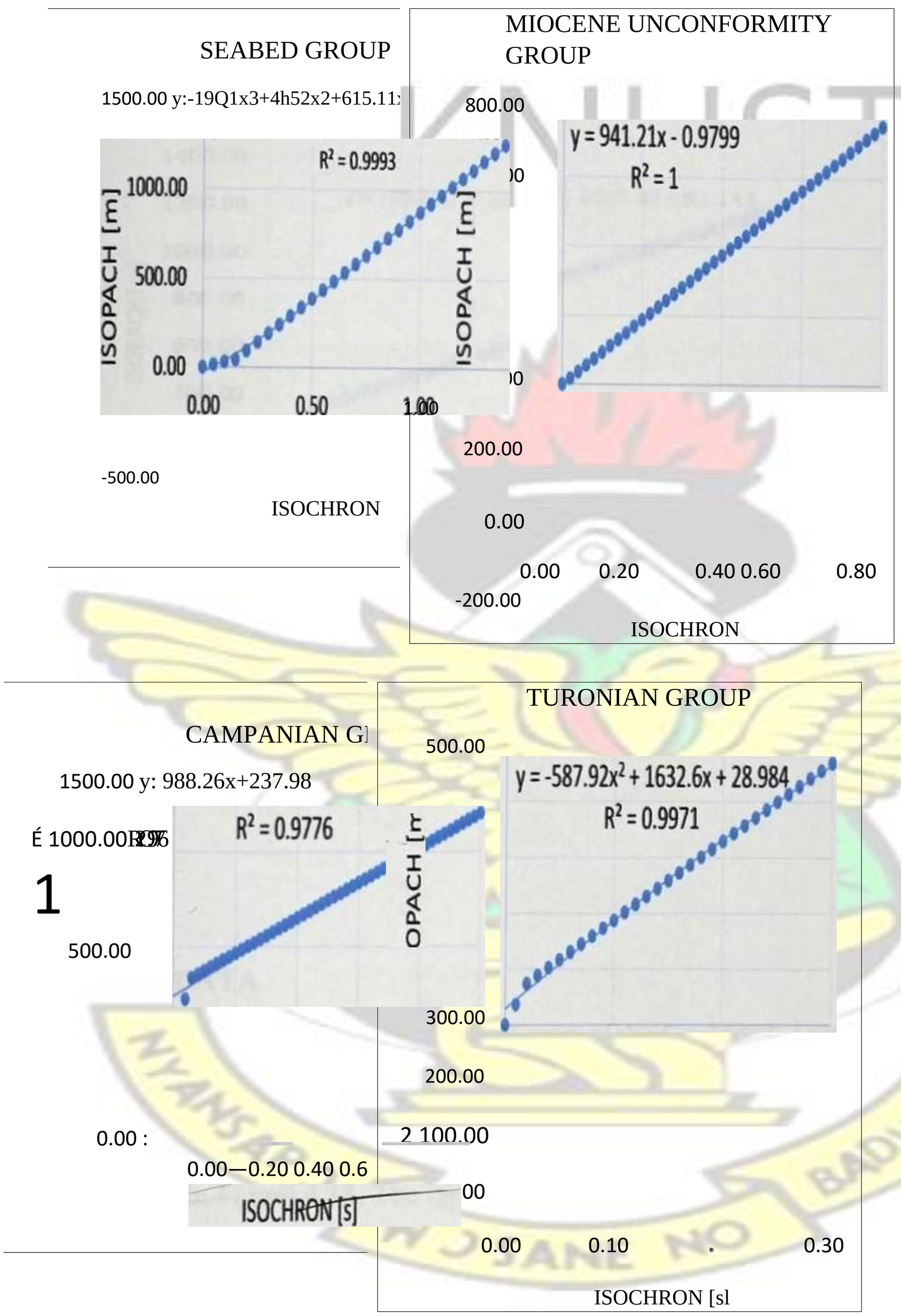

ÃfgGre 4.10: Graphs showing generated Isopach against Isochron with their trendline equations and correlation coefficients.

From Figure 4.11, the isopach-isochron graph of the Campanian group shows two distinct slopes. This observation seems to result from the fact that as the isochron gets smaller, the interval velocity becomes unacceptably large till it gets to zero. The linear regression trendline model appears to consider the thicker valtxs. A K»urthorder polynomial trendline fit to the graph, Figure considered 4.12, both but yielded an average deviation from well formation tops of 133 %. Which is not as good as 1.05 % average deviation yielded by the linear trendline, Table 4.4.

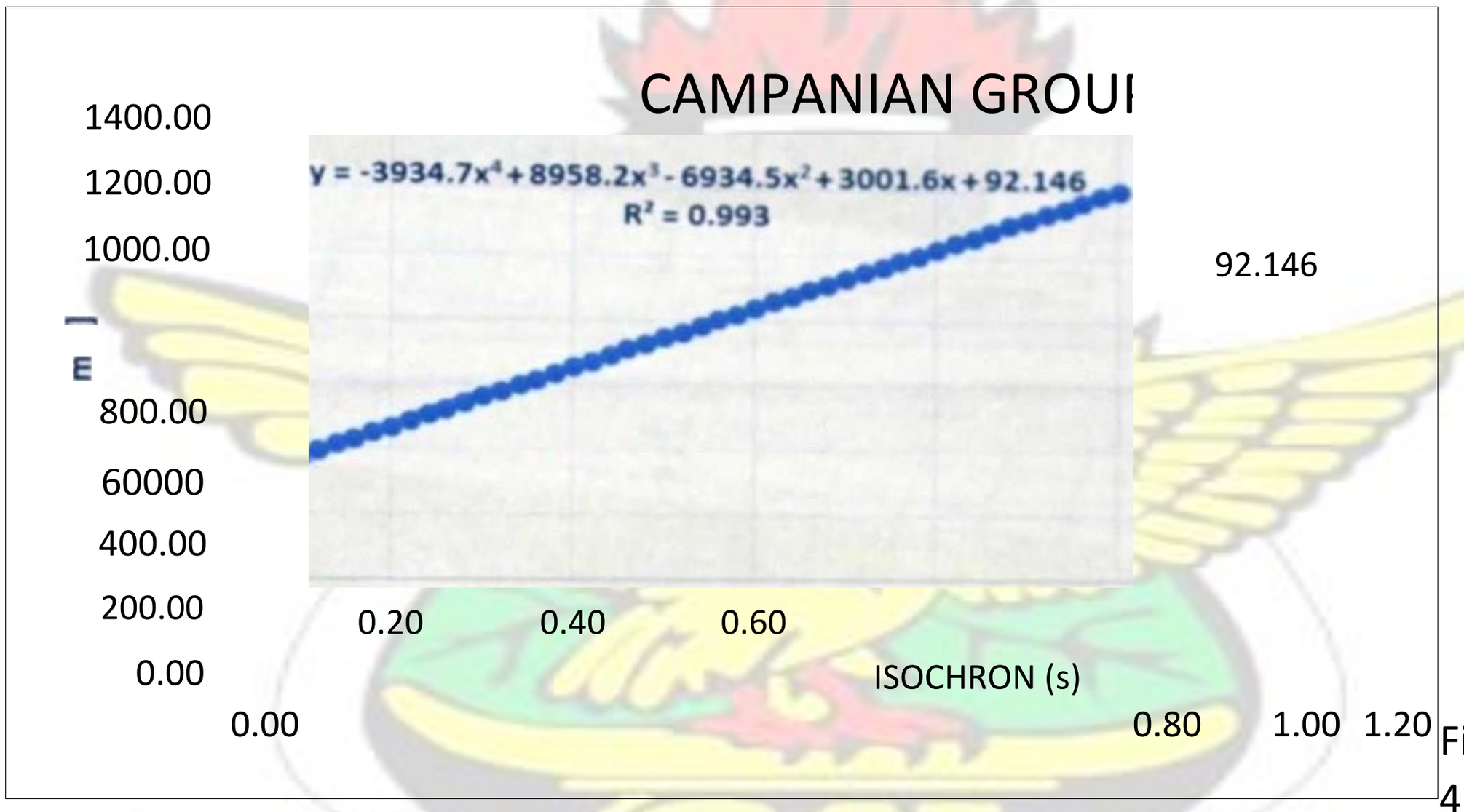

92.146

Figure 4.11: Graph showing isopach against isochron for the Campanian group with a polynomial fit

SEISMIC DATA

On seismic sections, the tops ofMU, CAM and TUR were picked, gridded, contoured and presented in Figure 4>1.3-Ãhetop of the Turonian fan was not extensive over the entire study area as shown in Figure 4.13c. From these maps, it is that the TWTs for the gridded surfaces

increases southwards. The TWT for the top of MU ranges from 0.843 s to 3.202 s, that of top of CAM, 1.938 s to 3.694 s and that for tiE

top of TUR ranges from 3.149 s to 4.453 s. TWT for Mioca•E Unconformity, 2.359 s, is the highest, followed by the top of Campanian, 1.7756 s, and finally that for top Turonian (fan), 1304 s.

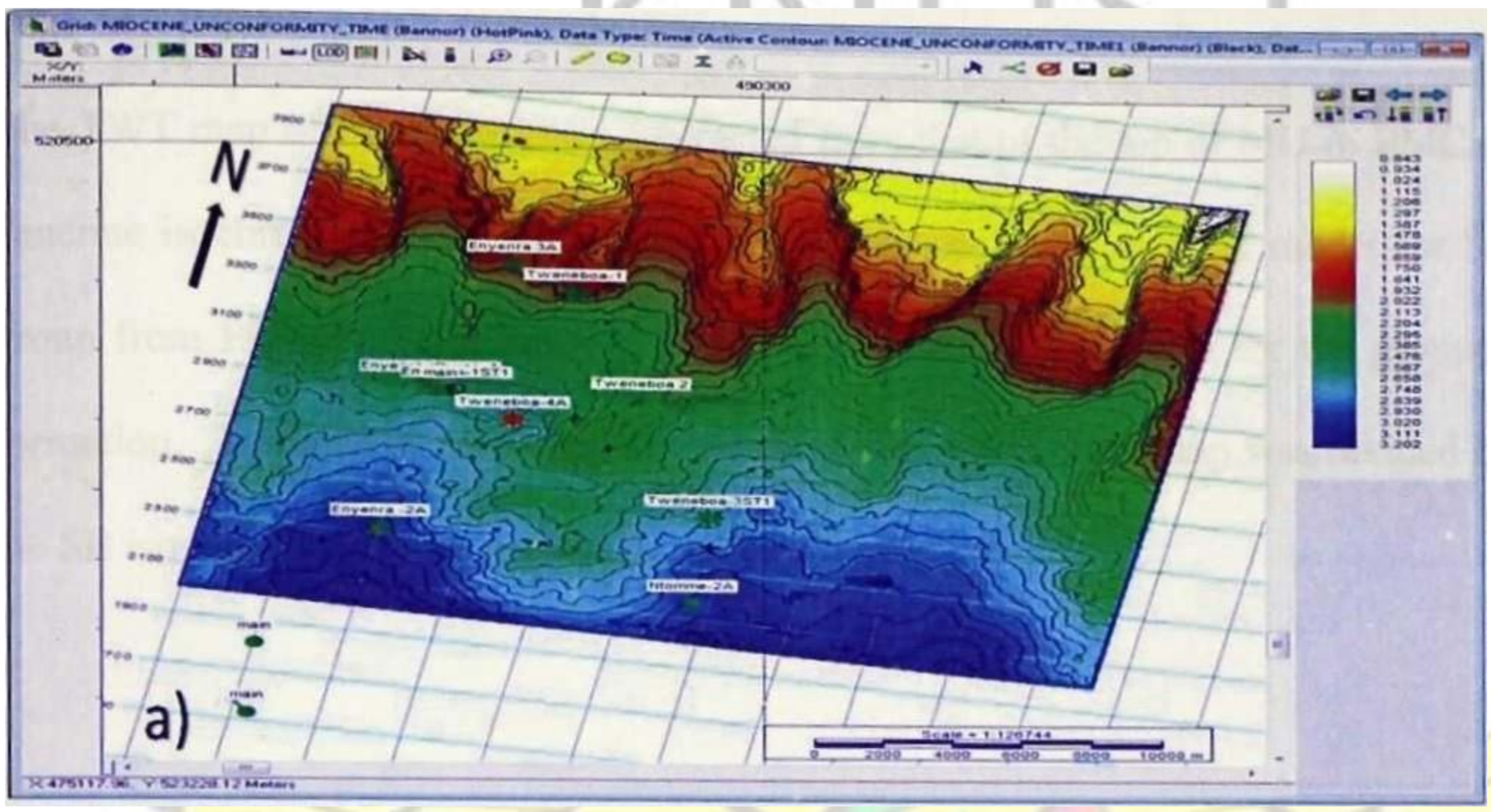

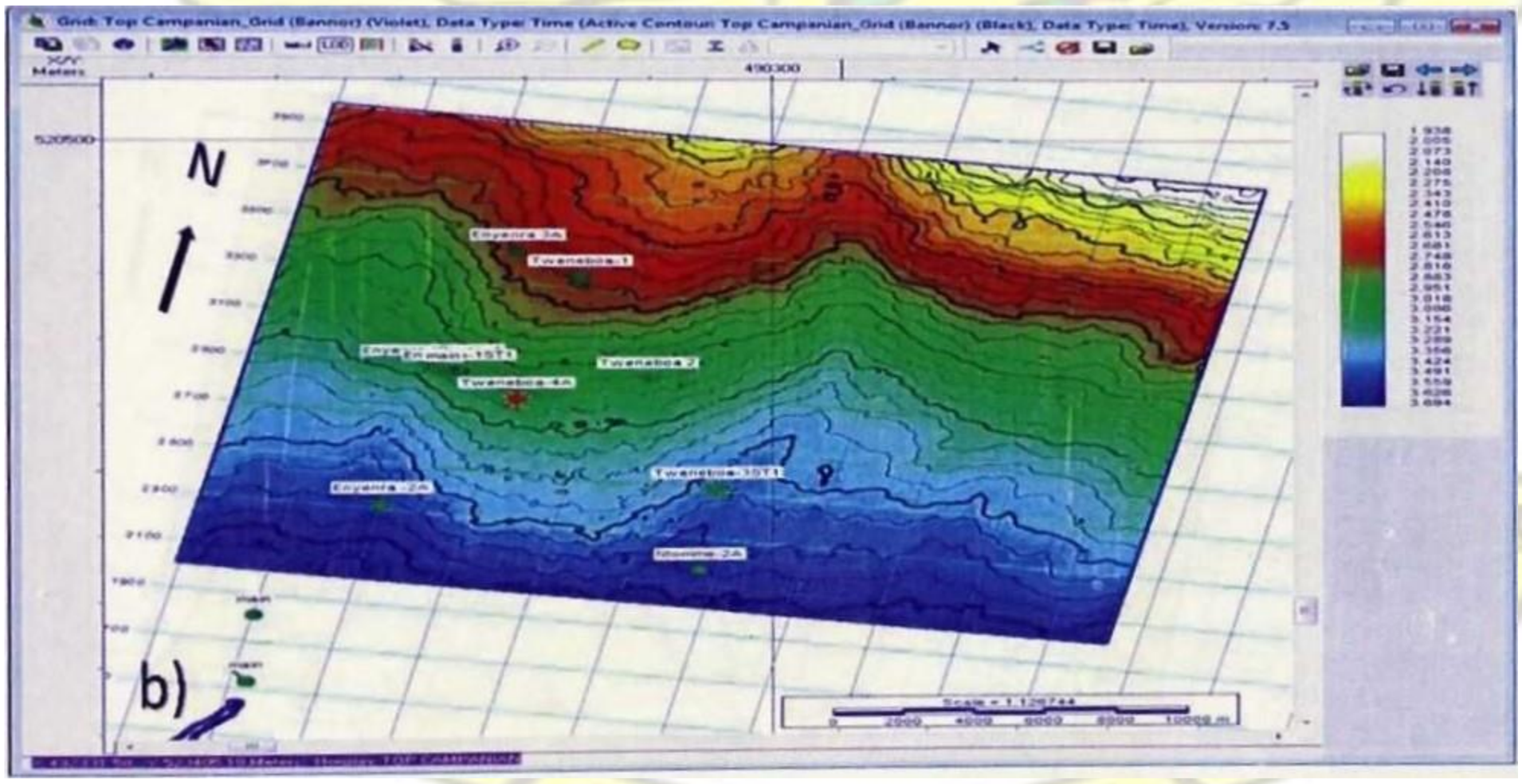

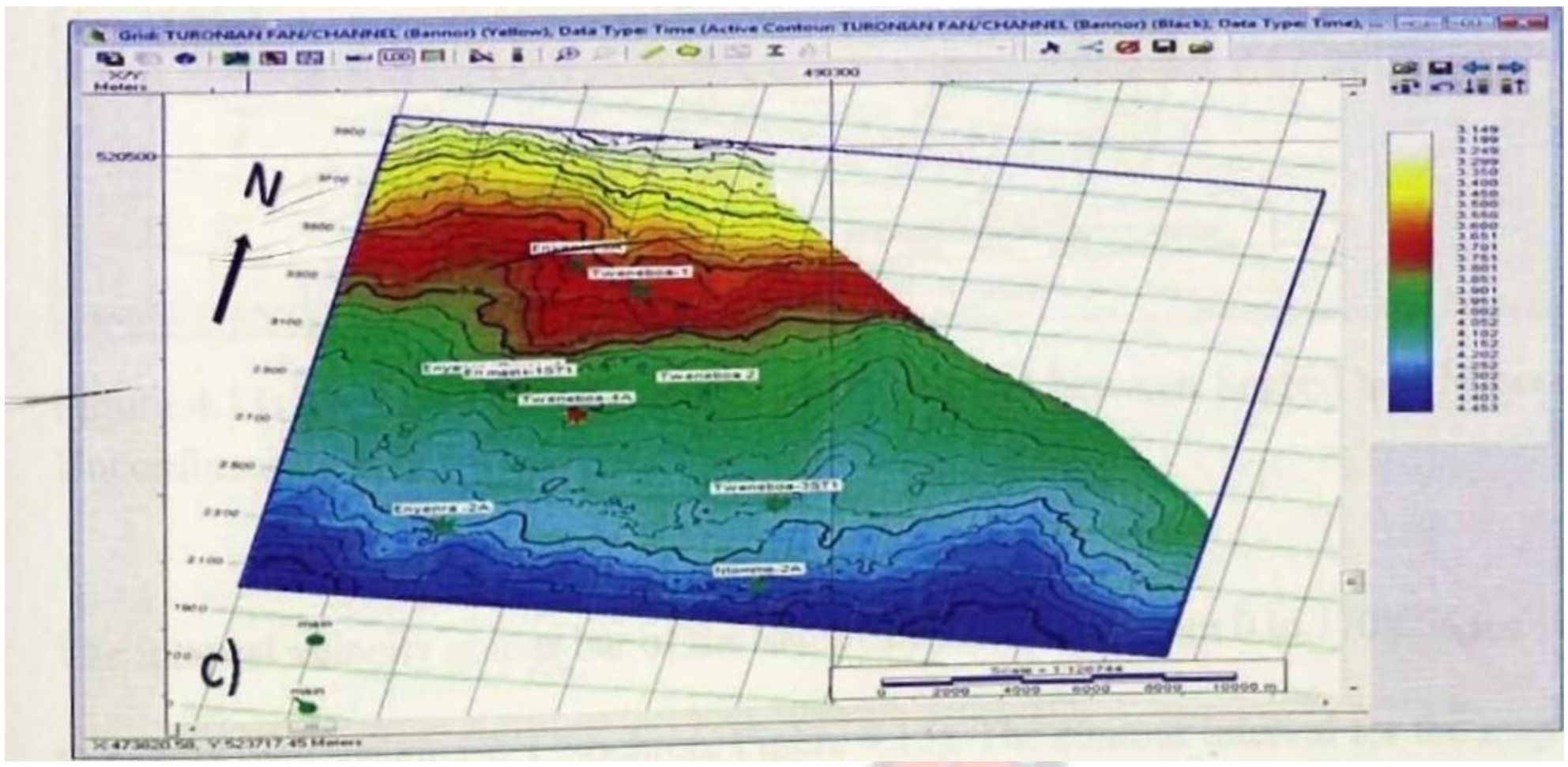

Figure 4.12: TWT Maps of a) Miocene Unconformity, b) Top Upper Campanian (Fan) and c) Top Turonian Fan

4.2.1 MIOCENE UNCONFORMITY

The TWT map of the seabed was subtracted from that of the top of MU in EMC to generate isochron map of the SB formation. The modified regression model for SB group from Figure 4.11 is input in EMC to generate isopach map for the grouped formation. To build the MIV map for the layer, the SB isopach map was divided by the SB isochron map. This gave MIV map shown in Figure 4.14.

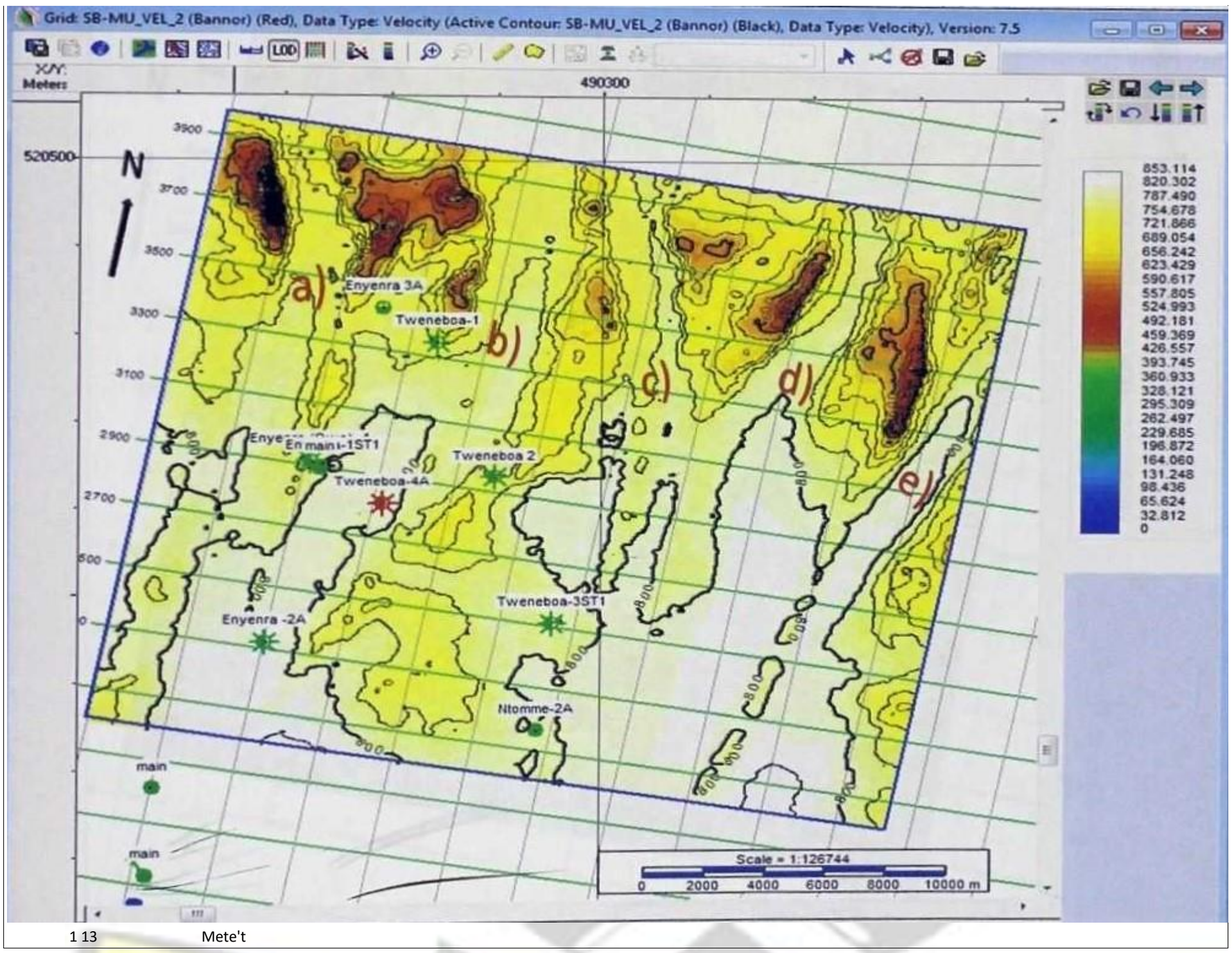

1 13 Mete't

—Fìýžre 4.13: Mapped Interval Velocity (MIV) Model between Seabed and Miocene Unconformity.

The interval velocity colour bar of the SB formation ranges from 0 to 1708.56 ms-I (0 to 854.28 ms-I, using TWT isochron, Figure 4.15). The contour interval for the map is

300 ms-I (150 ms-I, TWT). Generally, Vint appears to increase southwards. It is also

high within channels a, b, c, d and e. Areas in between the channels, north ofthe study area, have very low Vim. The Vint for the formation is between 919 ms-I to 1708 ms-I, above the green region on the colour bar.

Equation 3.7 was input into EMC to depth-convert Miocene Unconformity shown in Figure 4.15.

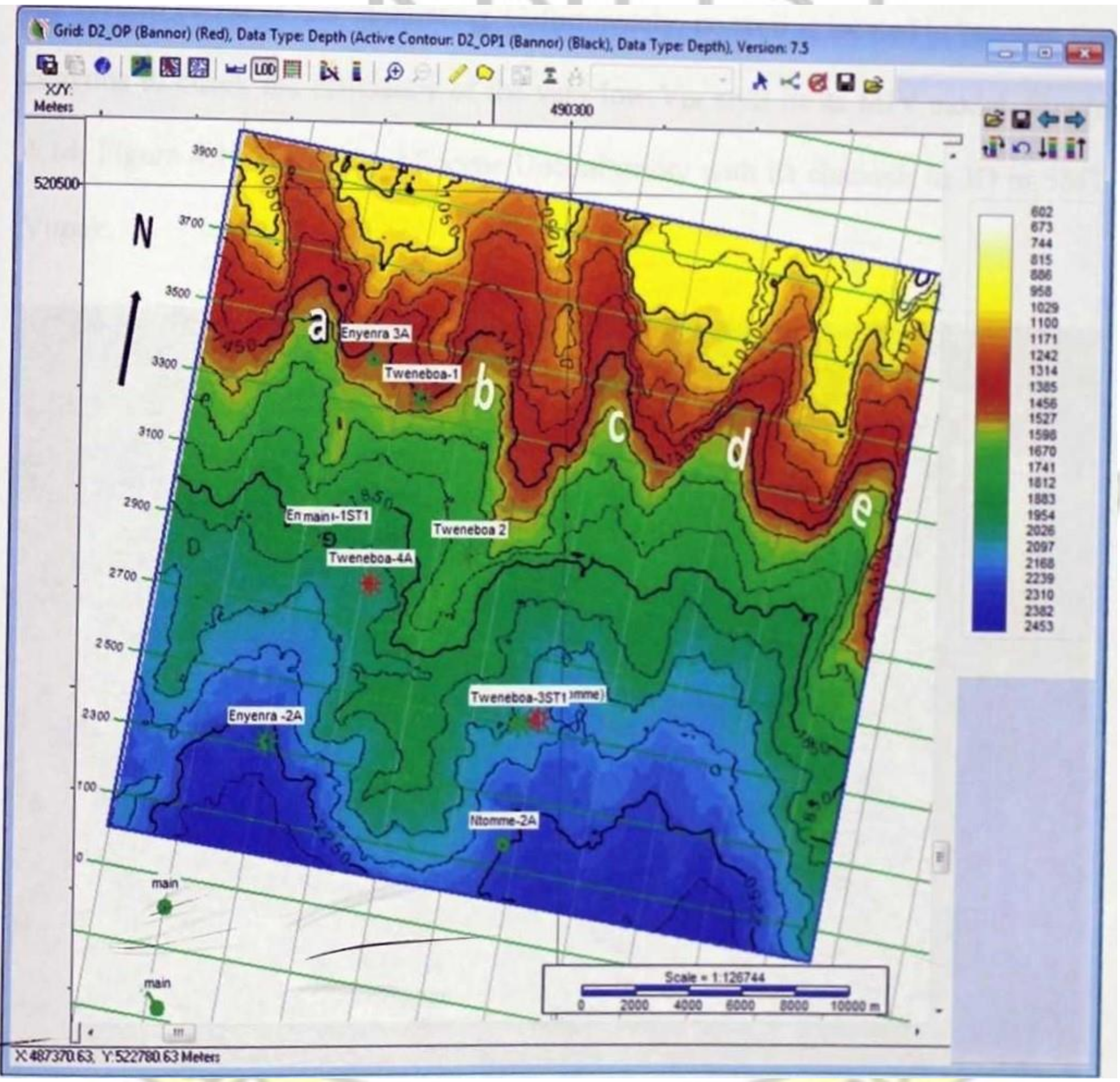

Figure 4.14: Depth converted Miocene Unconformity showing channels a, b, c, d and

The Miocene Unconformity also slopes southwards with depth (below MSL) ranging from 602 m to 2453 m, Figure 4.15. Thus, the surface ranged over a depth interval of

1851 m. The depth map also shows channels a, b, c, d and e. They appear to follow the paths of the canyons of the seabed. Like the canyons, channels a, b and c seem to head in the southeast direction whereas channels d and e are directed towards the southwest.

The five channels become less distinct at depths beyond 1954 m below MSL, blue colour scale. Channels a and b merge into one and c, d and e also merge into one. Beyond depths of 2000 m, blue range, the two merged channels seem to level off and the surface becomes less undulating. Unfortunately, no well is located in between the canyons to check the efficiency of the very low Vint seen in its MIV model, Figure 4.14. Figure 4.16 shows the Miocene Unconformity with its channels in 3D in SMT Vupak.

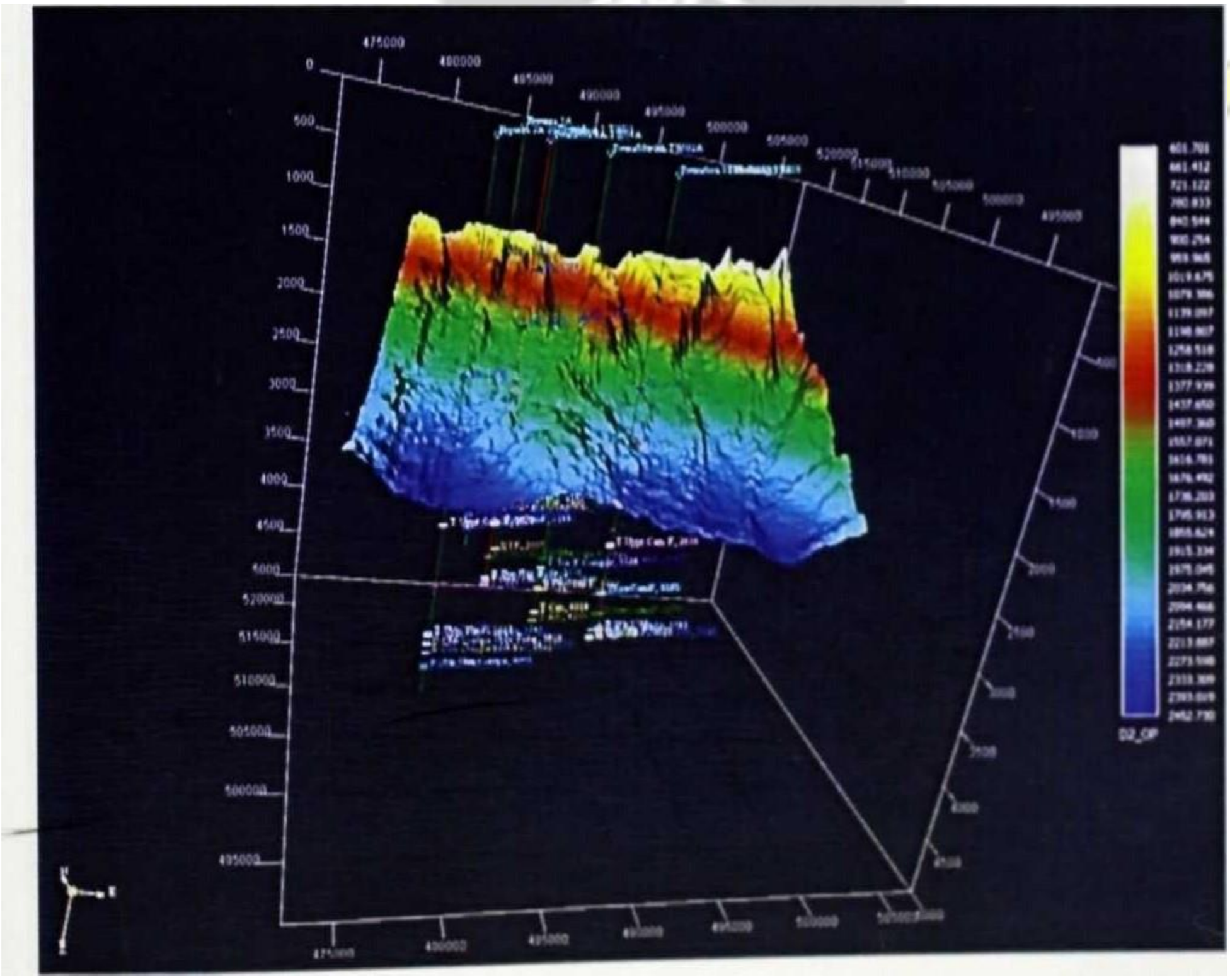

Figure 4.15: Depth-converted 3D view of the Miocene Unconformity in SMT VuPak showing channels a, b, c, d and e.

4.2.2 TOP UPPER CAMPANIAN (FAN)

The picked TWT horizon for top of Miocene Unconformity is subtracted from that of Upper Campanian (fan) to generate the isochron for the MU formation. The is also generated from the modified regression model and finally, isopach map is divided by the isochron map to build the MIV model for the MU formation, Figure 4.17.

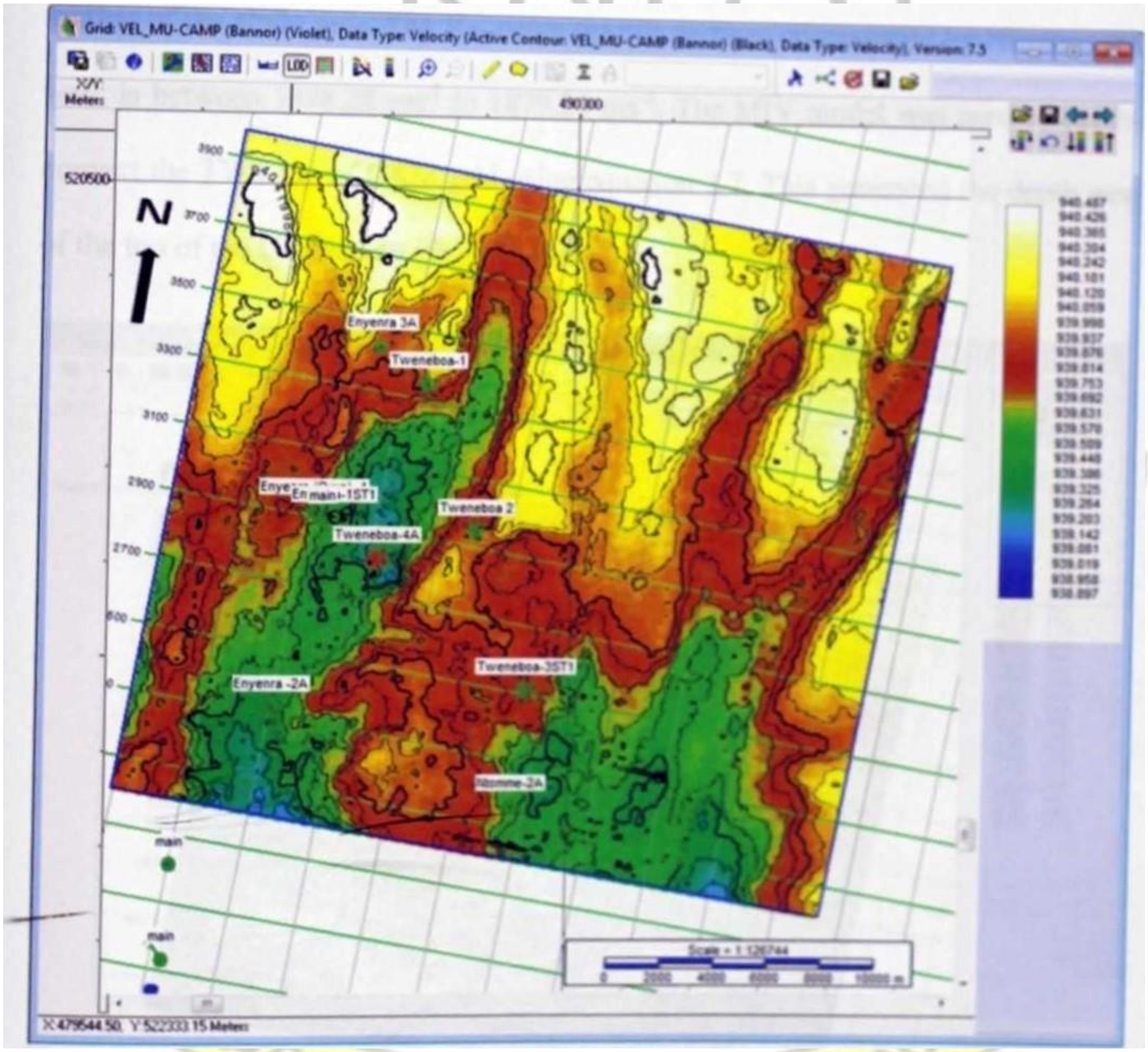

Figure 4.16: Mapped Interval Velocity (MIV) Model trtween MiocetE Unconformity and Top Campanian

Generally, from the colour bar for the MIV model, it is apparent that the Vint does not vary much laterally within this formation for the study area, Figure 4.17. The Vint ranges from 1877.90 ms-I to 1880.90 ms-I (936.9 to 940.47 ms-I, TWT isochron). Unlike the MIV for the SB formation, MU formation's MIV shows that

Vint decreases southwards. There appears to be a structure of low Vint ,shown in green, stranding between Tweneboa 1 and Tweneboa 2, passing through Tweneboa 4 and then through Enyera 2A in the southeast direction. The MIV model is also low at the southeast section of the study area. The Vint range for this section, encountered by Ntomme 2A well, is between 1878.28 ms-I to 1879.26 ms-I. The MIV model was used to depthconvert the TWT top of CAM grid using equation 3.7. This generated the depth map of the top of the Campanian (fan), Figure 4.18.

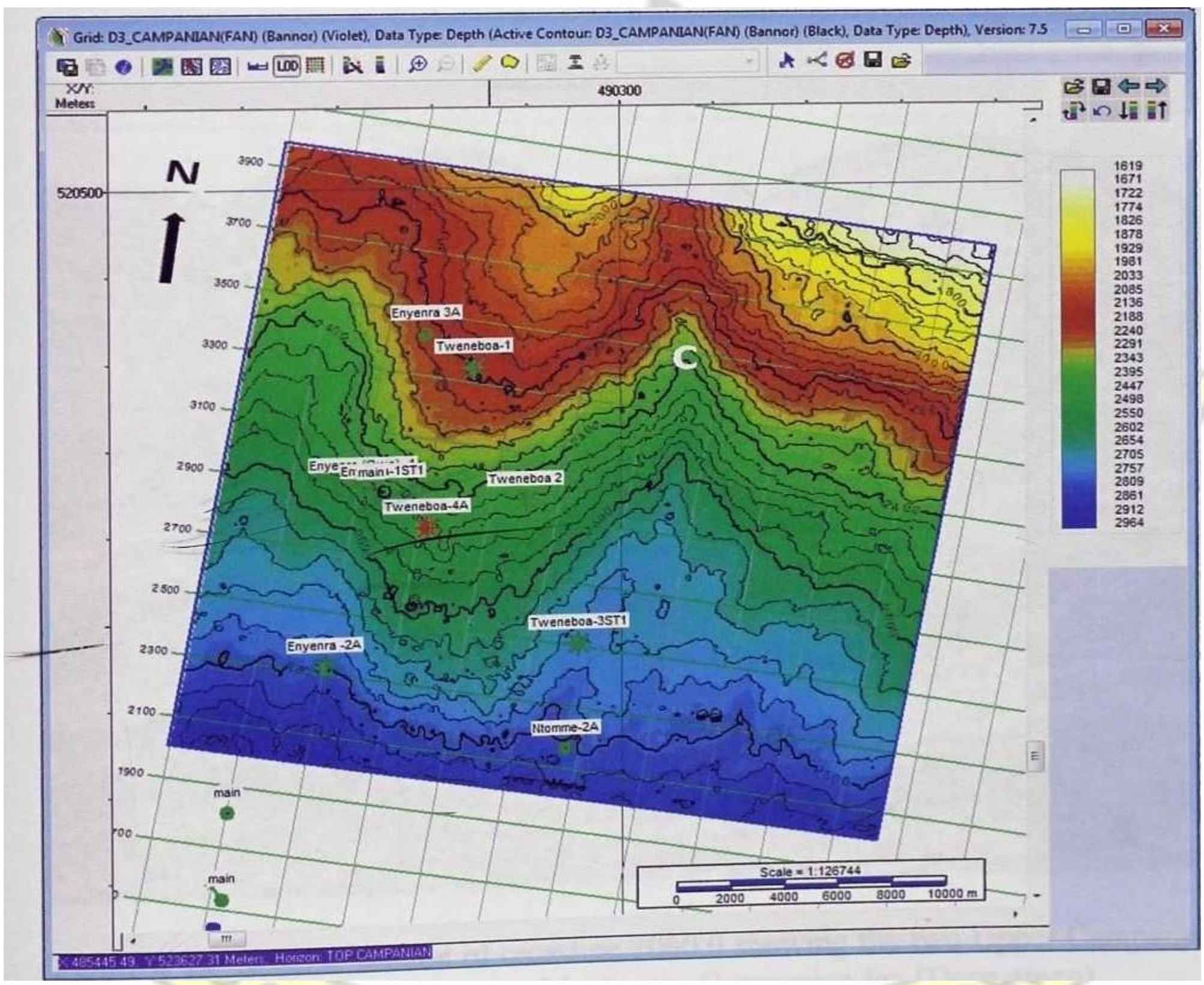

Figure 4.17: Depth converted Top Upper Campanian (fan)

The Depth map in Figure 4.18 shows that the top of CAM is a southward sloping surface. The depth from MSL of the surface ranges from 1619 m to 2964 m. The top of Miocene Unconformity sloped over a depth interval of 1345 m. A slight indication ofa channel is seen to follow a similar path as channel c ofthe Miocene unconformity and canyon c on the seabed. Channels a and b of the Miocene Unconformity seem to

have merged at the top of CAM. There is no indication of channels d and e of the Miocene Unconformity at the top of CAM.

The nature of the surface is appreciated when observed in 3D, in the SMT Vupak, Figure 4.20. The low depths where the Enyera 2A and Ntomme 2A are located are the tops of the two separate upper Campanian fans. Figure 4.19 shows the two upper Campanian fans and the lower Campanian fan.

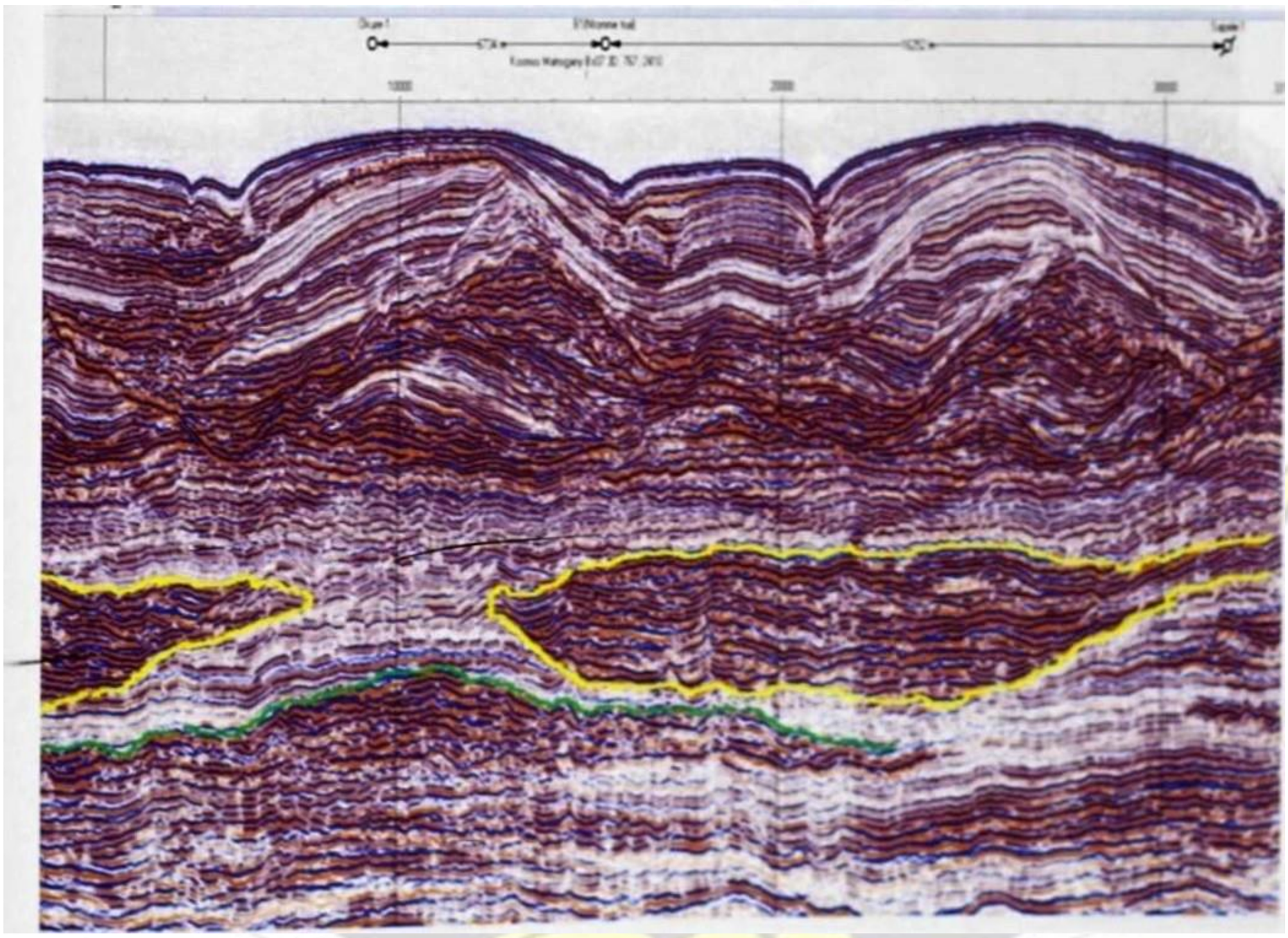

Figure 4.18: Seismic section of crossline 2060.0 showing the two t-Jprxr Campanian fans (Yellow outline) and the top of the Lower Campanian fan (Deep green)

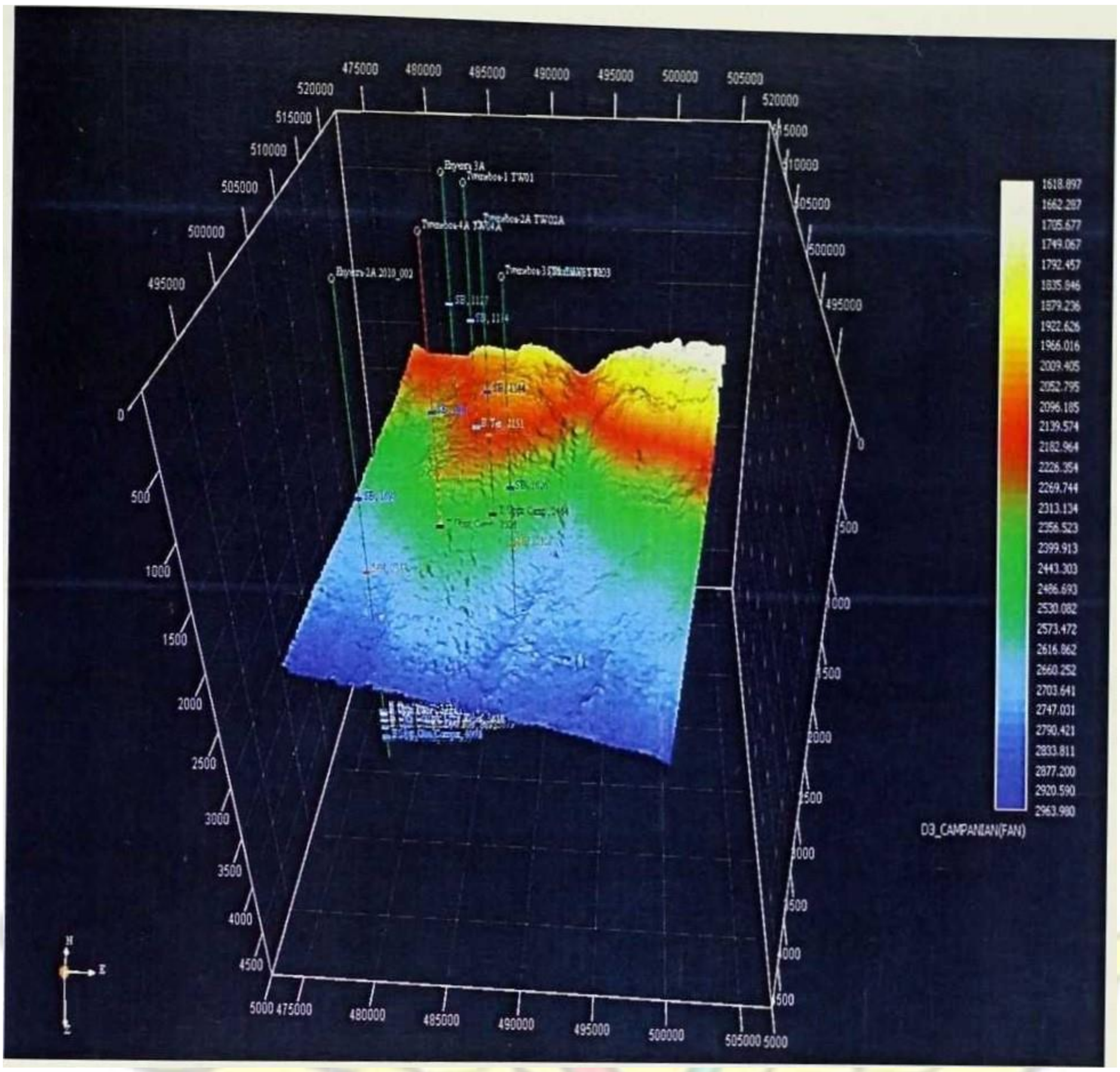

Figure 4.19: Depth-converted 3D view of the Top of Campanian (fan) in SMT VuPak

From Figure 4:20, Top Campanian (fan) shows undulation at the north with two prominent relatively raised parts or "highlands". One is at the northeast part of the study area whereas the other run m north to south through the middle section. The two are separated by valley-like channel c. The southern section appears less undulating compared to the northern section.

4.2.3 Top Turonian (fan)

The top of TUR formation which was not extensive over the study area was depth converted using the MIV ofthe CAM formation. The TWT map shown in Figure 4.13c had that of CAM subtracted from it in EMC to generate the isochron of the CAM formation. Then, its Isopach was then generated with EMC using modified regression model, which excludes the entries of the Enyera wells, for the

Campanian group in Figure 4.11. The MIV model was then built from the division of the Isopach map by the Isochron map, Figure 4.21.

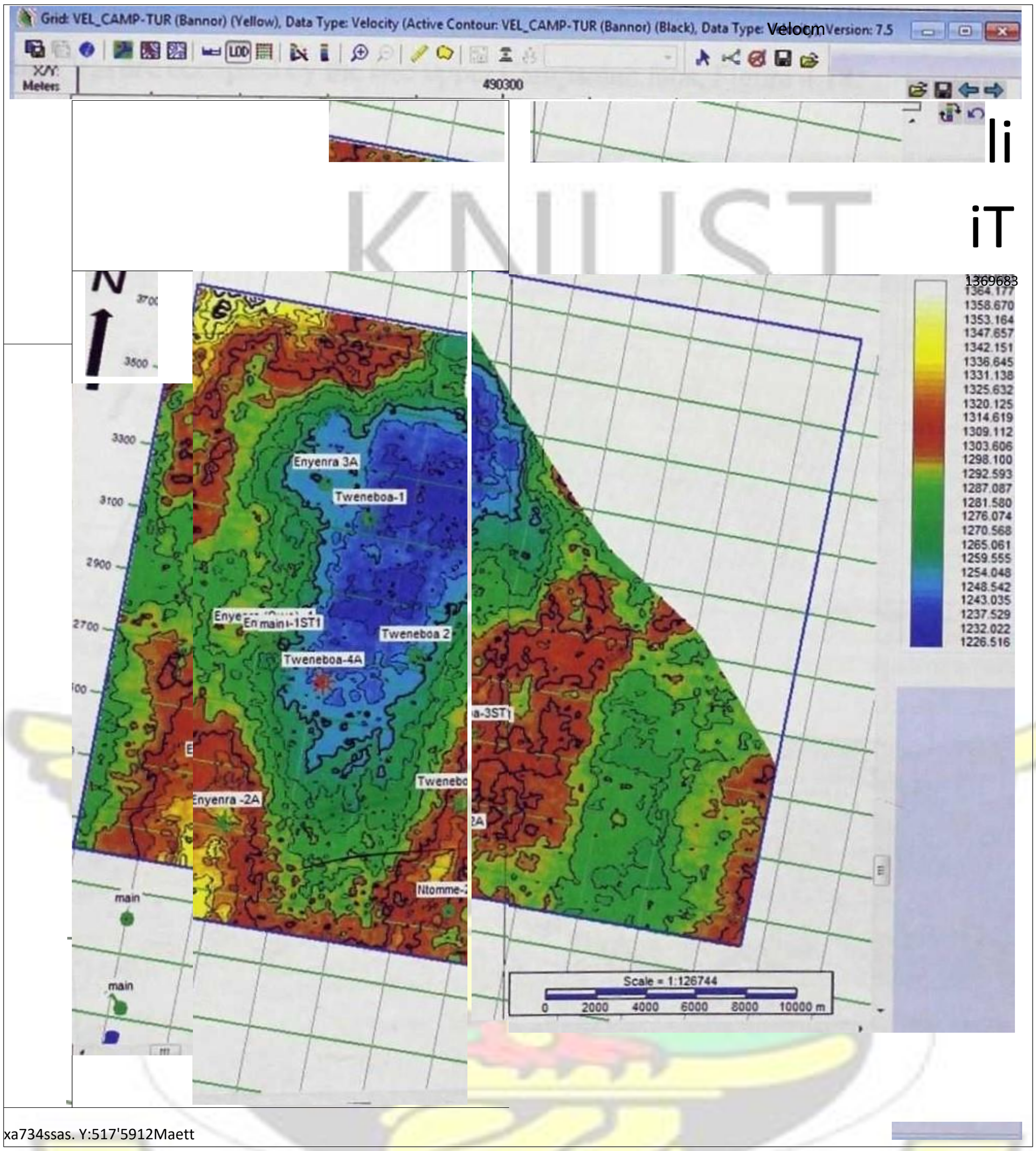

Figure 4.20: Mapped Interval Velocity (MIV) Model between Top Upper Campanian (Fan) and Top Turonian (Fan)

The Vint of the CAM formation ranges from 2453.03 ms-I to 2739.37 ms-I (1226.52 ms-I to 1369.68ms-l using TWT isochron, Figure 4.21). Areas of well of Tweneboa 1, Tweneboa 2 and Tweneboa 4 have relatively low Vat of below 2508.08 ms-I, shown in blue on the map. Relatively high Vint is observed within the area around locations of Enyera 2A and Ntomme 2A wells ranging between 2606.22 ms-I to 2728.36 ms-I. This is contrary to what is observed at Figure 4.8, CIV models of the Deepwater Tano wells, where for the CAM formation, the Enyera wells have the lowest Vint. This has resulted because the regression model for the conversion does not consider the entries of the Enyera wells for the CAM formation. Areas of apparent high Vint are occupied by the two upper Campanian fans, Figure 4.18.

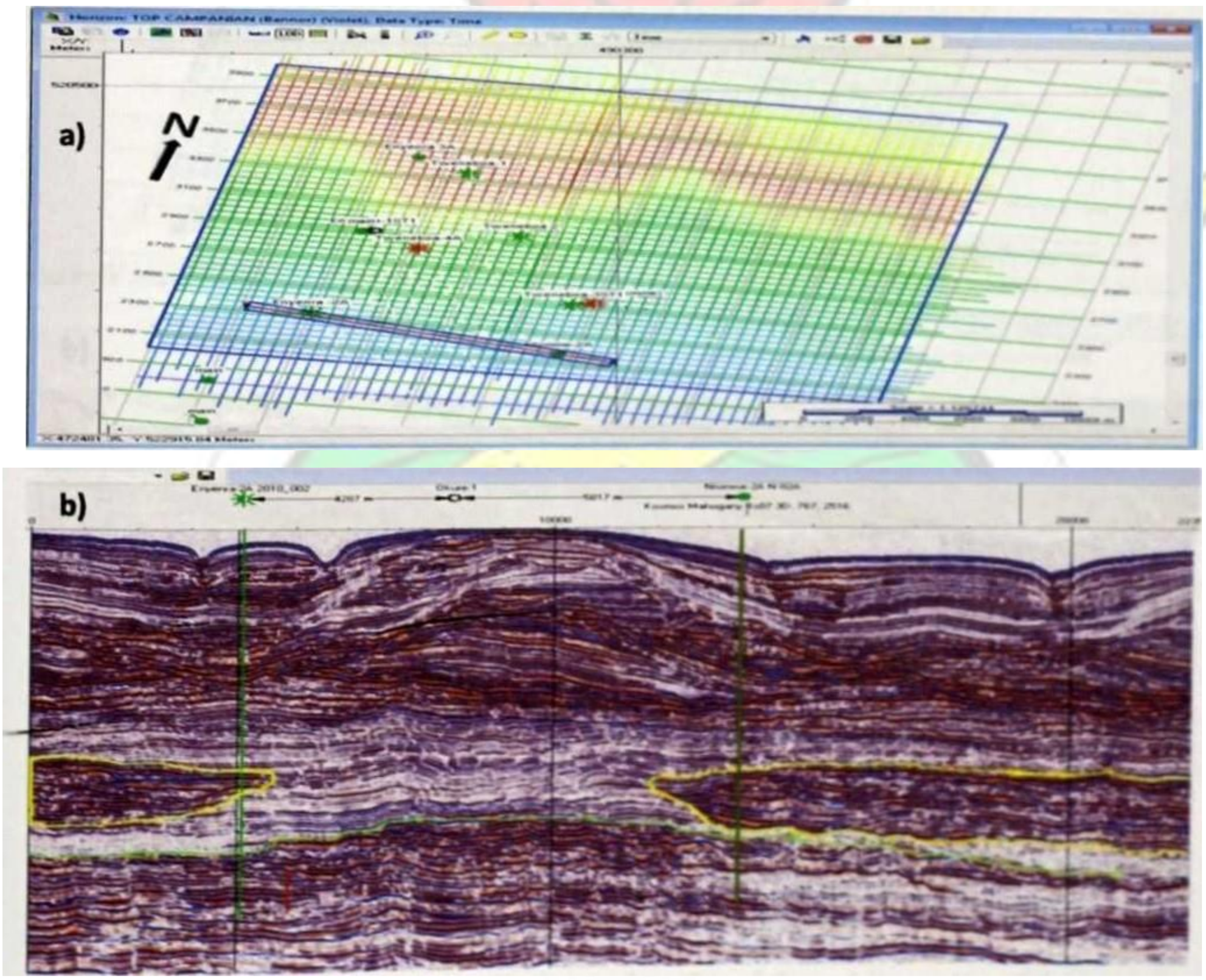

Figure 4.21: a) Base map and b) seismic section of the arbitrary line (across survey direction) showing the Enyera 2A and Ntomme 2A encountering the Upper Campanian fans.

When the lithology of the infill of the fans are not considered, the high Vint values are generally expected since the fans occupy areas of lower depths at the top of CAMP with relatively smaller isochrons resulting in higher interval velocity values.

The linear regression model that was later modified for the depth conversion excluded the entries ofboth Enyera wells. This was done to prevent the relatively low anomalous interval velocity values, at these wells for CAMP from affecting the model, Table 4.1 and figure 4.8.

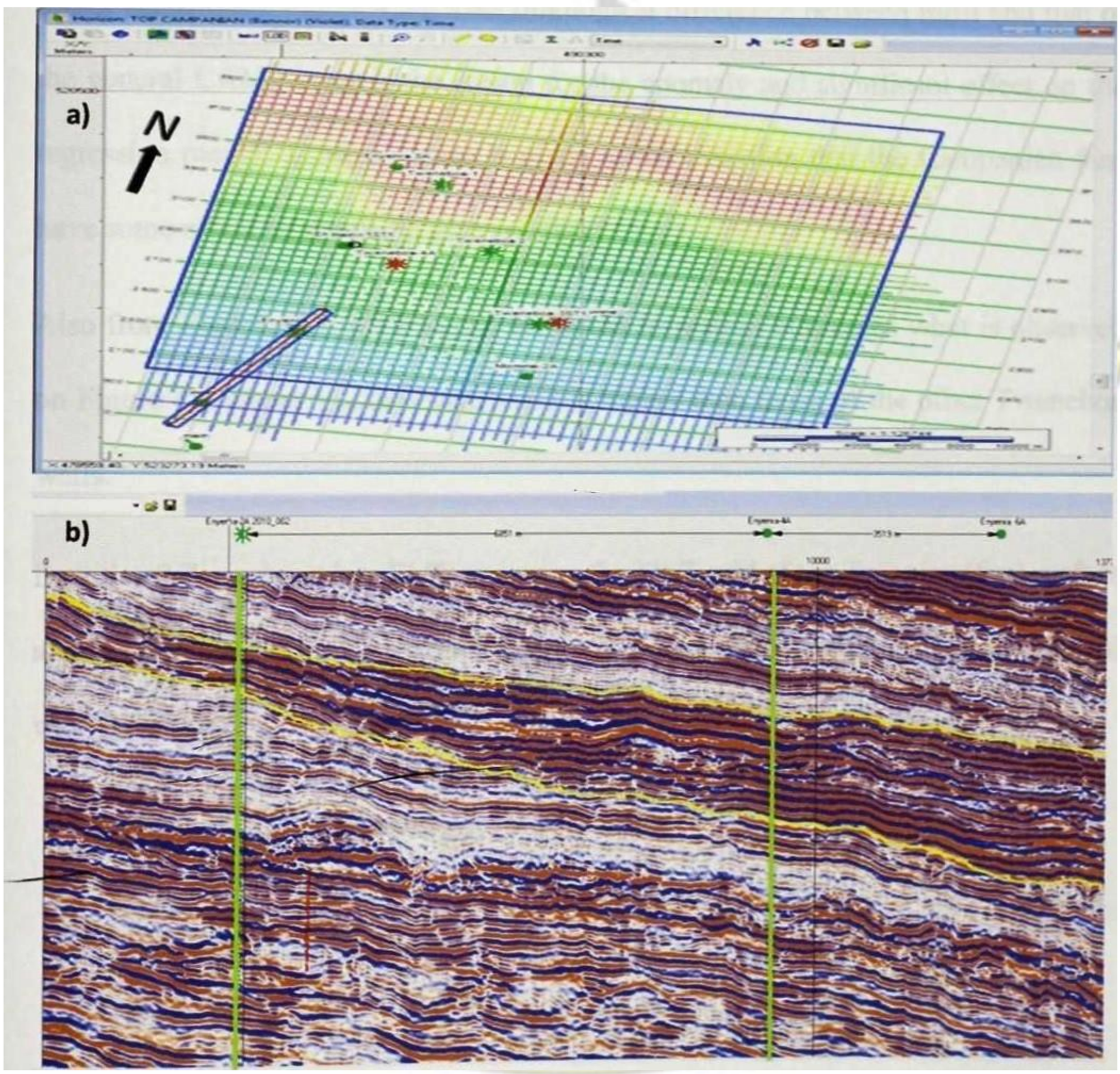

Figure 4.22: Base map (a) and seismic section (b) of the arbitrary line (along survey direction) showing the Enyera 2A and Enyera 4A encountering one of the Upper Campanian fans.

Even though Ntomme 2A encounters the top ofthe Campanian at the fan, Figure 4.22, it was not excluded because of the negligible difference it makes on the correlation coefficient, from 0.9523 to 0.9548. The Upper Campanian fan encountered by Ntomme 2A did not have substantial effect on the model for the CAMP formation because its infill is lithologically similar to that in between the two fans: sandstones, massive with sand/shale interbeds (or with claystone interbeds as at Tweneboa 4A).

The Upper Campanian fans encountered at the Enyera wells is mainly claystones with minor sandstones, Figure 4.23. This lithological difference between infill and that of the general CAMP layer is the reason for the anomaly and significant effect on the regression model. Thus, credence is given to the assertion that the Campanian fans have some effect on the depth conversions.

Also from Figure 4.21, MIV model for CAM formation buttresses what is observed on Figure 4.8 where Vint of Tweneboa 3 is higher than those of the other Tweneboa wells.

Equation 3.7 was input into EMC and using the TWT grid oftop Turonian (fan) surface and the MIV model for CAM, the depth-converted surface map of top Turonian (Fan) was generatsd-

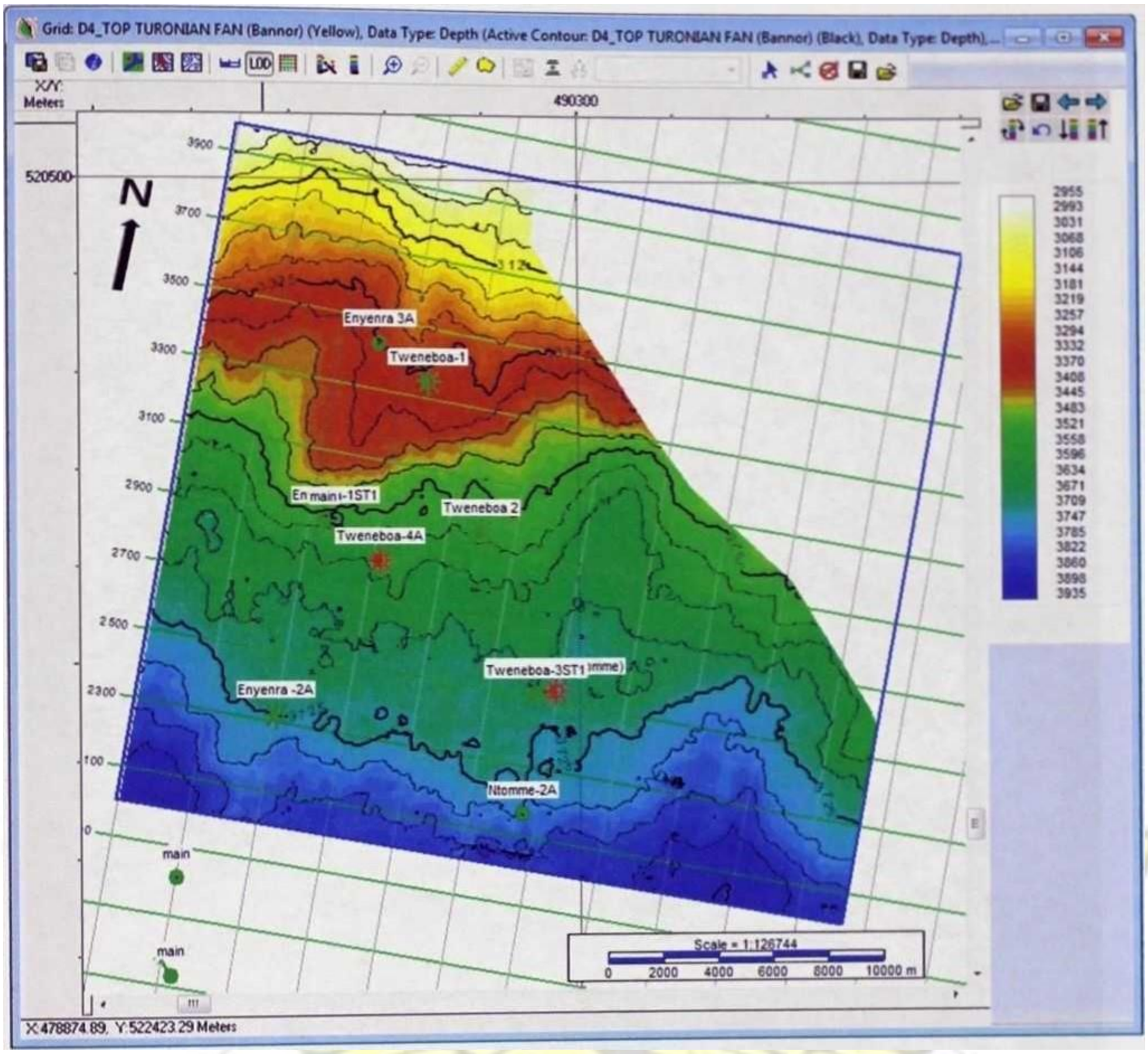

Figure 4.23: Depth converted Top Turonian (fan)

The depth map of the top of Turonian (fan) is a southward sloping surface of depth below MSL ranging from 2955 m to 3935 m, Figure 4:24. The surface, thus, sloped over some_980 m interval. The depth map does not reveal any channel. The depthconverted Top Turonian is shown in 3D in SMT Vupak in Figure 4.25.

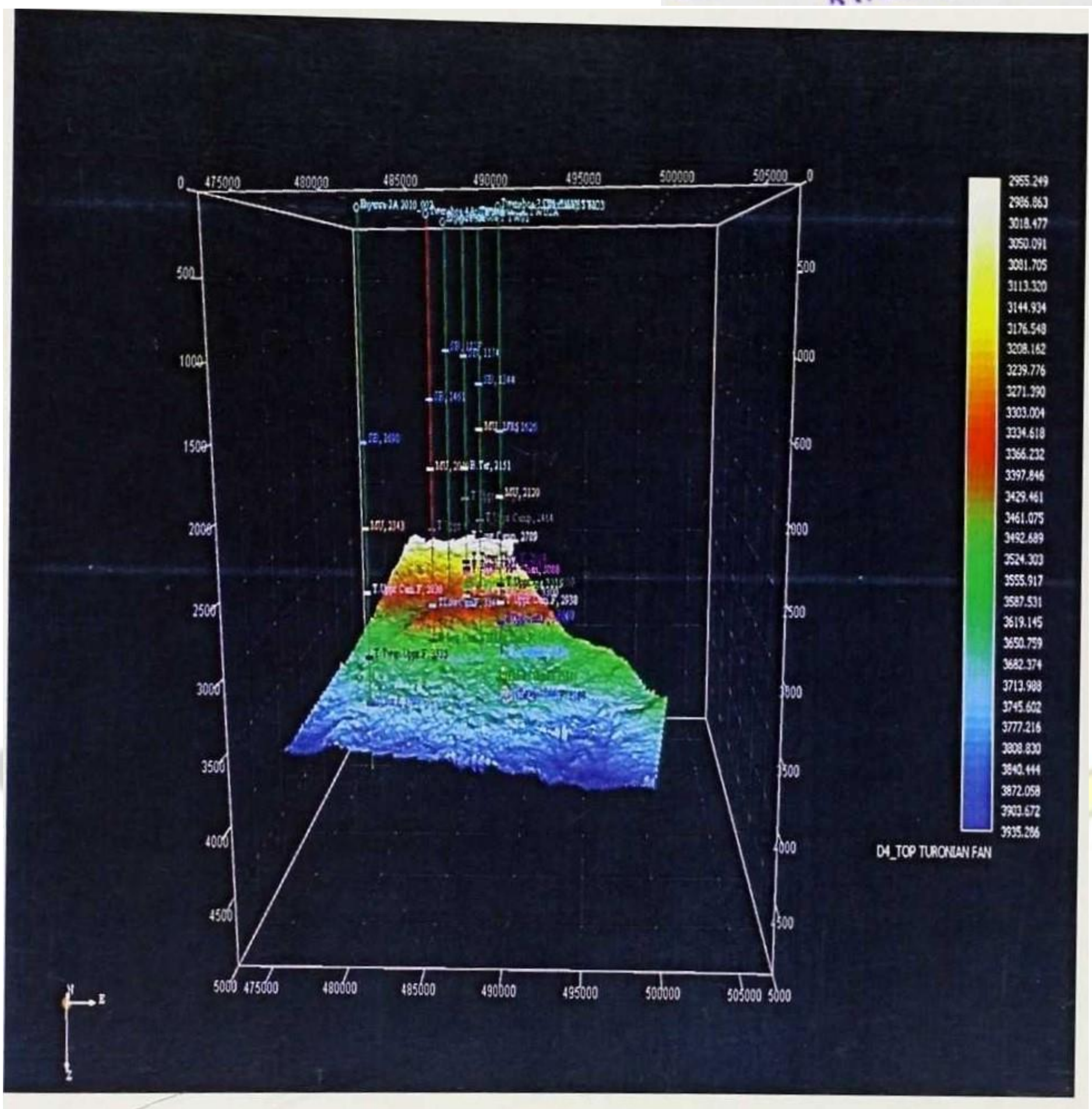

Figure 4.24: Depth-convefted-3Ðview ofthe Top Turonian (fan) in VuPak of SMT

The surface shows no undulation but a very gentle sloping surface. The depthconverted surfaces of the Miocene Unconformity, Campanian (fan) and the Turonian are shown in 3D in one Vupak for comparism, Figure 4.26. The colour bar shown is that for Top Turonian (fan). The surfaces are shown with Enyera 2A, Ntomme 2A and Tweneboa 3STl wells. Evidently, the Miocene Unconformity slopes most whereas Top Turonian (fan) does least. It seems that the deeper the layer the less undulating the surface.

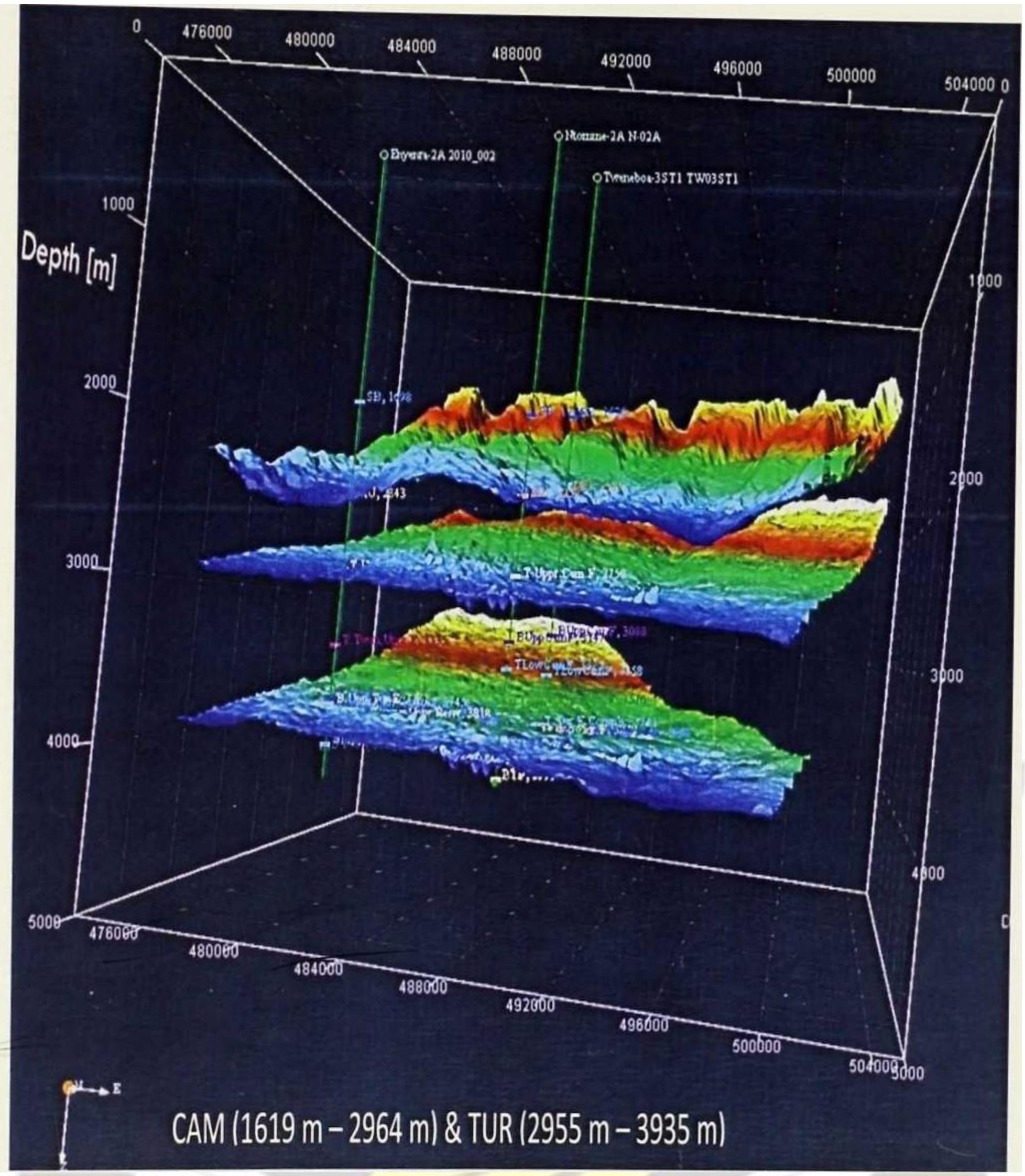

Figure 4.25: 3D view, in VuPak, the Miocene Unconformity, Top Upper Campanian (Fan) and Top Turonian (Fan).

To ascertain the reliability of the constant velocity value 1500 ms-I (used to convert the seabed) and the MIV models for depth conversion, their depth converted surfaces were compared with depths of formation tops from well data. Table 4.4 shows the well grouped formation top depths, MI V model converted depths, the difference between them and the percentage deviation.

Table 4.4: Comparison of depths of the Time-to-Depth converted grouped Formation Tops using MIV and grouped Formation Tops from wells.

WELLS	SEABED GROUP				MIOCENE UNCONFORMITY GROUP			
	WELL Z(ml	SEISMIC	DIFFERENCI	PERCENTAGE DEVIATION	WELL Z[ml	SEISMC	DIFFERENCE	PERCENTAGE DEVIATION
NTOWE	1626.00	1637.00	11.00	0.67	2120.00	2108.00	12.00	0.57
NTOWE 2A	1754.40	1749.00	5.40	0.31	2276.00	2253.00	23.00	1.01
TWENEBOA 4A	1461.00	1456.00	5.00	0.34	2019.00	2010.00	9.00	0.45
TWENEBOA 3	1626.00	1613.00	13.00	080	2120.00	208200	38.00	1.79
TWENEBOA 2A	134350	1338.00	550	0.41	1715.00	1719.00	4.00	0.23
MENEBOA 1	117350	1166.00	7.50	0.64				
ENYERA4A	1902.00				2413.00			
ENYEA2A	1698.00	1693.00	5.00	0.29	2343.00	2296.00	47.00	2.01
	Average		7.49	0.49	Average =		22.17	1.01

WELLS	CAMPANIAN GROUP				TURONIAN GROUP			
	WELL Z[ml	SEISMIC Zlm]	DIFFERENCI	PERCENTAGE DEVIATION	WELL Z[ml	SEISMIC Zlm]	DIFFERENCE	PERCENTAGE DEVIATION
NTOWE	20.00	274200	5800	207	3755.00	3693.00	62.00	1.65
NTOWE 2A	2749.00	2819.00	70.00	248	3756.00	3786.00	30.00	0.79
TWENEBOA 4A	2506.00	2498.00	8.00	0.32	3635.50	3603.00	3250	0.89
TWENEBOA 3	20.00	2755.00	45.00	1.61	374088	3686.00	5488	1.47
TWENEBOA 2A	246350	2457.00	6.50	0.26	3584.00	356000	24.00	0.67
MENEBOA	2422.00	2454.00	32.00	1.32	3406.00	3346.00	60.00	1.76
ENYERA	3004.70				3920.00			
ENYEA2A	2830.00	2795.00	35.00	1.24	370800	3712.00	4.00	0.11
	Average =		37.08	1.33	Avera e =		38.20	1.05

AVERAGE DEPTH DIFFERENCE [ml	AVERAGE PERCENTAGE DEVIATION [0/01
26.23	0.97

From Table 4.4, the constant velocity value of 1500 ms-I used to depth-convert the TWT picked surface performed best at depth conversion with the least deviation from the well depths of about 8 m. it had its least depth difference at Enyera 2A, 5.00

m, and its greatest at Tweneboa 3ST1, 13.00 m. The surface had a 99.5 % accuracy. The depth conversion of the Miocene Unconformity done using SB group's MIV model followed with an accuracy of 98.99%. It deviated least from well depth at Tweneboa 2A by 4.00m and greatest at Enyera 2A by 47.00 m.

In terms of relative reliability, the MIV of the CAM group is next with an accuracy of

98.95 0/0. Even though the regression model used for the depth conversion did not consider the isochron and isopach entries of the Enyera wells, it the depth converted surface had the least deviation from well depths at Enyera 2A by 4.00 m and the greatest at Ntomme, 62.00 m. Finally, the MIV model of MU used for depth conversion ofthe top of Campanian (fan) had the least accuracy of98.67 0/0. The depthconverted top of CAM deviated least for Tweneboa 2A by 6.50 m and greatest for Ntomme 2A by 70.00 m.

The MIV models built using regression are reliable for the time-to-depth conversion because the maximum percentage deviation computed between the observed field data and the estimated geostatistical depths, is less than 3 0/0. Moreover an average percentage-deviation of 0.97 % and average depth difference of26 m were the average error margins for the built interval velocity models.

CHAPTER 5: DISCUSSION AND CONCLUSION

5.1 CONCLUSION

Areal interval macrovelocity models were built for an area within the Deepwater Tano of the Western Basin, offshore Ghana. They were built from both checkshot data and seismic sections using regression geostatistical technique. The interval velocity values estimated using regression was reliable for the time-depth conversion because the maximum percentage deviation computed between the observed field

data and the estimated geostatistical depths, was less than 3 0/0. An average percentage deviation of

0.97 % and average depth difference of 26m were the average error margins for the built interval velocity models. The interval velocity models give an understanding of how the interval velocity varies laterally and vertically at the area. The interval macrovelocity models and their converted depths honoured lithological trends and geologic features within the subsurface. The interval velocity model for CAMP, without entries from Enyera wells resulted in a better correlation for the formation and converted the top of the Turonian very well. This gives some credence to the assertion that the Campanian fans have some effect on the velocity models and invariably affect depth conversions.

5.2 RECOMMENDATION

These depth deviations are due to the few well constraints for the research area. Generally the mapped interval model works best for areas with densely populated wells to ensure accurate picks and ensure representative gridding. In addition, tops of grouped formations as picked are subject to lithostratigraphic interpretation errors (Dalfsen et al, 2006). It is not uncommon to have incorrect well postings or inconsistencies in the interpreted tops. Often, record-keeping issues for well data normally result in incorrect well positioning (Rojano et al, 2005). Besides, acquisition and processing of seismic data is also subject to some errors which invariably affect interpretation.

Due to time constraints, fault analysis of study area was not undertaken. The margin of deviation of converted depths from well depths will be reduced when fault planes are incorporated in the seismic interpretation. Some degree ofspatial smoothing ofthe interval velocities is recommended to stabilize potential erratic velocities introduced

by the picking process for better conversions (Rojano et al, 2005). Since the Campanian group is made of upper and lower Campanian fans, further work should split the two as separate layers and find how the two affect the conversion models.

Since porosity, permeability and formation fluids such as hydrocarbons and water have significant effects on seismic velocities, further research should incorporate the impacts of these factors. Moreover, the methodology did not make use of any velocity data from seismic, which would have provided valuable additional information between well. For more ideal velocity models, seismic data should be calibrated to the wells and then the spatial and vertical coverage ofboth data sets can be benefited from.

Detailed analysis using other geostatistical techniques such as Sequential Gaussian

Simulation (SGS) and Kriging with External Drift (KED) technique which is particularly useful in areas where there is little well information (Olabode, 2008). The choice of gridding algorithms, least squares, kriging, etc., will lead to differences in depth maps between the well locations (Masden, 1992).

References

Al-Chalabi, M. (1997, MAY-JUNE). Parameter nonuniqueness in velocity versus depth functions. GEOPHYSICS, 62(3), P. 970-979.9.

Alaminiokuma and Ugbor C.C. (2010). Analytical Velocity Model foe Conærsion in the Subsurface Focies ofAgboda Formation in the Niger Nigeria. (Vol. 11). EnuguState: The Pacific Journal of Science and Technology.

Andreoletti, C, Panizzardi, J. & Bienati, N... (2012). Data And Technology Integration Improve Velocity Analysis For Seismic Imaging. ENI E&P.

Atta-Peters D & Salami M. B. (2004). Late Cretaceous To Early Pollen Grains From Offshore Tano Basin, Southwestern Ghana. University of Ghana, Department of Geobgy. Revista Espanola de Micropaleontología, 36(3).

Cameron, M & Sethian, J. (2006). Seismic Velocity Estimation And Time To Depth Conversion Of Time-Migrated Images. New Orleans Annual Meeting (p. 3066). SEG.

Cameron, M. S. (2006). Seismic Velocity Estimation And Time To Depth Conversion Of Time Migrated Images. New Orleans 2W6 Annual Meeting. SEG.

Cordier, J. P. (1985). Velocities In Reflection Seismology (Vol. 3). Springer.

Covautt, J. A (2011). Submarine Fans and Canyon-Channel Systems: A Review of Processes, Products, and Models.

Dalfsen, V. W., Doornenbal, J. C, Dortland, S. & Gunnink. L, L. (2006). A comprehensive seismic velocity model for the Netherlands based on lithostratigraphic layers. Netherlands. Journal of Geosciences. 85, 277.

Dheasúna M. N., Ballesteros M.. Leven J. (2012, Aug-Sept). A Regional Velocity Cube For Depth Con~~version On T~~he Northwest Shelf. PESA News Resovces, pp. 40-43.

Dix. C. H. (1955). Seismic velocities from surface measurements:. Geophysics, 20, 68—86.

—-Etris L Edward. Nick J. Crabtree, Jan Dewar. (2001. NovemberL TRUE DEPTH CONVERS&ON: MORE THAN A PRETTY PICTURE. ŒEG Recorder 11, 12-22.

Guilbot Jérðme and Brackin Smith. (2002, March). 4-0 onstrained onversion depth for reservoir compaction estimation: Application to Ekofisk Field. THE LEADING EDGE,
302-308.

H©nbotham, J. B. (2010). Depth MVation Vebcity Model W'th Wave Equation EAGE. 28.

Jones. l. F. T'Roriai: Time Conversion of MVated Data.. EAGE. 27.

Kearey. P.. Brooks. M. (2002). L 9. An ntroduction to Geophysical Exploration CVd. THIRD EDmON). Blackwell Science. 263Þ

Kissirw. (n.d.). Retrieved from http://www.agl.uh.edu/pdf/theses/kisin.pdf

Kuffour, O. (2008). Estimation Of Petrophysical Data For Assessing Hydrocarbon Potential In Western Ghana Oilfield (Tano Basin) Unpublished manuscript.

Leverette, S. J. (1977). Data Adaptive Velocity/Depth Spectra Estimation In Seismic Wide Angle Reflection Analysis. {Massachusetts Institute of Technology and Woods Hole Oceanographic Institution.

Lorie K. Bear, Thomas A. Dickens, Jerome R. Krebs, Jonathan Liu, and Peter Traynin. (2005, JUNE). Integrated velocity model estimation for improved positioning with anisotropic PSDM. THE LEADING EDGE, 622-628.

Marsden, D. (1989). Layer cake depth conversion. GEOPHYSICS: THE LEADING EDGE OF EXPLORATION, 10-15.

Marsden, D. (1998). A Practical Guide To Velocities In Exploration. London.

Masden, D. (1992, AUGUST). vo-K method of depth conversion. GEOPHYSICS: THE LEADING EDGE OF EXPLORA TION, 53-54.

Mavko G. (1990). Parameters That Influence Seismic Velocity, Conceptual Overview of Rock and Fluid Factors that Impact Seismic Velocity and Impedance. Stanford Rock Physics Laboratory .

Olabode O. P and Enikanselu P, A. (2008). Analysis ofSeismic Time-Depth Conversion Using Geostatistically- Derived Average (Vol. 1 (1)). Akure, Ondo State, Nigeria: Ozean journal ofApplied Science.

Rojano M. A, Garcia E. J, Mackay S,Goodoff L, Hamilton D. (2005). Creating accurate velocity models in maturefields: Poza Rica Field, Veracruz, México.

Stanford University. (n.d.). Retrieved from http://pangea.stanford.edu/courses/gp262/Notes/8.SeismicVelocity.pdf

Sutherland, R. (2008). Exploration History And Regional Geology. Tullow: Capital Markets Day, _____

Tano Basin - Onshore to Shallow Offshore. (n.d.). Retrieved March 14, 2013, from http://www.clontarfenergy.com/app_user_files/file/Ghana-Tano-Basin_PresentationAGM.ppt

Telford, W. M., Geldart, L. P., & sheriff, R. E. (2001). Applied Geophysics (Second Edition ed.). Cambridge university press.

TEN Development Project, Deepwater Tano License, Ghana. (2012). Retrieved March 5, 2013, from Offshore Technology, In association with Worldexpro: http://www.offshore-technology.com/projects/ten-development-projectdeepwater-tano-ghana/

TNO, I. K. (2007). Seismic velocity model building based on sonic data of boreholes in the Netherlands (Vols. Beno uGE 05105-2007). Netherlands: TNO Built Environment and Geosciences.

Tullow Oil Ghana. (2012, November 14). Retrieved March 5, 2013, from TEN: http://www.tullowoil.com/ghana/index.asp?pageid=12

Uduanochie, K. O. (2011). Building Subsurface Velocity Models Using Ocean-Bottom Seismic Data:. Green Canyon, Gulf of Mexico.

Velocity Analysis In Practice. Version 1.0 released. (1999, 1 29). Retrieved 12 4, 2012, from http://www.xsgeo.com/course/velan.htm

Wang, B. Y., Mason, K. C . & Zeng, X. (2008). Advances in velocity model-building technology for subsalt imaging. . 73(No. 5 September-October 2008_; P. Ve173—Ve181, 17 Figs.10.1190/1.2966096.).

Yilmaz, O. & Doherty, S.M. (1987). Seismic Data Processing. Investigation In Geophysics.